Evaluation of Fiber-Matrix Interfacial Shear Strength in Fiber Reinforced Plastics

by

Philippe Jacques Sabat

Thesis submitted to the Faculty of the
Virginia Polytechnic Institute and State University
in partial fulfillment of the requirements for the degree of
Master of Science
in
Engineering Mechanics

APPROVED:

H. F. Brinson, cochairman

D. W. Dwight, cochairman

J. C. Duke

September, 1985

Blacksburg, Virginia

Evaluation of Fiber-Matrix Interfacial Shear Strength in Fiber Reinforced Plastics

by

Philippe Jacques Sabat

H. F. Brinson and D. W. Dwight, cochairmen

Engineering Mechanics

(ABSTRACT)

The role of the interphase in fiberglass reinforced composites was studied by a combination of theoretical analysis, mechanical tests, and several high resolution analytical techniques. The interphase was varied in composition by using epoxy and polyester matrix polymers with and without added coupling agents, as well as four fiber surface modifications. Different coupling agents on the fibers were shown to change the fiber tensile strength markedly. Filament wound unidirectional composites were tested in short beam "shear". Corresponding samples were fabricated by embedding one to seven fibers in the center of polymer dogbone specimens that were tested in tension to determine critical fiber lengths. Those values were used in a new theoritical treatment (that combines stress gradient shear-lag theory with Weibull statistics) to evaluate "interfacial shear strengths". The fact that results did not correlate with the short beam data was examined in detail via a combination of polarized light

microscopy, electron microscopy (SEM) and spectroscopy (XPS or ESCA) and mass spectroscopy (SIMS). When the single fiber specimens were unloaded, a residual birefringent zone was measured and correlated with composite properties, as well as with SIMS and SEM analysis that identified changes in the locus of interphase failure. Variations in the interphase had dramatic effects upon composite properties, but it appears that there may be an optimum level of fiber-matrix adhesion depending upon the properties of both fiber and matrix. Fiber-fiber interactions were elucidated by combining tensile tests on multiple fiber dogbone specimens with the high resolution analytical techniques. In general, this work exemplifies a multidisciplinary approach that promises to help understand and characterize the structure and properties of the fiber-matrix interphase, and to optimize the properties of composite materials.

ACKNOWLEDGEMENTS

The author wishes to express his sincere gratitude to:

- Drs. D. W. Dwight and H. F. Brinson for their consistent guidance, assistance, and encouragement throughout this work.

- Drs. J. C. Duke, and for their guidance and support.

- Drs. and and their graduate students for the use of their laboratory equipment and for their repeated assistance.

- for his assistance and support of this work by running ESCA and SEM analysis.

- The compagny VETROTEX SAINT-GOBAIN for their financial support and also for the supply of the samples and products absolutely necessary for this work.

- The French Government, the association of E.N.S.A.M.'s engineers and the association Ingénieurs et Scientifiques

de France (I.S.F.) for their financial support which made possible this very interesting year of studies.

TABLE OF CONTENTS

LIST OF FIGURES

LIST OF TABLES

LIST OF PLATES

LIST OF SYMBOLS

Rf	Radius of the fiber
Ri	Radius of the interphase
Rm	Radius of the matrix
Ra	Radius of the average material
L''	Half length of the average material
L'	Half length of the fiber
L	Length of the fiber
Ef	Effective Young's modulus of the fiber
Ei	Effective Young's modulus of the interphase
Ea	Effective Young's modulus of the average material
Gi	Shear modulus of the interphase
Gm	Shear modulus of the matrix
Xf	Tensile strength of the fiber
σ	Tensile stress
σf	Tensile stress in the fiber
σi	Tensile stress in the interphase
σa	Tensile stress in the average material
τi	Shear stress in the interphase
τm	Shear stress in the matrix
γi	Shear strain in the interphase
γm	Shear strain in the matrix

Uf	Extension of the fiber
Ui	Extension of the interphase
Ua	Extension of the average material
α	Coefficient ($\sigma i = \alpha . \sigma f$)
β	Coefficient ($\tau i = \beta . \tau m$)
c	Coefficient of stress concentration
δ	Ineffective length
Lc	Critical fiber length
ν	Poisson's ratio
Vf	Volume fraction of fiber
R	Reliability
f	function (f(L)=1, f(0)=0)
f'	Density function
μ	Mean
α'	Weibull shape factor
σo	Weibull characteristic strength

INTRODUCTION

The current rapid development of composite materials comes from the ability to design their properties by combining the properties of their constituents for a specific application, i.e. to satisfy given specifications. Conventionally, the constituents of fibrous composites are the fiber and the matrix. In order to calculate their combined properties, the rule of mixtures can be applied as a first approximation. This method is based on the volume fraction of the two constituents and assumes perfect bonding between fibers and matrix. Differences between the predictions of the rule of mixtures and experimental data have led in the past to numerous studies to understand and to attempt to model the stress transfer between the fibers and the matrix at a region of zero thickness called the interface.

With the development of analytical techniques such as X-ray Photoelectron Spectroscopy (XPS or ESCA) and Fourier Transform Infrared Spectroscopy (FTIR) it has been possible to show that the bulk properties of two constituents A and B bonded together may be quite different from those of a region around the A-B interface. There is a gradient of chemical structure and mechanical characteristics as one goes from the bulk of material A to the bulk of material B. This region of

finite thickness between the two bulk materials is called the interphase. This is an important element of a composite because of its critical role in stress transfer. Good interphase properties are necessary as there is no benefit from putting two elements together if one cannot combine their characteristics because of a poor interphase. Therefore it has to be considered as a real constituent of the composite and thus must be designed for specific purposes.

Historically, two different approaches have been adopted to study the interphase in fibrous composites: One is mechanical, its goals are the development of models for the mechanism occuring at the interface and the evaluation of the mechanical properties in this region. It should be noticed that the term interface is used here because few studies deal with the concept of an interphase [1,2]. The second approach is physicochemical and involves the understanding the chemistry and physics in the interphase and the evaluation of the surface chemistry of constituents using various analytical techniques. Moreover recent studies have been done in an attempt to correlate those two approaches [3,4].

Faced with the complexity of the problem and the diversity of the postulates about the interphase, it is of interest to develop some approaches to gain new insights on the interphase.

LITERATURE REVIEW

INTRODUCTION

In order to understand why the subject of the interphase is obscure and controversial but above all, in order to elucidate the background and motivation for this research, it is of interest to go through the literature and comment about what has been done in the past. As stated before, researchers have used two different approaches to model the interphase: mechanical and physicochemical. Both are very important and complementary for a better understanding and prediction of the phenomena occuring in the interphase. On account of the difference in scale or dimension, the two approaches provide information which can be compared to one another, thus permiting a comprehensive description of the problem. Unfortunately their complementary characters have been virtually ignored by researchers. Emphasis here will be on the mechanical approach as this one provides property data essential to the design of composite parts which is the final goal of any complete study of composite materials.

PHYSICOCHEMICAL APPROACH

With the development of glass fiber reinforced composites, the detrimental effects of moisture was noticed on the properties of such composites due to the debonding fiber-matrix by the penetration of water at the interface. In order to tackle this phenomena, numerous empirical changes in the interface chemistry and/or morphology have been done in the past by coating the fibers with different chemical agents. A first approach was empirical treatments on the fibers to promote chemical bonds between fiber and matrix, followed by testing the composites made with those fibers and then classifying the treatments. However the empirical method induced researchers to develop and use analytical techniques in order to quantify and understand the adhesion between fiber and matrix. One of these techniques is related to the adsorption theory of adhesion which has been discussed in detail by many authors [5,6,7], and proposes the evaluation of the work of adhesion through the measurement of contact angles of glass surfaces and surface tension of polymers [3,4,7,8,9,10]. The fiber-matrix adhesion may also be evaluated using modified inverse gas chromatography technique [11]. In order to know the chemical composition and bonding occuring on glass surfaces, many means have been used such as X-ray Photoelectron Spectroscopy (XPS or ESCA) [12,13], Auger Electron Spectroscopy (AES) [14], Fourier Transform InfraRed

spectroscopy (FTIR) [15,16,17], Ion Scattering Spectroscopy and Secondary Ion Mass Spectroscopy (ISS/SIMS) [18]. It is also possible to observe a composite cross section and obtain its morphology by Scanning Electron Microscopy (SEM/STEM) or its point chemical composition by Energy Dispersive X-ray Spectroscopy (EDXS) or AES or ISS/SIMS [18]. It should be noted that it is impossible to access the glass surfaces or interphases inside the composite with those techniques without cuting into sections or the fabrication of ideal specimens suitable for observation. Therefore the results obtained with those analytical techniques are representative of the interphase for the specific kind of sample used. The question is: Are there any relationships between this "interphase" and the one which exists in real composite materials? For instance, a method to analyze the interphase would be to coat a single fiber with a very thin layer of matrix such that, using ESCA, one can obtain a depth profile of the chemical composition and bonding across the interphase. In order to obtain this thin layer, one can mix the matrix with a solvent and then use a centrifugal technique. Unfortunately the influence of the solvent on the interphase is unknown, just as is that of the surrounding matrix and other nearby fibers in the real composite. That makes this method difficult to relate with the real world. However these analytical techniques do give information and promote a better understanding, they just have to be analysed with care.

MECHANICAL APPROACH

Mechanical Analysis

The literature on the mechanical approach to the interface can be classified according to the analysis applied, the nature of the interface chosen and whether or not of the influence of other fibers was considered.

Five mechanical analysis have been used in general by researchers for a better understanding of the phenomena occuring at the interface between fiber and matrix:

1. The theory of elasticity [19,20,21] where one tries to find the exact solution for a cylindrical inclusion in an infinite medium under a certain applied load. The validity of this analysis lies in the answer to the question: Can a composite material be considered as homogeneous and perfectly elastic at the microscale of one of its fibers?

2. The finite element method [22,2,23] where the validity of the results obtained depends mainly on the size of the elements and on the values chosen for the input parameters. The lack of knowledge of the mechanical properties

around the interface makes these choices very difficult and thus the predictions uncertain.

3. The photoelasticity method [24-28]. Considering the very small thickness of the interphase [29] it is impossible to obtain the stress field in the interphase. The only experiment one can do is the observation of the patterns as close as possible to the interface in a sample containing one fiber or several widely spaced and then tries to infer the mechanism in the interphase.

4. The fracture mechanics approach [30-35] whose purpose is the study of crack propagation along the interface or perpendicular to the fiber direction or of crack creation due to fiber breaks.

5. The shear-lag analysis [36-41]. This is the most used approach because it is very simple, though less rigorous. It is generally assumed in this theory that the matrix transfers only shear and the fiber carries only tensile stresses. It is also assumed that at a fiber end, an interfacial shear stress applied on a length "delta" (ineffective length [30,31]) provides stress transfer, thereby building up tensile stress in the fiber. This analysis promotes a better understanding of the stress transfer between fiber and matrix. One of the most famous

examples of this approach which is frequently used in the literature is Rosen's model [30,31]. It will be modified as part of this research in order to introduce the notion of the interphase.

Another important point in this field is the nature of the interface and the properties of fiber and matrix. Four concepts have been proposed in the literature:

1. The bonding between fiber and matrix is assumed to be perfect, fibers and matrix have an elastic behaviour [36].

2. The bonding between fiber and matrix is assumed to be perfect, fibers behave elastically, the matrix plastically [37,38].

3. The stress transfer is governed by the friction between fiber and matrix caused by the normal stress component due to the differential thermal expansion coefficient and Poisson's ratio of the two constituents [42,43,44].

4. Combinations of the above concepts [35,45].

Here also, there is no satisfactory experimental evidence to date to support one of those proposals. The reason for that

is the enormous difficulty in performing meaningful experiments and analysing them properly, as will be shown later.

Finally, there is a great extent of literature on the influence of other fibers on the stress transfer between the fiber and the matrix due to stress concentrations around a particular fiber caused by adjacent fiber breaks. Several models have been proposed and are used to predict the strength of unidirectional composites under tensile load in the direction of the fibers [46-50].

Mechanical Tests

There are two categories of mechanical tests according to whether they provide a direct or indirect evaluation of the interphase. The first case calculates the interfacial shear stress on one fiber embedded in a matrix strained in tension. The others measure mechanical properties of composite samples that are greatly influenced by the quality of the fiber-matrix adhesion.

1. Direct evaluation of the interphase

   Three tests are available, however two presently are used in a large extent by researchers and industries in their studies about the interface: The measure of the critical

fiber length and the pull out test. Emphasis here will be on the pull out test as it has been the subject of many publications on its theoretical modelling. Critical fiber length tests are among the principal experimental studies later in this report.

- Single filament interfacial shear and tranverse tensile test [51,52,53]. Compressive stress is applied on a specimen containing a single filament in the stress direction. The shape of the sample determines whether the interfacial shear is measured (the sample is parallelepiped) or the transverse tensile strength (the sample is concave on its sides in order to take advantage of the Poisson effect).

- Measure of the critical fiber length [3,8,54,55,56] A sample containing a single filament is subjected to a tensile load. As the volume fraction of fiber is negligible and the strain at failure of the matrix is much higher than that of the fiber, the filament should break into smaller fragments as the elongation increases. This process will continue untill the point where the fragments are too small to carry enough shear at their surface to cause failure in tension. This dimensional limit is called the

critical fiber length. It is characteristic of the nature of the adhesion between fiber and matrix.

- The pull out test. It consists in embedding a length L of a fiber in a block of matrix and applying a force on the other part of the fiber in order to pull out the embedded length. L and the force are recorded. These two quantities permit the calculation of the interfacial shear strength. Several shapes of sample have been proposed: the button type [51], the block type [44], the three fibers type [57] and the droplet type [58]. The latter avoids the formation of a meniscus around the fiber, therefore to eliminate any errors on L. This test does represent a qualitative evaluation of the interface. However it cannot be considered as a quantitative measurement because of the lack of knowledge of the mechanism occuring at the interface and because of the scatter in the results due to the influence of uncontrolled experimental variables. The alignment between fiber and applied force, the clamping quality of the fiber and matrix, the elasticity of the fiber, the viscoelasticity of the matrix and the fact that the fiber has to be embedded in exact alignment in the matrix, make this test very difficult to perform correctly. Moreover there is no satisfactory answer

to the question: what is measured with this technique? Is it the energy required to initiate or to propagate fiber/matrix debonding, or a combination of the two? It should be noticed that if debonding starts at the fiber end, or at the interface along L, or at the meniscus each represent very different cases. The lack of knowledge of this starting point makes the interpretation of the results very hazardous. Besides, the fiber end geometry has an important influence [59]. Numerous publications deal with the theoretical analysis of this test [33,34,60-63].

2. Indirect evaluation of the interphase

- Short beam shear test (Three point bending). This test is standardized: ASTM D 2344-76 or NFT 57-104. On account of the shear failure of the samples, the interface properties are very important in the failure process. However this experiment can only be considered as qualitative, the value of the apparent horizontal shear strength should not be used for design purposes [64]. This is a very common test used in industry, this is the reason why it has been chosen for part of the experiments in this thesis.

- Traction on an off-axis unidirectional sample [65].

- Double cantilever beam cleavage test [66]. This test permits the measurement of energy of failure and how it is influenced by the nature of the interface.

- Charpy impact test [65]. It shows the influence of the interface on the impact strength of a composite.

- Viscoelastic tests [66]. Creep and relaxation experiments are performed on spherical filler reinforced composites for different surface treatments on the spheres.

DEFINITION OF THE PROBLEM : MOTIVE OF THE RESEARCH

At this point, one should notice that the tests used for a direct evaluation of the interphase are performed on single fiber specimens, inspite of the fact that practical fibrous composites contain a large number of fibers. This contradiction does not seem to have induced concern among researchers in the past. However even with single fiber tests, the practical purpose of all studies of this interphase is the improvement, prediction and control of composite properties. Therefore, this leads to two key questions, the answers to which will improve to a large extent the understanding of the role of the interphase in composites.

1. What is the influence of adjacent fibers on the interphase around a particular fiber?

2. Are the values of interfacial shear strength obtained with single fiber tests valid for commercial composites?

Now we shall emphasize the influence of other fibers. This influence can be of two kinds: Mechanical, Physicochemical.

- Mechanical influence: The proximity of fiber breaks around a certain one will induce stress concentrations

and therefore have a great infuence on the stress transfer as one can see on Figure 1 and as it has been shown in [46,47,48]. Besides, adjacent fibers will imply a mechanical constraint in a region around the fiber and therefore change the mechanical behavior of the surrounding matrix. Moreover, other fibers through the volume fraction (0.6-0.7 for usual industrial composites) may also invert the phenomena which would occur in a single fiber sample due to differential thermal expansion and poisson coefficient, i.e. the shrinkage of the matrix on the fiber creating a normal stress component. This is shown in Figure 2.

- Physicochemical influence: A high volume fraction of fibers may modify the interphase during the curing process because of potential catalytic effects of the glass or coating layer (e.g. silane) on chemical reactions. Examples of this very important factor have already been reported [67,68].

Faced with the lack of studies about the interphase taking into account the influence of other fibers, it has been considered of interest to define a research based on such an approach of the interphase.

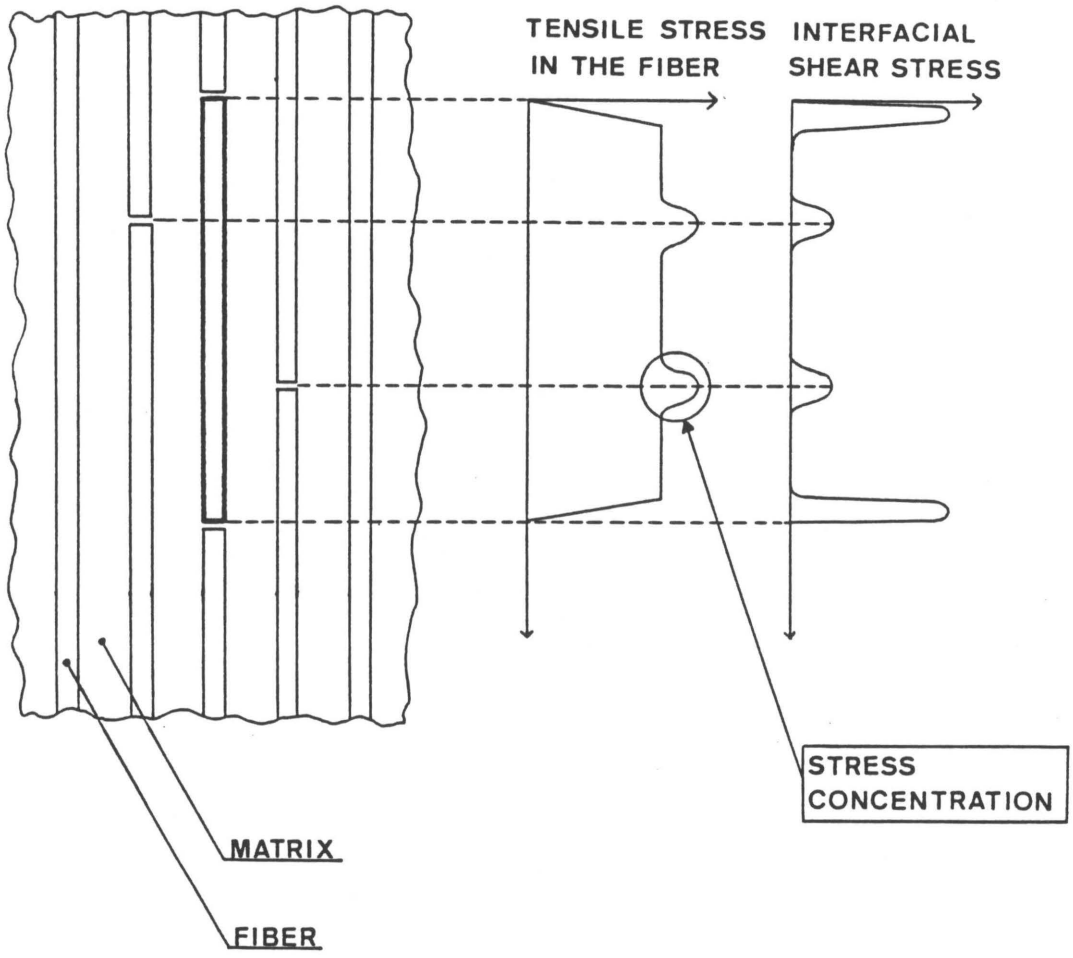

Figure 1. Stress concentration due to fiber breaks: influence on the fiber tensile stress and interfacial shear stress.

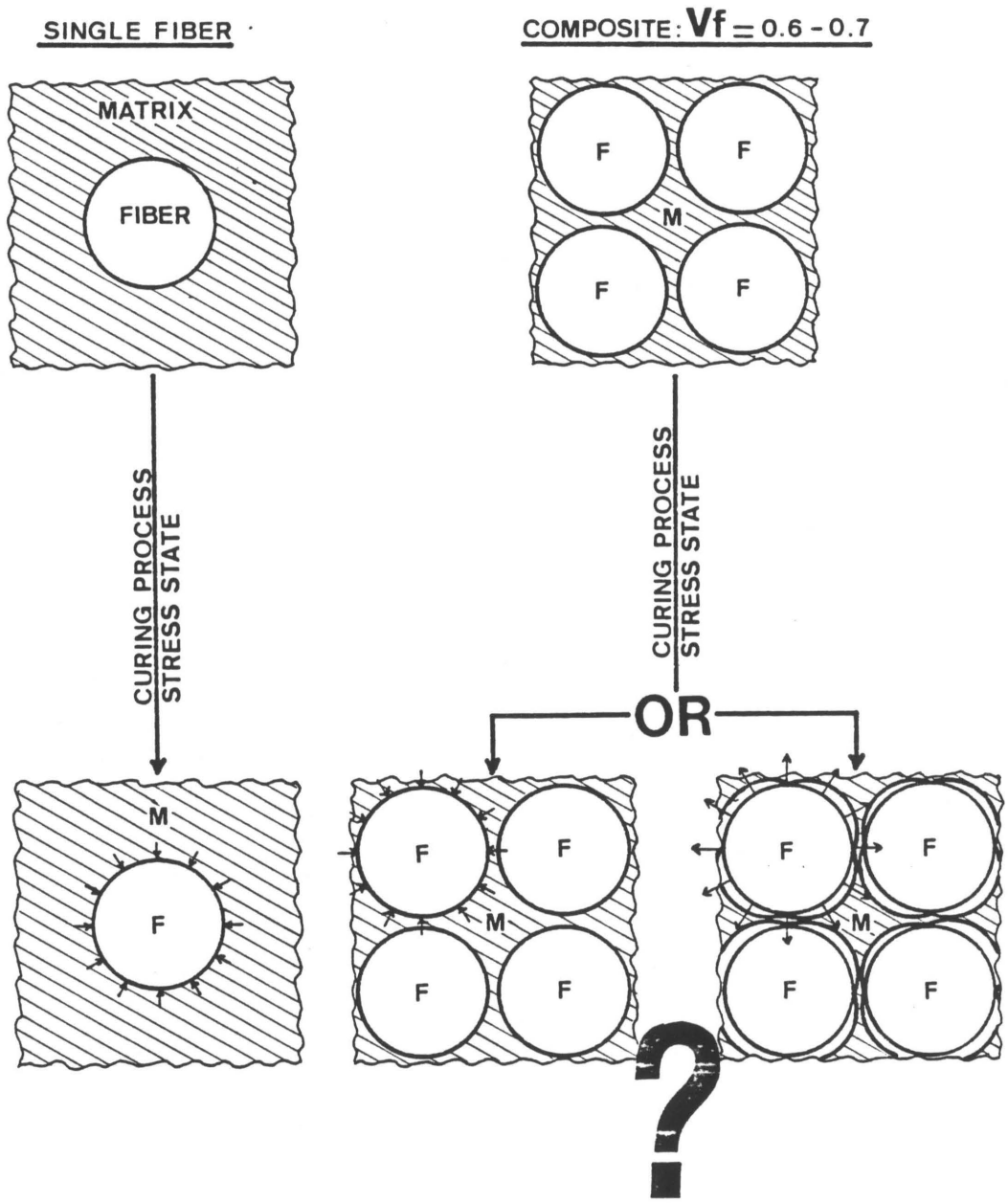

Figure 2. Differential thermal expension and Poisson's ratio: the difference of fiber volume fraction between a single fiber sample and a composite may invert the effect of the shrinkage of the matrix.

RESEARCH PROJECT

OBJECTIVES

The overall objective of this research is to obtain new insights about the role of the interphase in commercial fiber reinforced composites.

In order to achieve this goal, theoretical and experimental approaches will be used as follows:

- I. Develop a mechanical model including the notion of interphase in order to:

    A. Evaluate the influence of properties of the constituents in a composite on the interfacial shear strength.

    B. Improve the understanding of the stress transfer between fiber and matrix.

    C. Analyse the experimental procedures and results of this thesis and try to make predictions.

- II. Use a statistical model to:

A. Complete the analysis of the model with an interphase.

B. Calculate the interfacial shear strength from the experimental results.

- III. Observe and analyse the influence of different interphases and fiber treatments on the critical fiber length test and on the three point bending test.

- IV. Develop a new method for the evaluation of the fiber-matrix adhesion based on the applications of polarized light.

- V. Correlate results from embedded single filament tensile test with results from three point bending tests on unidirectional composites.

- VI. Analyse surfaces and interphases using ESCA, SIMS and SEM in order to:

A. Correlate properties with structure and bonding before and after fabrication.

B. Determine fracture modes and locus of failure.

MECHANICAL ANALYSIS OF THE INTERPHASE

Introduction

Faced with the lack of mechanical models including the notion of interphase, it was decided to develop such a model. With it and the use of a statistical model to analyse and predict the experimental results in this thesis, we will intend to improve the understanding of the interphase. Comparisons will be made with theoretical approaches and experimental results given in the literature.

Development of a model with an interphase

A model with an interphase is developed here using Rosen's approach [36] and introducing an interlayer between fiber and matrix called interphase. Its diagram is presented in Figure 3. The assumptions of this model are:

1. The fibers carry only tensile loads and normal stresses.

2. The interphase carries part of the tensile load of the fiber and part of the shear stress of the matrix: $\sigma i(x,y) = \alpha(x,y).\sigma f(x)$ and $\tau i(x,y) = \beta(x,y).\tau m(x)$.

3. The matrix carries only shear stress.

4. The average material carries only tensile loads.

5. Shear transfer is limited to the matrix-interphase region.

6. The bonds between fiber-interphase, interphase-matrix and matrix-average material are perfect.

The additional assumptions compared to Rosen's model are due to the interlayer and to the concept of gradient behavior assumption (no 2). The interphase is supposed to match the properties of the fiber with those of the matrix.This assumption may not be verified in a real composite.

For a first approach one considers:

$\alpha(x,y) = \alpha,\ \beta(x,y) = \beta \quad (\alpha,\beta) \in RxR$

Notations:

$\sigma i(x) = \sigma i,\ \tau i(x) = \tau i,\ \sigma f(x) = \sigma f,\ \tau m(x) = \tau m,\ \sigma a(x) = \sigma a.$

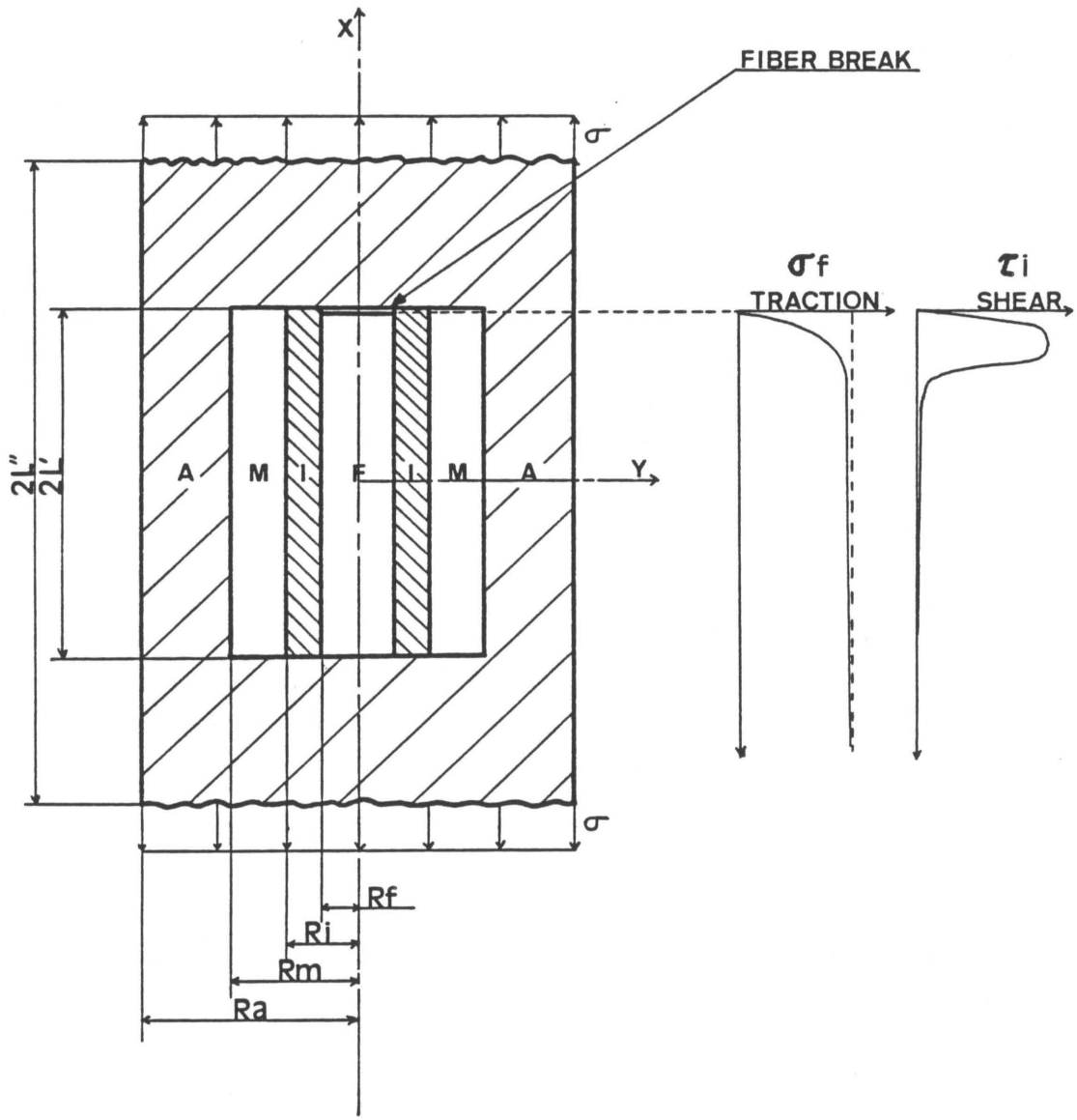

Figure 3. Diagram of the model with interphase

Calculation of the ineffective length

Equilibrium of the fiber:

$$2\pi\ Rf\ \tau i(x,Rf) + \pi\ Rf \frac{d\sigma f(x)}{dx} = 0 \tag{1}$$

Equilibrium of the interphase:

$$-2\pi\ Rf\ \tau i(x,Rf) + \pi\ (Ri^2-Rf^2) \frac{d\sigma i(x)}{dx} + 2\pi\ Ri\ \tau m(x) = 0 \tag{2}$$

Equilibrium of the composite:

$$\pi\ Rf^2\ \sigma f(x) + \pi\ (Ri^2-Rf^2)\ \sigma i(x) + \pi\ (Ra^2-Rm^2)\ \sigma a(x) = \pi\ Ra^2\ \tau \tag{3}$$

Kinematics Figure 4:

$$\gamma m = \frac{Ua - U}{Rm - Ri} \tag{4}$$

$$\gamma i = \frac{U - Uf}{Ri - Rf} \tag{5}$$

Perfect bonding between fiber and interphase is assumed, thus this leads to:

$$U = Ua - \gamma m\ (Rm-Ri) = Uf + \gamma i\ (Ri-Rf) = Ui + \gamma i\ (Ri-Rf)/2 \tag{6}$$

Inserting (5) into (4), differentiating twice and using the stress-strain relation yield:

$$\frac{Rm-Ri}{Gm} \frac{d^2\tau m}{dx^2} = 1/Ea \frac{d\sigma a}{dx} - 1/Ef \frac{d\sigma f}{dx} - \frac{Ri-Rf}{Gi} \frac{d^2\tau i}{dx^2} \tag{7}$$

where:

Ea = effective Young's modulus of the average material

Ef = effective Young's modulus of the fiber

Ei = effective Young's modulus of the interphase

Gi = shear modulus of the interphase

Gm = shear modulus of the matrix

Differentiating equation (3) yields:

$$Rf^2 \frac{d\sigma f}{dx} + (Ri^2-Rf^2) \frac{d\sigma i}{dx} = - (Ra^2-Rm^2) \frac{d\sigma a}{dx} \quad (8)$$

Equation (1) leads to:

$$\frac{d\sigma f}{dx} = - 2/Rf\ \tau i \quad (9)$$

Inserting (9) into (8):

$$- 2\ Rf\ \tau i + (Ri^2-Rf^2) \frac{d\sigma i}{dx} = - (Ra^2-Rm^2) \frac{d\sigma a}{dx} \quad (10)$$

Inserting (9) and (10) into (7) one obtains:

$$\frac{Rm-Ri}{Gm} \frac{d^2\tau m}{dx^2} + \frac{Ri-Rf}{Gi} \frac{d^2\tau i}{dx^2} = \left(\frac{2\ Rf}{Ea\ (Ra^2-Rm^2)} + \frac{2}{Ef\ Rf}\right) \tau i - \frac{(Ri^2-Rf^2)}{Ea\ (Ra^2-Rm^2)} \frac{d\sigma i}{dx} \quad (11)$$

Equation (2) leads to:

$$\frac{d\sigma i}{dx} = \frac{2\ Rf}{(Ri^2-Rf^2)} \tau i - \frac{2\ Ri}{(Ri^2-Rf^2)} \tau m \quad (12)$$

(12) into (11):

$$\frac{Rm-Ri}{Gm}\frac{d^2\tau m}{dx^2} + \frac{Ri-Rf}{Gi}\frac{d^2\tau i}{dx^2} - \frac{2}{Ef\ Rf}\tau i - \frac{2\ Ri}{Ea\ (Ra^2-Rm^2)}\tau m = 0 \qquad (13)$$

Recalling: $\tau i = \beta\ \tau m$ yields:

$$\frac{d^2\tau m}{dx^2} - \eta^2\ \tau m = 0 \qquad (14)$$

where

$$\eta^2 = \frac{2\ Ri/(Ea\ (Ra^2-Rm^2))\ 2\ \beta/(Ef\ Rf)}{(Rm-Ri)/Gm + \beta\ (Ri-Rf)/Gi} \qquad (15)$$

The solution to equation (14) is of the form:

$$\tau m = A\ \sinh(\eta x) + B\ \cosh(\eta x)$$

The boundary conditions are: $\tau m(0) = 0$, $\sigma f(L') = 0$

(1) and the 2nd boundary condition imply:

$$\tau m = A\ \sinh(\eta x) \qquad (16)$$

$$\sigma f = \frac{2\ \beta\ A}{Rf\ \eta}\ (\cosh(\eta L') - \cosh(\eta x)) \qquad (17)$$

(7) yields:

$$\left(\frac{Rm-Ri}{Gm} + \beta\ \frac{Ri-Rf}{Gi}\right)\frac{d\tau m}{dx} = \frac{\sigma a}{Ea} - \frac{\sigma f}{Ef} \qquad (18)$$

Evaluating (18) and (3) at $x=L'$ leads to:

$$\left(\frac{Rm-Ri}{Gm} + \beta\ \frac{Ri-Rf}{Gi}\right)\ A\ \eta\ \cosh(\eta L') = 1/Ea\ \sigma a(L') \qquad (19)$$

$$\sigma a(L') = \frac{Ra^2}{Ra^2-Rm^2}\ \sigma \qquad (20)$$

Therefore:

$$A = \frac{Ra^2\ \sigma}{Ea\ (Ra^2-Rm^2)}\ \frac{1}{\eta\ \cosh(\eta L')\ ([Rm-Ri]/Gm + \beta\ [Ri-Rf]/Gi} \tag{21}$$

and

$$\sigma f = \mu\ (1 - \frac{\cosh(\eta x)}{\cosh(\eta L')}) \tag{22}$$

with

$$\mu = \frac{2\ \beta\ Ra^2\ \sigma}{Rf\ Ea\ (Ra^2-Rm^2)}\ \frac{1}{2\ Ri/(Ea\ [Ra^2-Rm^2] + 2\ \beta/(Ef\ Rf)} \tag{23}$$

and

$$\tau m = \frac{Ra^2\ \sigma}{Ea\ (Ra^2-Rm^2)}\ \frac{1}{([Rm-Ri]/Gm + \beta\ [Ri-Rf]/Gi)}\ \frac{\sinh(\eta x)}{\eta\ \cosh(\eta L')} \tag{24}$$

At mid point of a fiber of length $2L'$:

$$\sigma fo = \mu\ \frac{\cosh(\eta L') - 1}{\cosh(\eta L')}$$

Consider c the coefficient of stress concentration due to breaks in adjacent fibers and ϕ such that:

$$\phi = \frac{\sigma f(L'-\delta)}{c\ \sigma fo} = \frac{\cosh(\eta L')}{c\ (\cosh(\eta L') - 1)}\ (1 - \cosh(\eta\delta) + \tanh(\eta L')\ \sinh(\eta\delta))$$

It can be shown that for L' of the order of milimeters or more:

$\tanh\eta L' \# 1$ and $\cosh\eta L' >> 1$

Therefore one can define the "ineffective length":

$$\delta = 1/\eta\ \cosh^{1}(\frac{1 + (1 - c\ \phi)^2}{2\ (1 - c\ \phi)}) \tag{25}$$

This is the distance at the end of the fiber where the tensile stress is lower than the one at a point far enough from a fiber break. Therefore the chance of fiber breakage within the "ineffective length" is very small; the fiber will more probably break in its central part. It can be noticed that as soon as the choice of ϕ is made, the ineffective length depends only on material properties. Consequently the fiber should not be able to break into fragments smaller than δ. Two times the ineffective length is, thus, the critical fiber length mentioned in the literature review.

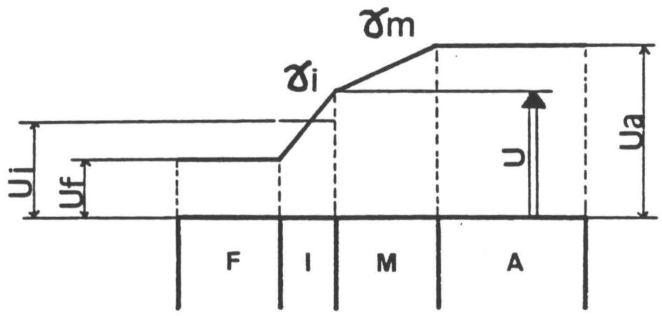

Figure 4. Kinematics of the model with interphase

Calculation of α/Ei

Recalling equation (6) and Figure 4:

$$Ui - Uf = \gamma i \, (Ri-Rf)/2$$

Therefore:

$$(\alpha/Ei - 1/Ef) \frac{d\sigma f}{dx} = \frac{Ri-Rf}{2\,Gi} \beta \frac{d^2\tau m}{dx^2}$$

Thus, with (1):

$$\alpha/Ei = 1/Ef - \frac{Rf\,(Ri-Rf)}{4\,Gi} \eta^2 \qquad (26)$$

Relation between α and β

Equation (2) leads to:

$$-2\,Rf\,\beta\,\tau m + (Ri^2-Rf^2)\,\alpha \frac{d\sigma f}{dx} + 2\,Ri\,\tau m = 0 \qquad (27)$$

Recalling (17) and differentiating:

$$\frac{d\sigma f}{dx} = - \frac{2\,\beta\,A}{Rf} \sinh(\eta x) \qquad (28)$$

Inserting (28)into (27):

$$\alpha = \frac{Ri - \beta\,Rf}{Ri^2 - Rf^2} \frac{Rf}{\beta} \qquad (29)$$

Evaluation of the data for this model

Two cases will be considered here:

1. A sample containing a single filament.

2. A fiber reinforced composite with a volume fraction of fiber: Vf = 0.6

In both cases, the specimens have the geometry described by Figure 5, the matrix is an epoxy resin and fibers are glass fibers.

The matrix is assumed to have a poisson's coefficient of 0.4 and fiber of 0.25. The shear moduli will be calculated with the formula:

$$G = \frac{E}{2\ (1 + \nu)}$$

According to Figure 3 and Figure 5, in order to have a Vf of 0.6 the radius of the matrix must be equal to: Ra = 1.6 mm

Considering the fiber break at the middle of the sample, Figure 5 implies: $L' \leq 25$ mm

Table 1 gives the input data for the model with an interphase. The values taken have been determined during the experiments described later on.

Assumptions:

$$Em \leq Ei \leq Ef,\ Gm \leq Gi \leq Gf$$

Figures 6-18 represent the influence of the variation of the model's parameters.

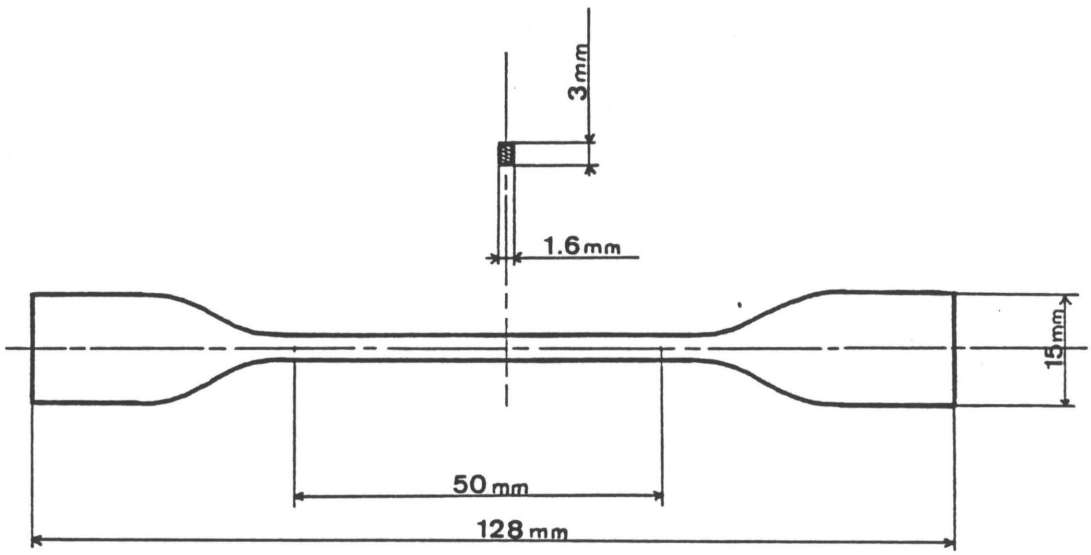

Figure 5. Description of the samples

Table 1. Data for the model with an interphase

case number 1	case number 2
a : bulk epoxy resin m : matrix adjacent to the fiber i : interphase f : fiber	a : average composite m : matrix adjacent to the fiber i : interphase f : fiber
Ef = 65000. MPa Rf = 12. µm Gi = 15000. MPa Ri = 12.01 µm Gm = 964. MPa Rm = 15.49 µm Ea = 2700. MPa Ra = 1.6 mm	Ef = 65000. MPa Rf = 12. µm Gi = 15000. MPa Ri = 12.01 µm Gm = 964. MPa Rm = 15.49 µm Ea = 45000. MPa Ra = 1.6 mm

Results and discussion

From Figures 6 through 16 that follow, it stands to reason that the order of δ obtained with this model (# 80 μm) is lower than the one generally found in the literature [3,8,55,69] (# 300 μm). Figure 6 shows the influence of Ri on δ, using the properties of the fiber and matrix given by [69]. It can be seen that the maximum value of δ one can obtain is 62 μm. However, according to the experimental data of [69], δ should be of the order of 220 μm for good bonding fiber-matrix and 300 μm for poor bonding. Coming back to the values given in the section "Evaluation of the data for this model" Figure 7 implies that in order to have δ equal to 300 μm, β must be equal to 0.1 which means a very weak stress transfer occur between interphase and fiber. However a β of 0.1 is unacceptable because this would imply an α greater than 1 and a Young's modulus for the interphase greater than the fiber (Figure 8,9). The assumptions of perfect fiber-interphase, interphase-matrix and matrix-average material bonding induce a dependence between α, β, Gi and Ei (Figure 4) (equations 26, 29). In fact β has to be less than 0.999 for α to be smaller than 1 (Figure 10). Therefore up to this point one may conclude (1) that the assumption of perfect bonds is probably not met completely in the real world, and

(2) that δ has no simple relation with the critical fiber length. This model is unable to predict the critical fiber length as it is defined in the literature. Future evolutions of this model will have to include the notion of imperfect bonds and variable coefficients $\alpha(x,y)$ and $\beta(x,y)$. Nevertheless, if an elastic zone exits at the end of the fiber as described by Figure 3 or if the shear going beyond the yield point of the matrix implies a plastic zone, one should be able to give with this model an approximation of the magnitude of the ineffective fiber length. Since this ineffective length, δ, is characteristic only of the material properties (Equations 15, 25), the measurement of this length should provide a characterization of the interphase properties. To do that, photoelastic measurements have to be performed around a single fiber. These will be described later in the experimental section.

Despite the overly constraining assumption (perfect bonds), it was possible to observe the influence of different parameters.

Figures 11,12,13 express the influence of Ri on δ, α and Ei. One can notice the great influence of Ri on δ and on Ei for Ri greater than 14.5 μm. This means that the modification of the matrix properties in the close neighborhood of a fiber

due to other fibers may imply a δ for a composite two times smaller than for a single fiber sample.

According to Figure 14, Gi seems to have a negligible effect on δ if Ri is small. Its influence becomes somewhat larger with increasing Ri. However it should be remembered at this stage that perfect fiber-interphase bonding and gradient behavior for the interphase have been assumed. Therefore if the interphase constitutes a weak boundary layer, this model will not take that fact into account and thus Gi may have a much more important effect on δ than shown by Figure 14.

On the other hand Figure 15 reveals the great influence of Gm on the ineffective length. This is a very important parameter and its influence will be emphasized in the experimental section.

Finally, Figure 16 shows the negligible effect of Ea on δ. According to this model, the average material influences the ineffective length only through the coefficient c (stress concentration due to adjacent fiber breaks) and through the values of Gi and Gm which may be affected by the nature of this material.

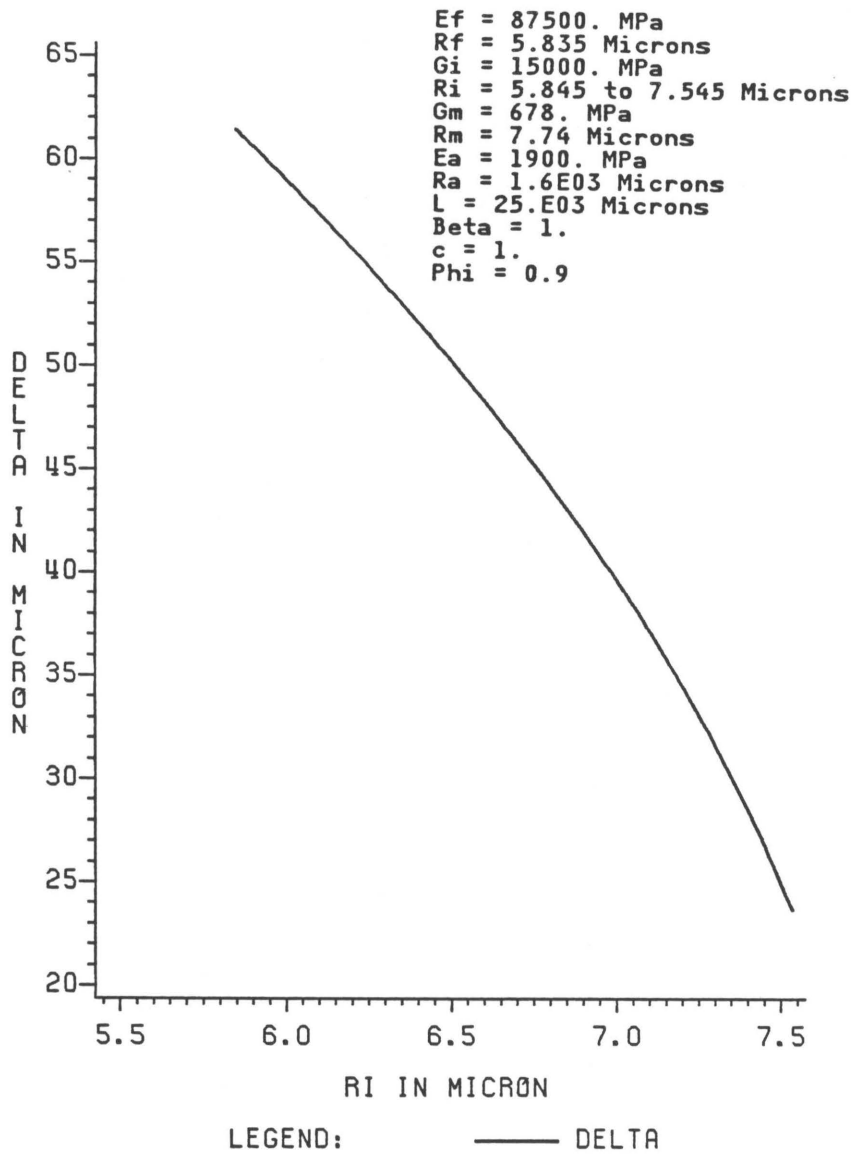

Figure 6. Model with an interphase: Comparison with [69].

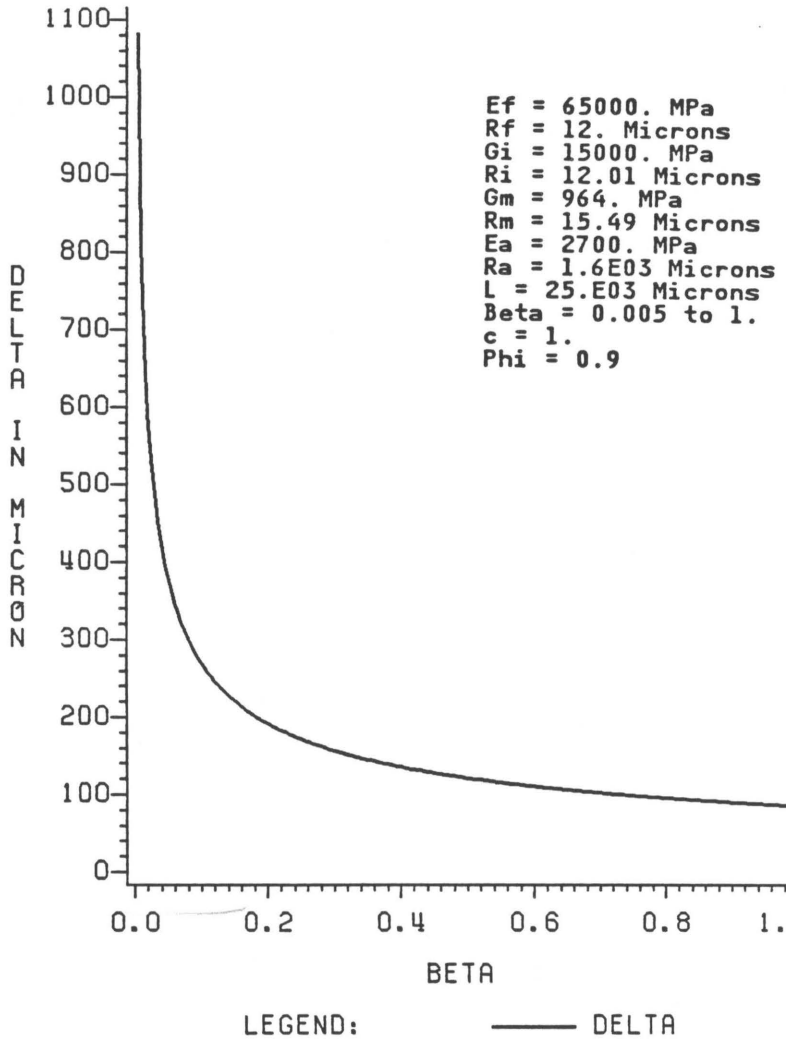

Figure 7. Model with an interphase: Influence of Beta on the ineffective length.

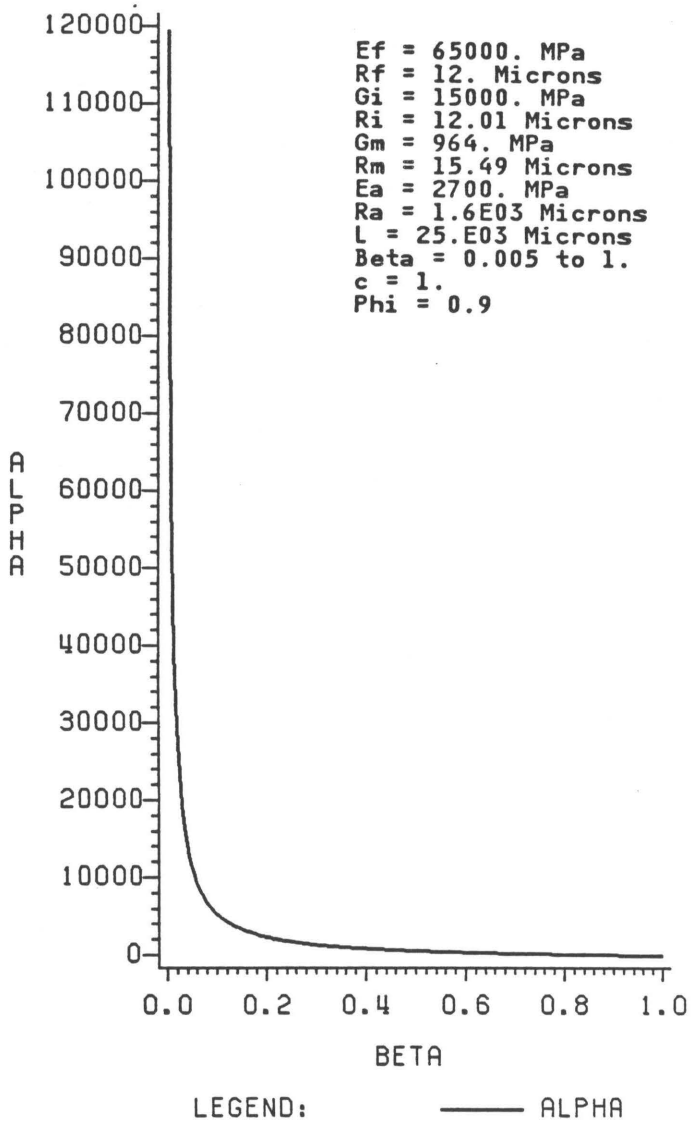

Figure 8. Model with an interphase: Influence of Beta on Alpha.

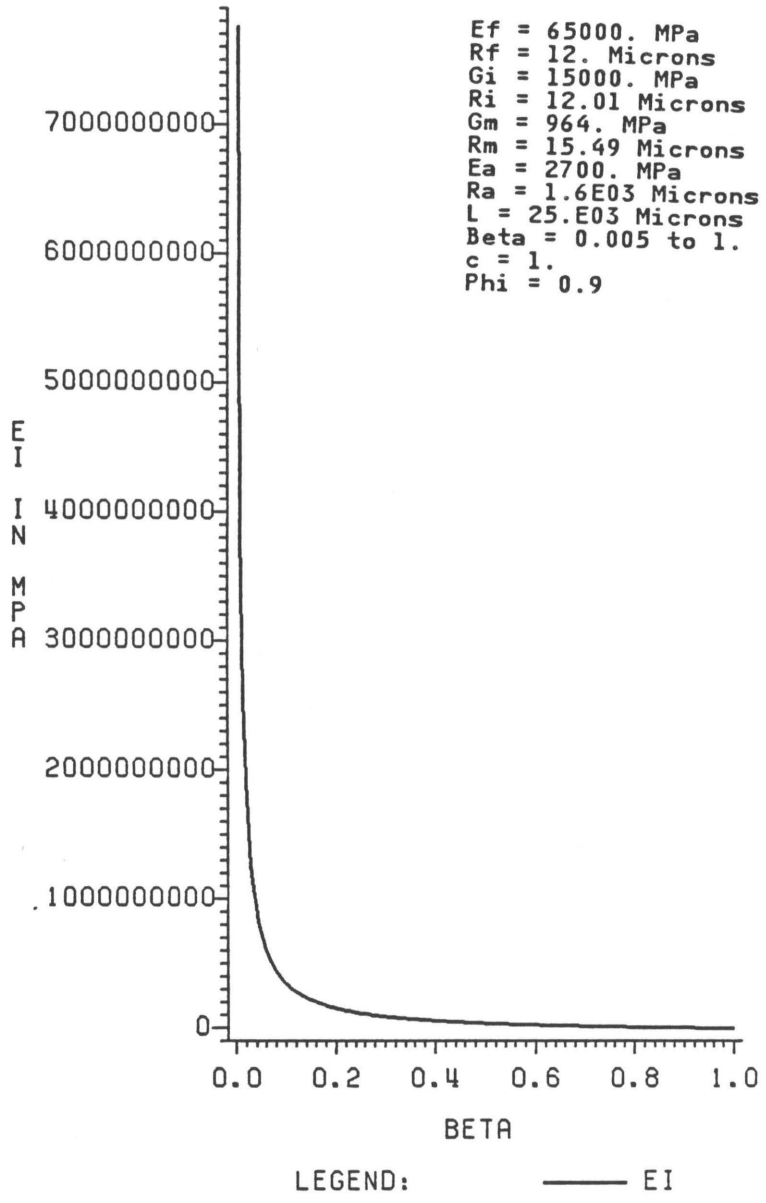

Figure 9. Model with an interphase: Influence of Beta on the Young's modulus of the interphase.

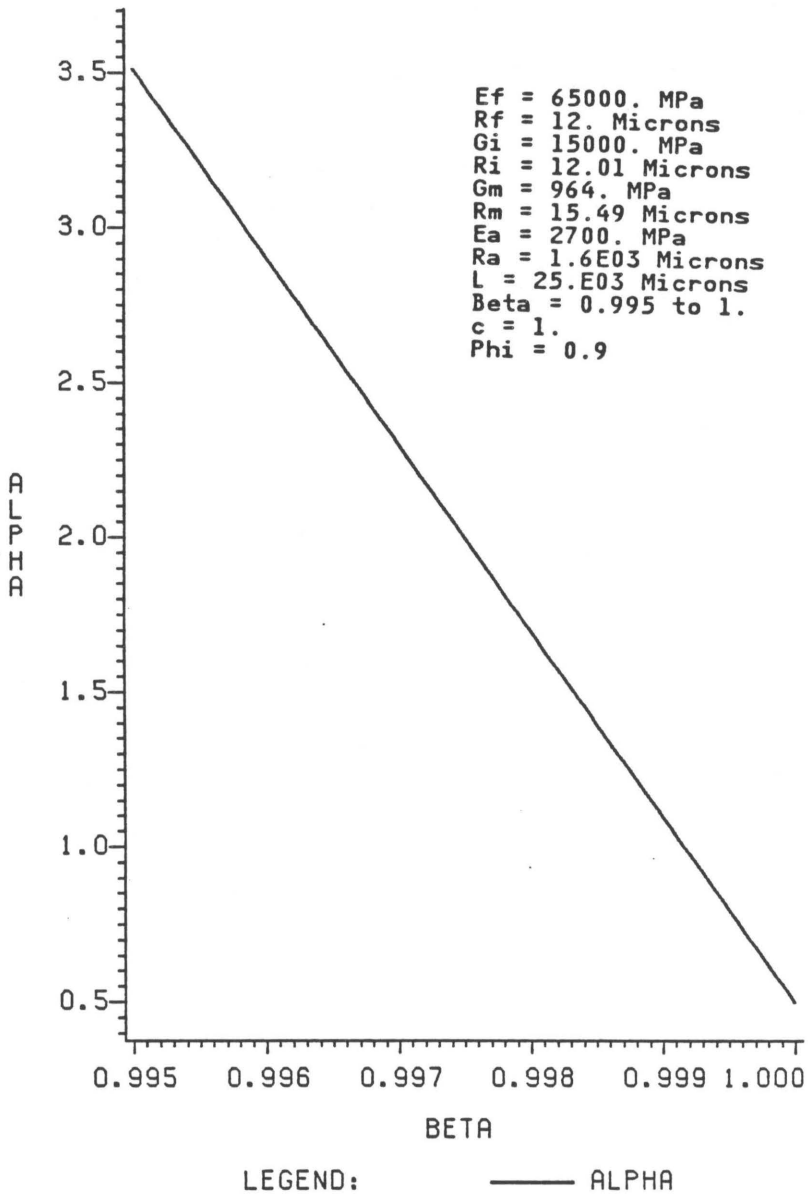

Figure 10. Model with an interphase: Influence of Beta on Alpha for Beta close to 1.

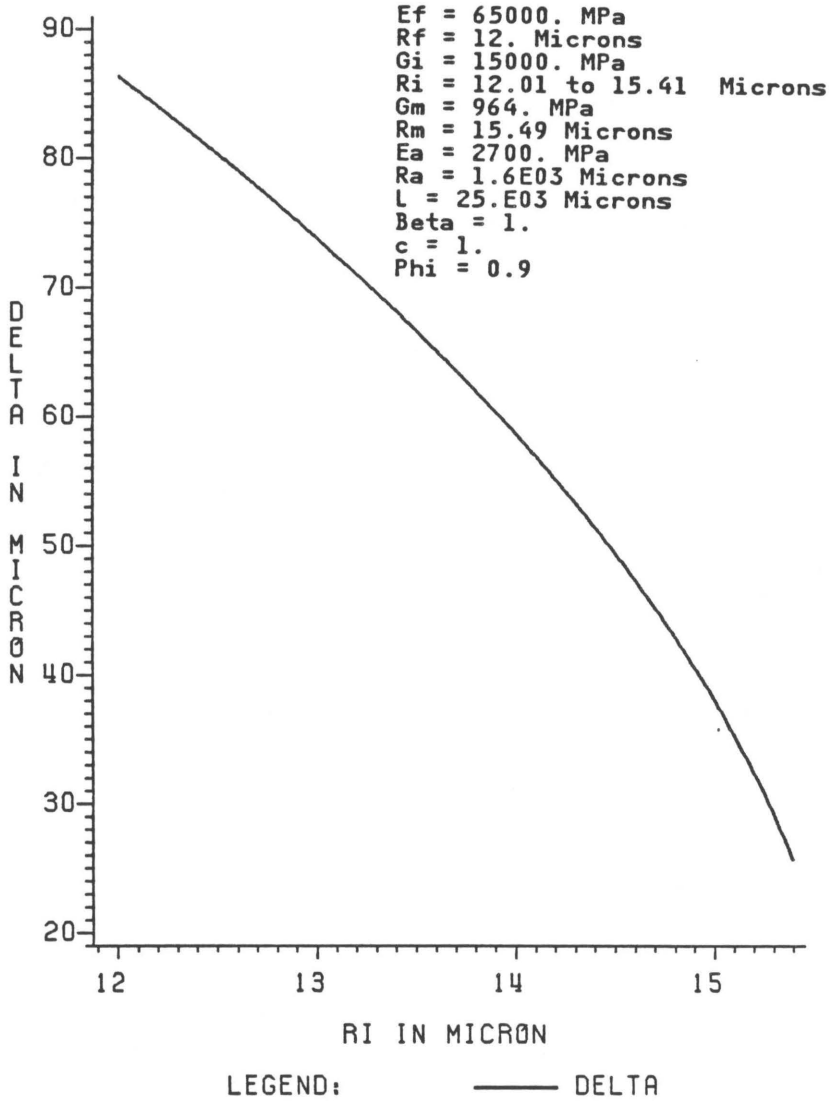

Figure 11. Model with an interphase: Influence of Ri on the ineffective length.

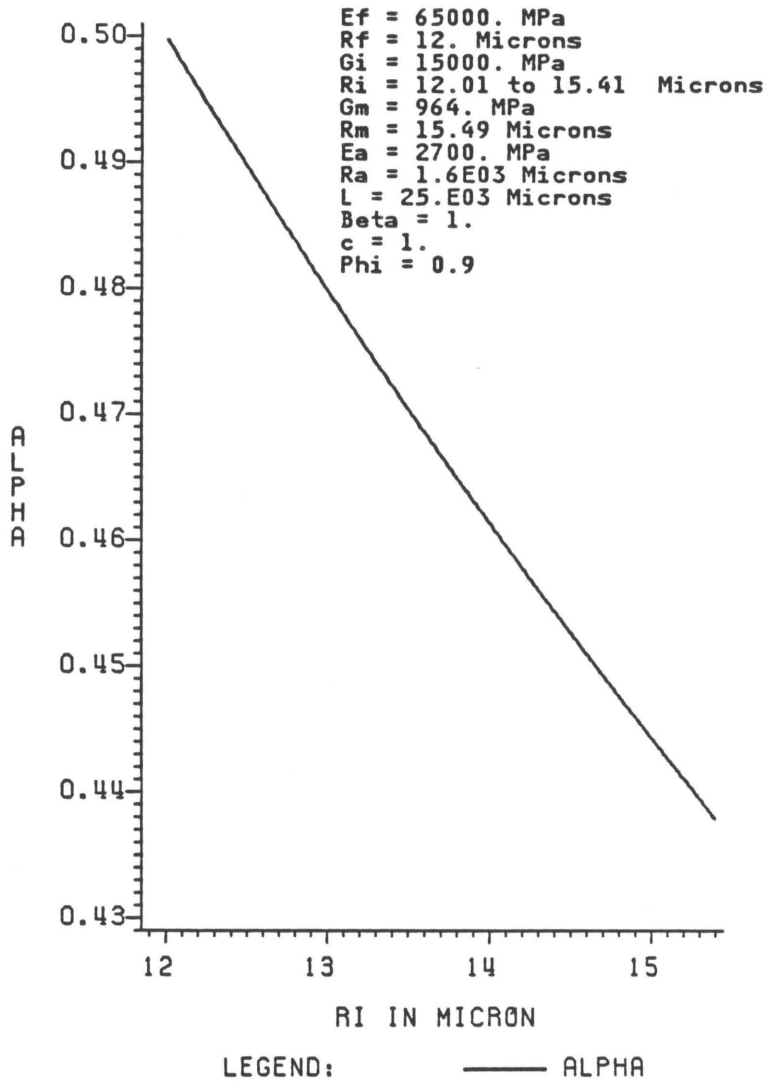

Figure 12. Model with an interphase: Influence of Ri on Alpha.

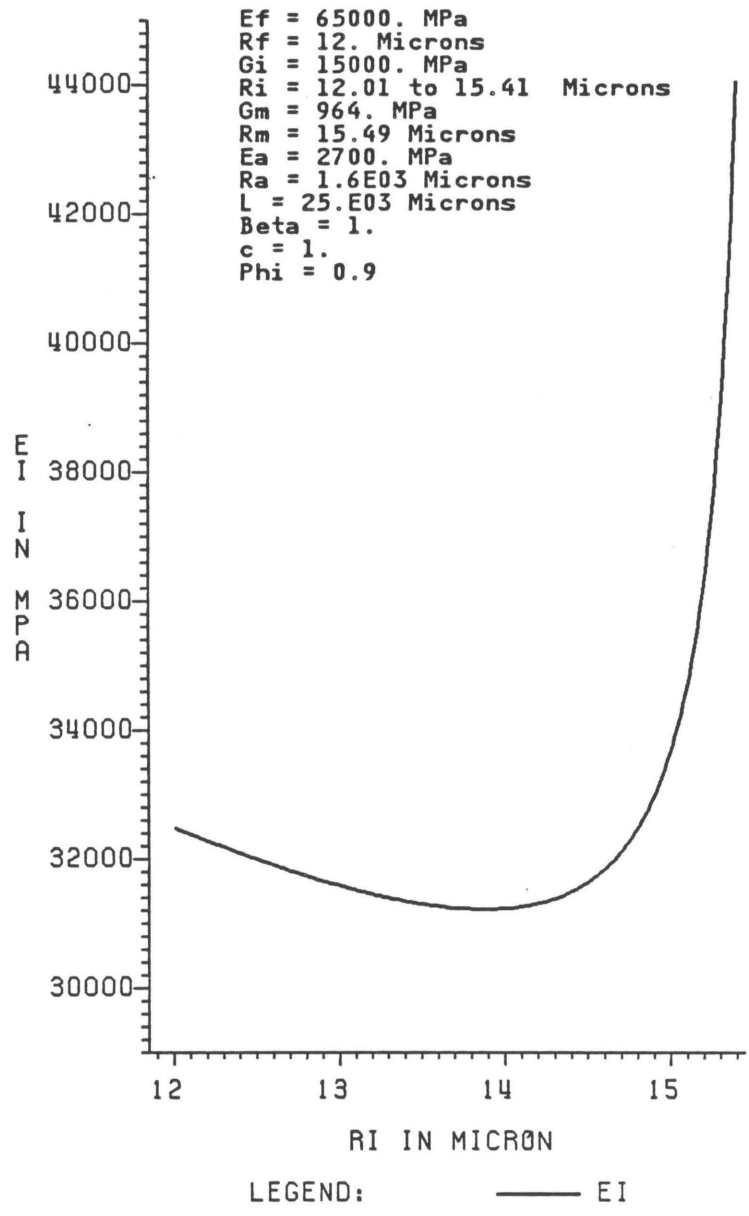

Figure 13. Model with an interphase: Influence of Ri on the Young's modulus of the interphase.

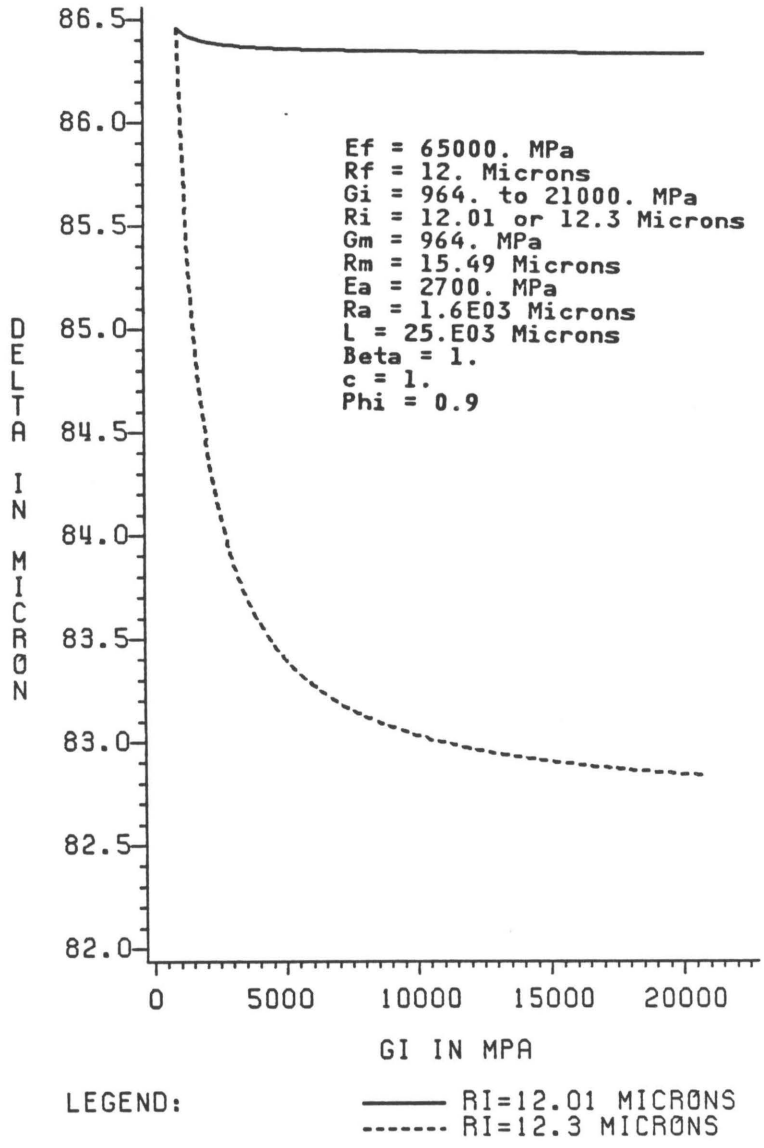

Figure 14. Model with an interphase: Influence of the shear modulus of the interphase on the ineffective length.

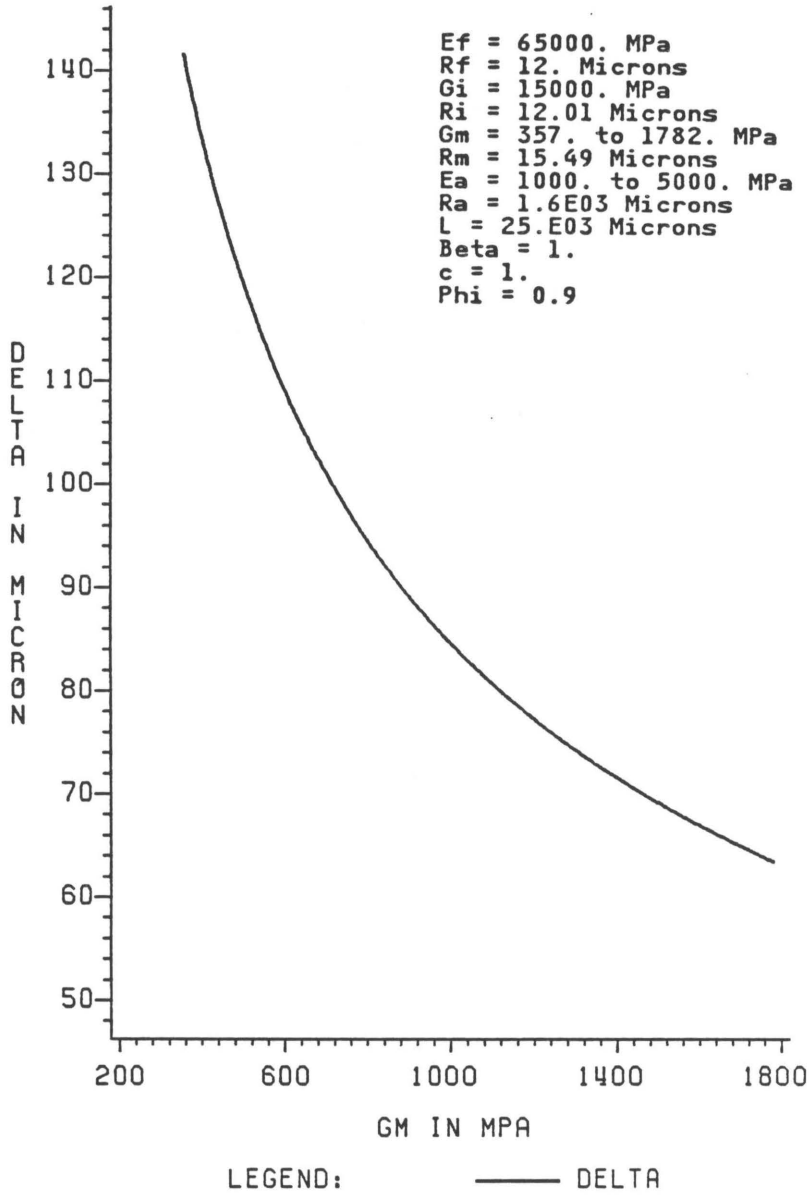

Figure 15. Model with an interphase: Influence of the shear modulus of the matrix on the ineffective length.

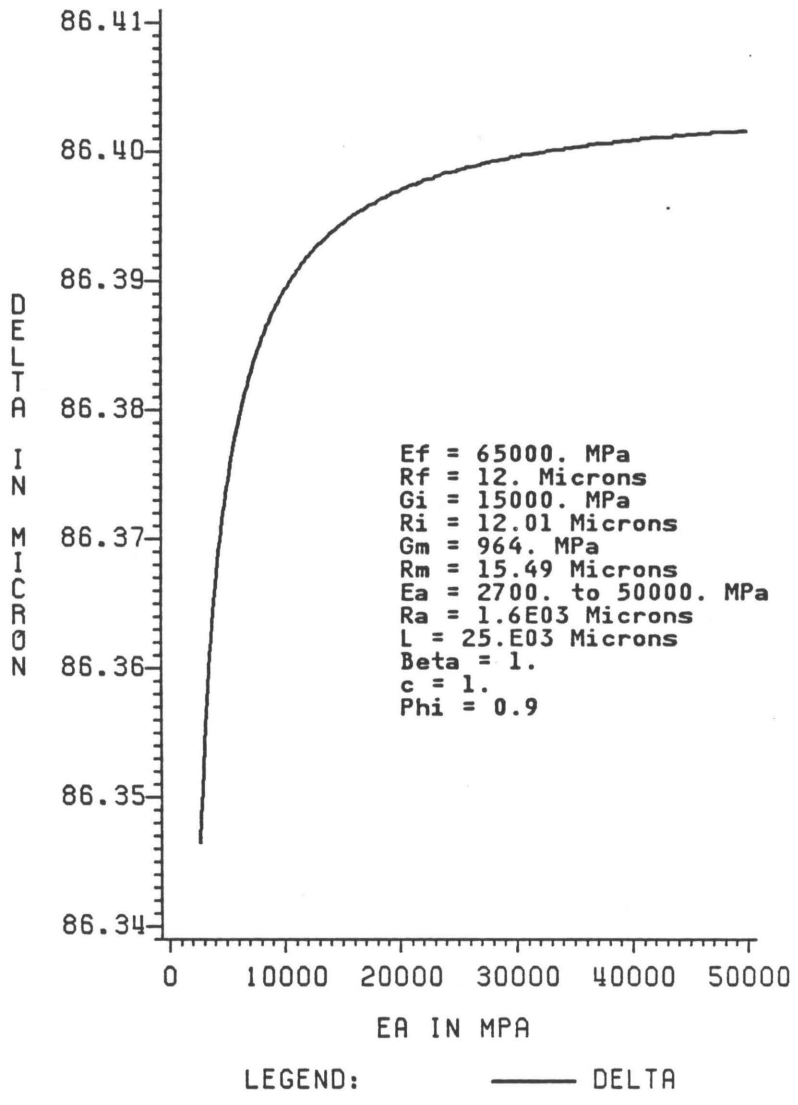

Figure 16. Model with an interphase: Influence of the Young's modulus of the average material on the ineffective length.

Statistical model

Using the formula of the reliability for a fiber proposed by Dr K.L. Reifsnider [70], it is possible to obtain an average of the ineffective length as a function of the interfacial shear strength.

If one considers a fiber of length L and the stress in this fiber to be:

$\sigma(x) = f(x)\ \sigma a$ where $f(L) = 1$ and $f(0) = 0$, σa = applied stress

One can divide the fiber in N segments. Then considering the stress in each part, one can write the probability of the ith segment of length Xi to survive the stress σi to be:

$$[Ro(\sigma i)]^{\Delta Xi}$$

Therefore the probability for the entire fiber surviving is:

$$R = \prod_{i=1}^{N} [Ro(\sigma i)]^{\Delta Xi}$$

Now if one takes the logarithm of this expression and lets:

$$N \rightarrow \infty$$

The reliability of the fiber can be written as:

$$R(\sigma) = \exp\left[\int_0^L \mathrm{Ln}(Ro(\sigma))\, dx \right] \qquad (1)$$

With Ro = Reliability per unit length

Although a bi-linear logarthmic plot has been found [18,37,71] to fit the experimental data for the strength of the fiber as a function of its length, a Weibull distribution has been chosen here, in order to represent the tensile strength of the fiber versus L. The reason for this choice is the good representation of the data with this distribution [8,55], as well as the fact that the smaller slope in the bi-linear logarithmic plot seems due to the clamp effects during testing [72] rather than a "double box" distribution function for the strength-length behavior.

The reliability of a Weibull distribution is given by:

$$Ro(\sigma) = \exp[-(\sigma/\sigma o)^{\alpha'}] \qquad (2)$$

where α' = shape factor and σo = characteristic strength

Hence

$$R = \exp[-(\sigma a/\sigma ao)^{\alpha'}] \qquad (3)$$

with

$$\sigma ao = \sigma o \left[\int_0^L f^{\alpha'}(x)\, dx \right]^{-1/\alpha'}$$

Calculation of the average fiber strength

Taking f(x)=1 and recalling (3):

$$R = \exp[- L (\sigma a/\sigma o)^{\alpha'}] \qquad (4)$$

If the reliability is such that (4), the density function is:

$$f'(\sigma) = \alpha' L \sigma o^{-\alpha'} \sigma a^{\alpha'-1} \exp[- L (\sigma a/\sigma o)^{\alpha'}] \qquad (5)$$

and the mean:

$$\mu = \sigma o \, L^{-1/\alpha'} \Gamma(1 + 1/\alpha') = Xf \qquad (6)$$

Calculation of the ineffective length

If the stress transfer between fiber and matrix is represented by Figure 17, the ineffective length is given by:

$$\delta = \frac{\sigma f^{\infty} Rf}{2 \tau} \qquad (7)$$

It should be noticed that this stress transfer model does not require a specific kind of interface. Therefore it can represent, for instance, the case of a plastic matrix or the case of fiber-matrix friction.

According to Figure 17: $f(x) = \frac{x}{\delta}$ for $x \in [0,\delta]$

Hence

$$R = \exp[-\frac{\delta}{\alpha'+1}(\sigma a/\sigma o)^{\alpha'}] \quad (8)$$

Then similarly to (4) the density function is:

$$f'(\sigma) = \alpha' \frac{\delta}{\alpha'+1} 1/\sigma o^{\alpha'} \sigma a^{\alpha'-1} \exp[-\frac{\delta}{\alpha'+1}(\sigma a/\sigma o)^{\alpha'}] \quad (9)$$

and the mean:

$$\mu = \sigma o (\frac{\delta}{\alpha'+1})^{-1/\alpha'} \Gamma(1 + 1/\alpha') \quad (10)$$

So the average stress that the fiber can carry for a length δ from a break is: μ

In other words μ equals σfmax that the portion $[0,\delta]$ can carry without breaking.

Inserting (10) into (7) one obtains:

$$\delta = [\frac{Rf\ \sigma o}{2\ \tau} \Gamma(1+1/\alpha')]^{\alpha'/(\alpha'+1)} (\alpha'+1)^{1/(\alpha'+1)} \quad (11)$$

or using (6):

$$\delta = [\frac{Rf\ \sigma o}{2\ \tau}]^{\alpha'/(1+\alpha')} [(\alpha'+1)\ L]^{1/(\alpha'+1)} \quad (12)$$

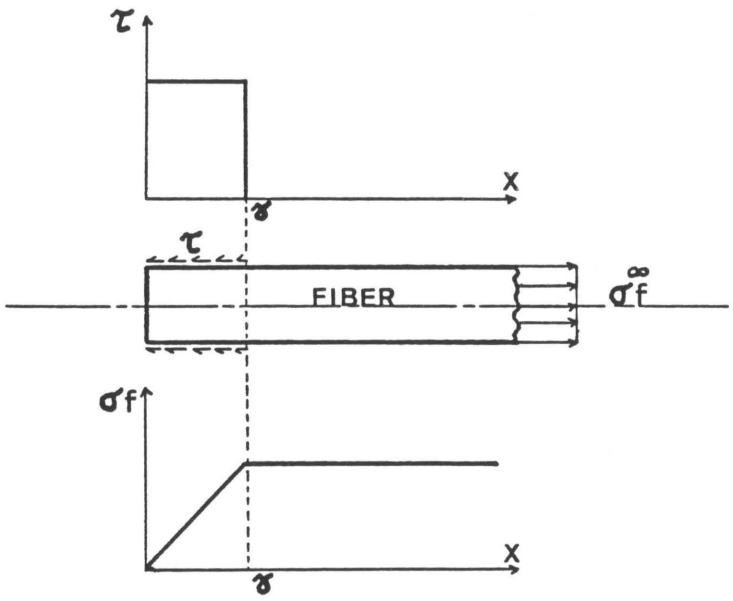

Figure 17. Statistical model: Stress transfer fiber / matrix.

Determination of α' and σo

From equation (6):

$$\text{Log}(Xf) = \text{Log}(\sigma o) - 1/\alpha' \text{Log}(L) + \text{Log}(\Gamma(1+1/\alpha'))$$

So:

$$\text{Log}(Xf) = -1/\alpha' \text{Log}(L) + \text{Log}(\sigma o) + \text{Log}(\Gamma(1+1/\alpha')) \qquad (13)$$

The above equation is the equation of a straight line. Therefore, to determine the shape factor and the characteristic strength for a particular fiber, a tensile test has to be performed for at least two gage lengths.

This test has been done for three gage lengths on glass fiber coated with surface treatments used later on in this research. Results are given in Table 2.

Figure 18 implies α' and σo given in Table 3.

The curves of $\delta = f(\tau)$ are plotted in Figures 19,20 and 21.

Table 2. Strength of the fibers.

Gage length in mm		78.	30.	10.
No treatment	Xf in MPa	737.	867.	1301.
A174 (*)	Xf in MPa	954.	1301.	1691.
A1100 (**)	Xf in MPa	2038.	2754.	3122.

(*) A174: γMPS (**) A1100: γAPS

Table 3. α' and σ_o for each treatment.

Treatment	α'	σo (MPa)
None	3.59	2628.7
A174	3.54	3622.9
A1100	5.	5515.6

Results and discussion

It should be noticed that the formlation for this model is different from what is generaly used in the literature [8,36,54,55]. This difference comes from the term $(\alpha'+1)^{1/(\alpha'+1)}$. in equation (12). Most of the researchers do not take into account the variable tensile sress at each fiber end when they calculate the average strength of the segment $[0,\delta]$. In fact they take $f(x)=1$ and obtain a similar equation to (6) instead of (10) by replacing L with δ. This implies a δ 1.4 times smaller than the one found with equation (12) and can induce according to Figure 20 very different results in τ for δ less than 0.25 mm.

Figures 19,20,21 indicate that for a very good fiber-matrix adhesion (i.e. τ > 240 MPa) the measurment of δ does not give sensitive evaluation of the interfacial shear strength. A small variation in τ will not be detected.

According to Figure 21 a δ of the order of 0.3-0.4 implies an interfacial shear strength between 70 and 180 MPa which is much higher than shear force due to friction [44] (about 20 MPa for an epoxy resin). One may conclude that friction is not the only mechanism occuring at the interface.

As it has been already said, this model does not make any assumption about the matrix or on the nature of the interface. The only points to be assumed are the stress transfer described by Figure 17 and the kind of reliability for the fiber (Equation (3)). For these reasons, this model seems to be quite realistic and will be applied in order to calculate τ from the measurements of δ.

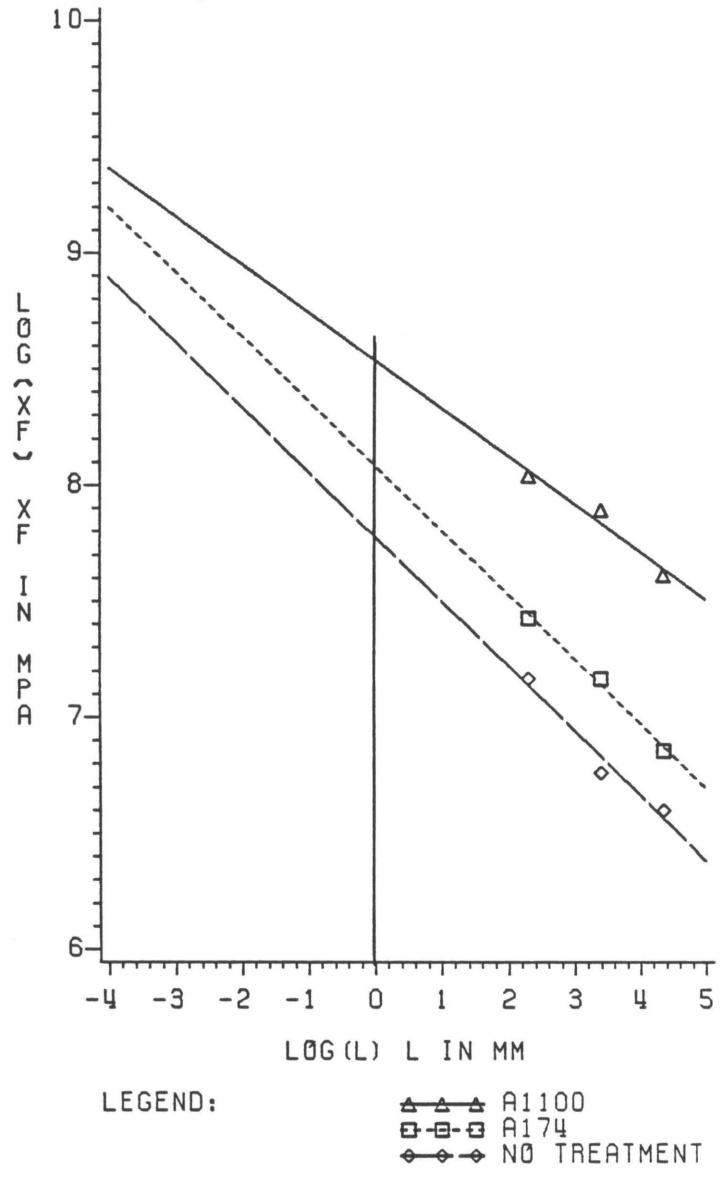

Figure 18. Statistical model: Plot of equation (13).

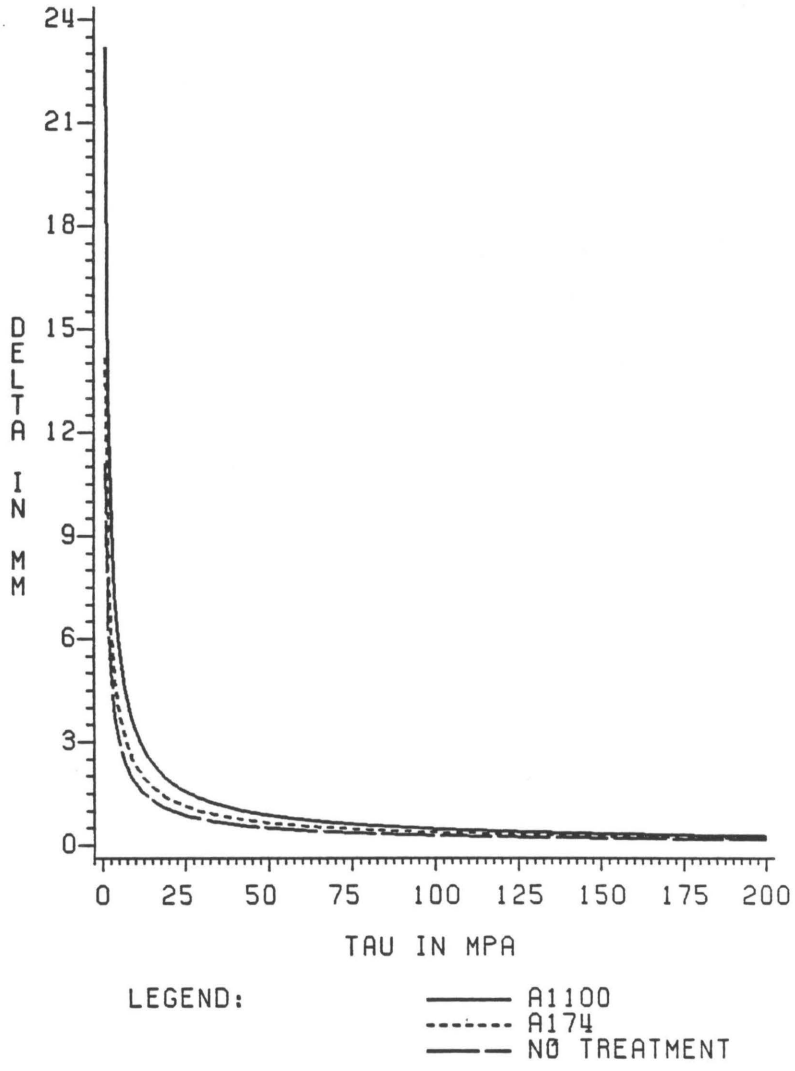

Figure 19. Statistical model: δ function of τ for δ between 0 and 21 mm.

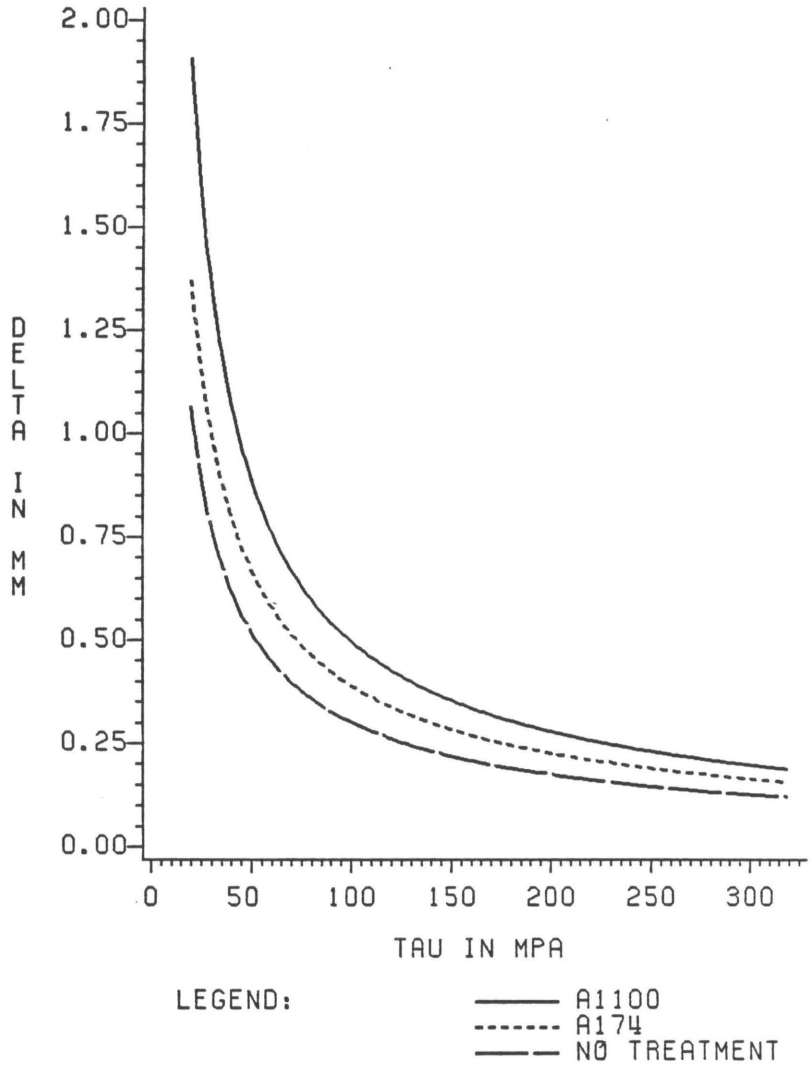

Figure 20. Statistical model: δ function of τ for δ between 0 and 2 mm.

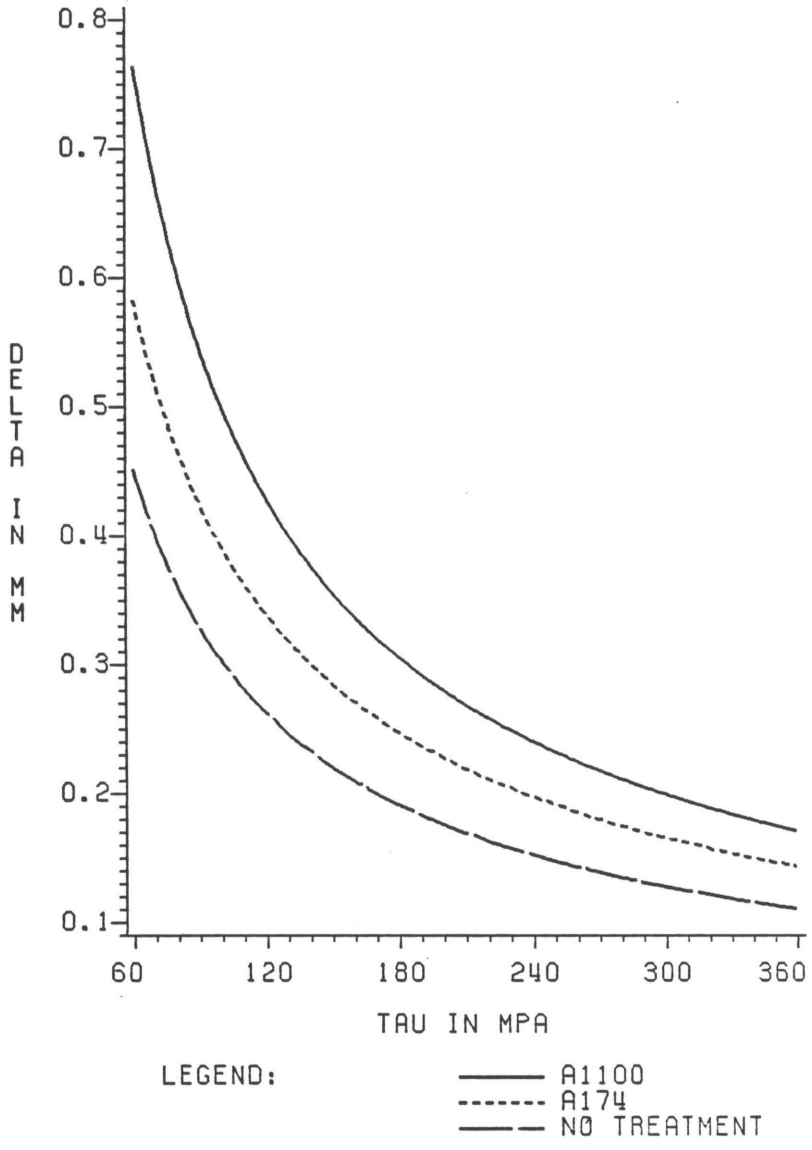

Figure 21. statistical model: δ function of τ for δ between 0 and 0.7 mm.

EXPERIMENTAL PROCEDURES

Constituents of the specimens

Fibers

They are E-glass fibers (24 µm diameter, 24000 tex) produced by Vetrotex Saint-Gobain (France)

Matrices

They are of two kinds, epoxy and polyester. Both are used by the company Vetrotex Saint-Gobain for their industrial quality control tests. Their compositions are given in Table 4 and their cure cycles in Figure 22.

Interphases

For each matrix, four different interphases are investigated in this study and are described in Table 5. It should be noted that each surface treatment has been applied on bare fiber directly. It is not commercial glass fiber where one has removed an initial sizing by boiling or burning before specific

coating application. Therefore that eliminates the possible residual of a previous treatment on the fiber. On the other hand that makes the handling of the fiber more difficult. Thus the presence of flaws due to handling is a parameter to be considered as it will be shown later.

Table 4. Composition of the matrices.

EPOXY		
• CY 205 (ARALDITE F) (Giba Geigy).....	100	parts
• DY 026 (Reactive diluent).....	20	parts
• HT 972 (Hardening agent) (Giba Geigy).....	32.4	parts
POLYESTER		
• STRATYL A 123 (Unsaturated resin) (Rhone Poulenc).....	100	parts
• STRATYL 302 (Unsaturated resin) (Rhone Poulenc).....	20	parts
• Styrene.....	16.4	parts
• TRIGONOX (Hardening catalyst) (Nourylande)..	1.5	parts

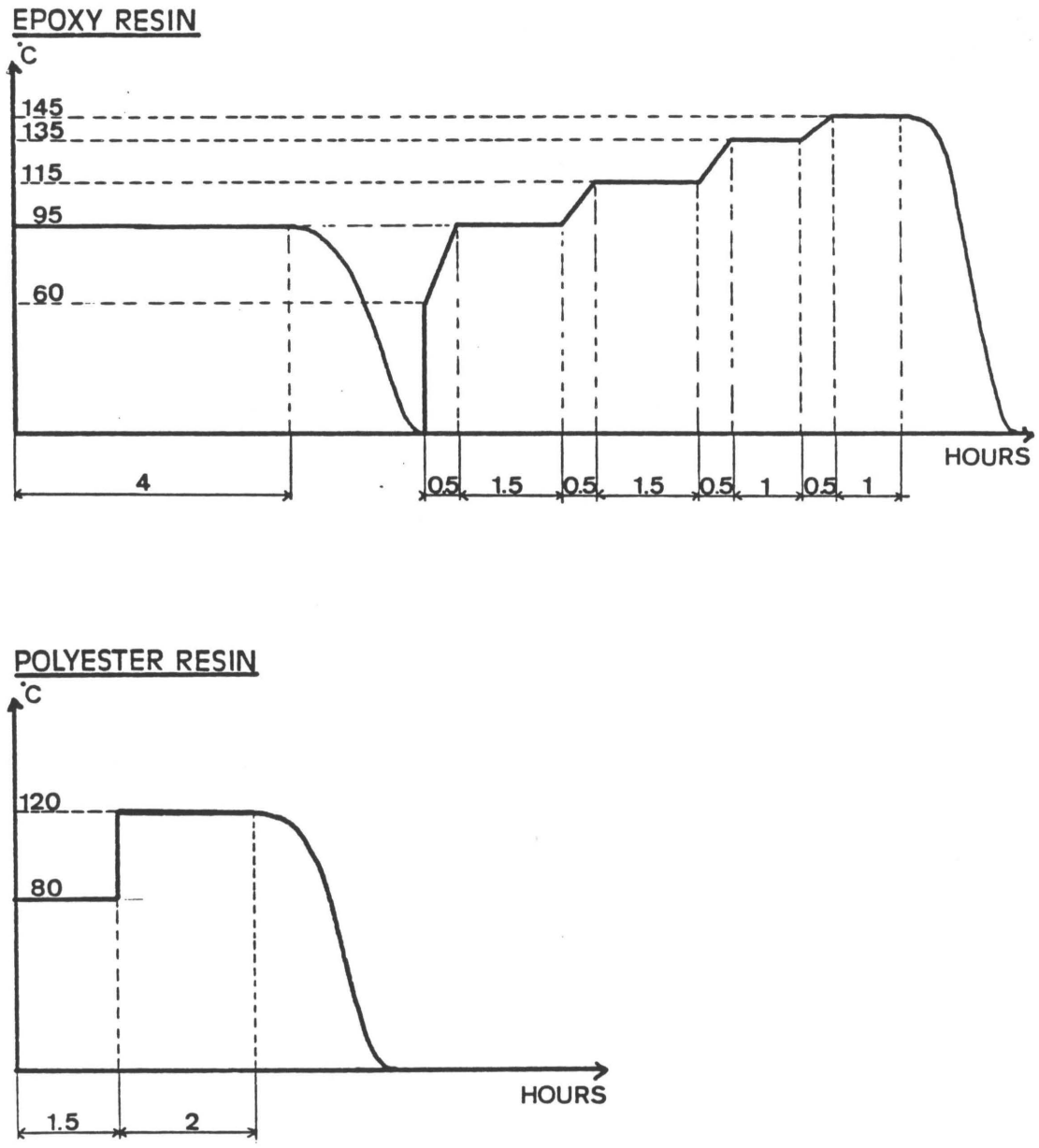

Figure 22. Cure cycles: Resin epoxy and polyester.

Table 5. Nature of the interphases.

Matrices Treatments on fibers	Epoxy	Epoxy + γAPS (1 part)	Polyester	Polyester + γMPS (1 part)
None	★	★	★	★
γAPS	★			
γMPS			★	
Silicone SN 2050 (*)	★		★	

(*) Produced by General Electric

Specimen preparation

Two kinds of specimens are considered: Dogbone samples containing a single glass filament and unidirectional glass fiber reinforced composites.

Unidirectional composites

They have been produced by Vetrotex Saint-Gobain using a filament winding technique. The plates (310 x 210 x 3 mm) obtained with this process were then cut into parallepipeds (19 x 6 x 3 mm) with a diamond saw.

Single fiber samples

They have been molded by mounting the fiber as shown in Figure 23 and then by pouring slowly the degassed matrix at room temperature into the mold. An RTV 664 silicone rubber (General Electric Co) has been chosen for the mold because of its properties: wide versatility, easy reproduction of duplicate dogbones from standard specimens, high temperature resistance and ease of specimen release. Release agents could have contaminated the fiber treatment during the mounting process

of the fiber into the mold. After curing the samples obtained have the geometry shown in Figure 23.

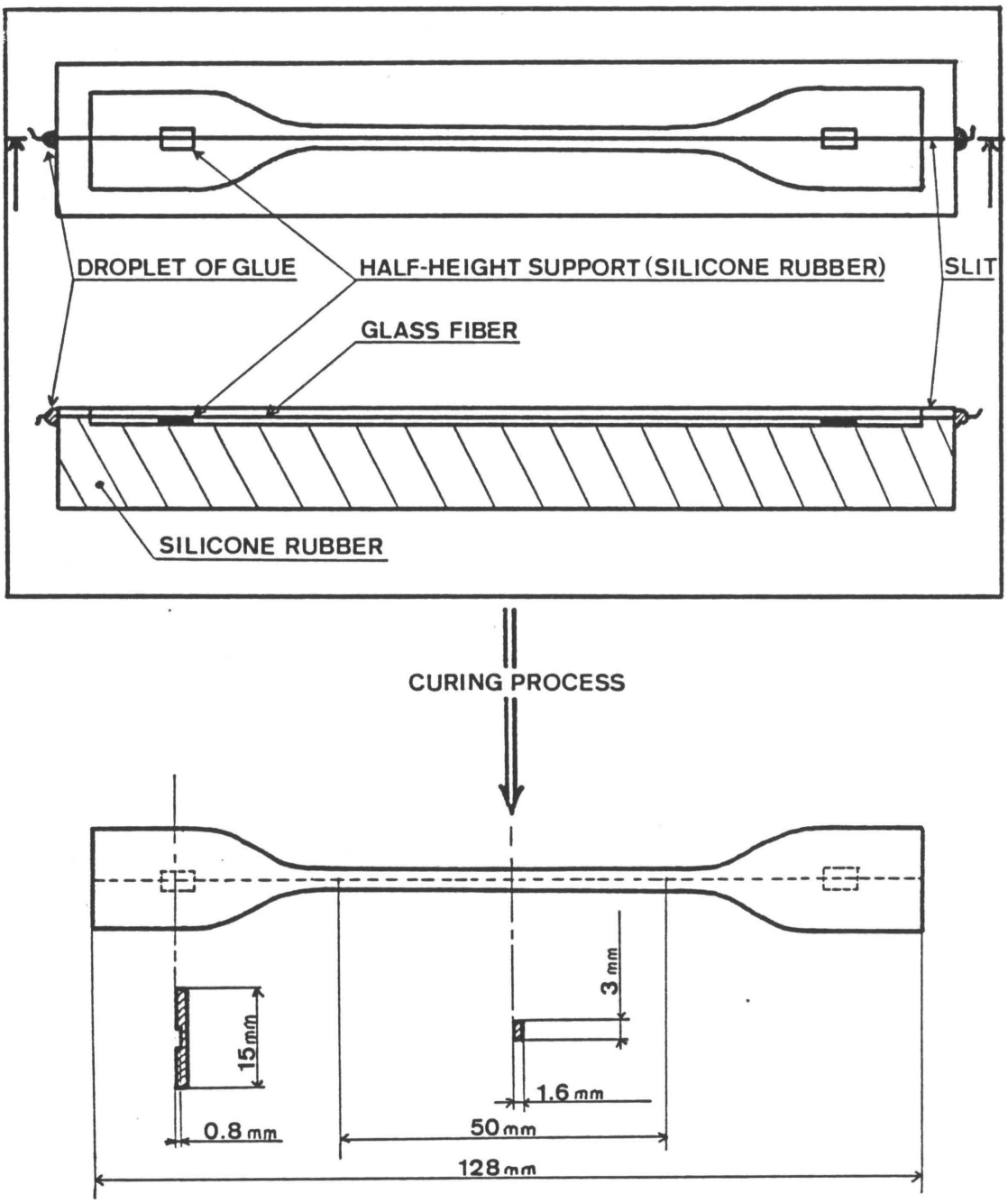

Figure 23. Single fiber sample: Preparation and geometry.

Critical fiber length test.

This test consists of embedding a single filament in a matrix having an elongation at failure greater than for the fiber, followed by tensile loading. Since one filament is not able to reinforce the sample, the fiber will break into fragments due to the load transfer. However this process will stop when the fragments become too small to carry enough shear at their interface to fail further in tension. This dimensional limit is called critical fiber length Lc. If the fiber is slightly longer than Lc failure will occur one more time. Therefore the fragment distribution has to be bounded by Lc/2 and Lc or δ and 2δ (ineffective length). This is summarized in the schematic diagram of the critical fiber length test: Figure 24.

Previous work [8,54,55,69] shows that in fact the distribution of fragment length is broader than Lc/2. The reason for that is variable properties and geometry along the length of the fiber.

If one assumes the fiber/matrix stress transfer described in the section about the statistical model (Equation 7 and Figure 17), after loading one has to measure the fragment length, then to calculate the mean Lm in order to determine δ:

$$\delta = 2/3 * Lm$$

Knowing δ one can use Figures 20 and 21 to evaluate the interfacial shear strength.

Evaluation of the strength of the fiber as a function of its length

Recalling Equation (13) of the section 'Statistical model' it has been demonstrated that a tensile test has to be performed on the fiber for three gage lengths. The results have already been given in Table 2. The test has been performed according to ASTM 3379-75 using an Instron machine (model 1122 S/N 4470) with a cross head speed of 0.2 mm/min. The specimen mounting method is given in Figure 25.

Loading of the single fiber sample

In order to observe and analyse the fiber breakage, the test has been performed on an MTS machine (model 445 servo controller testing system) with polarized light with the apparatus shown in Figure 26. The cathetometer used provides a 50X magnification. For reasons explained in the next section 'Results and Discussion' samples made of epoxy were tested with a cross head speed of 0.025 mm/min at room temperature

and for those made made of polyester, the cross head speed was 0.05 mm/min and the temperature 60° C.

Measure of the fragments' length

Measurements were made on a Zeiss microscope at 160X magnification with 5 μm precision. About 100 fiber fragments were measured for each of the eight interphases.

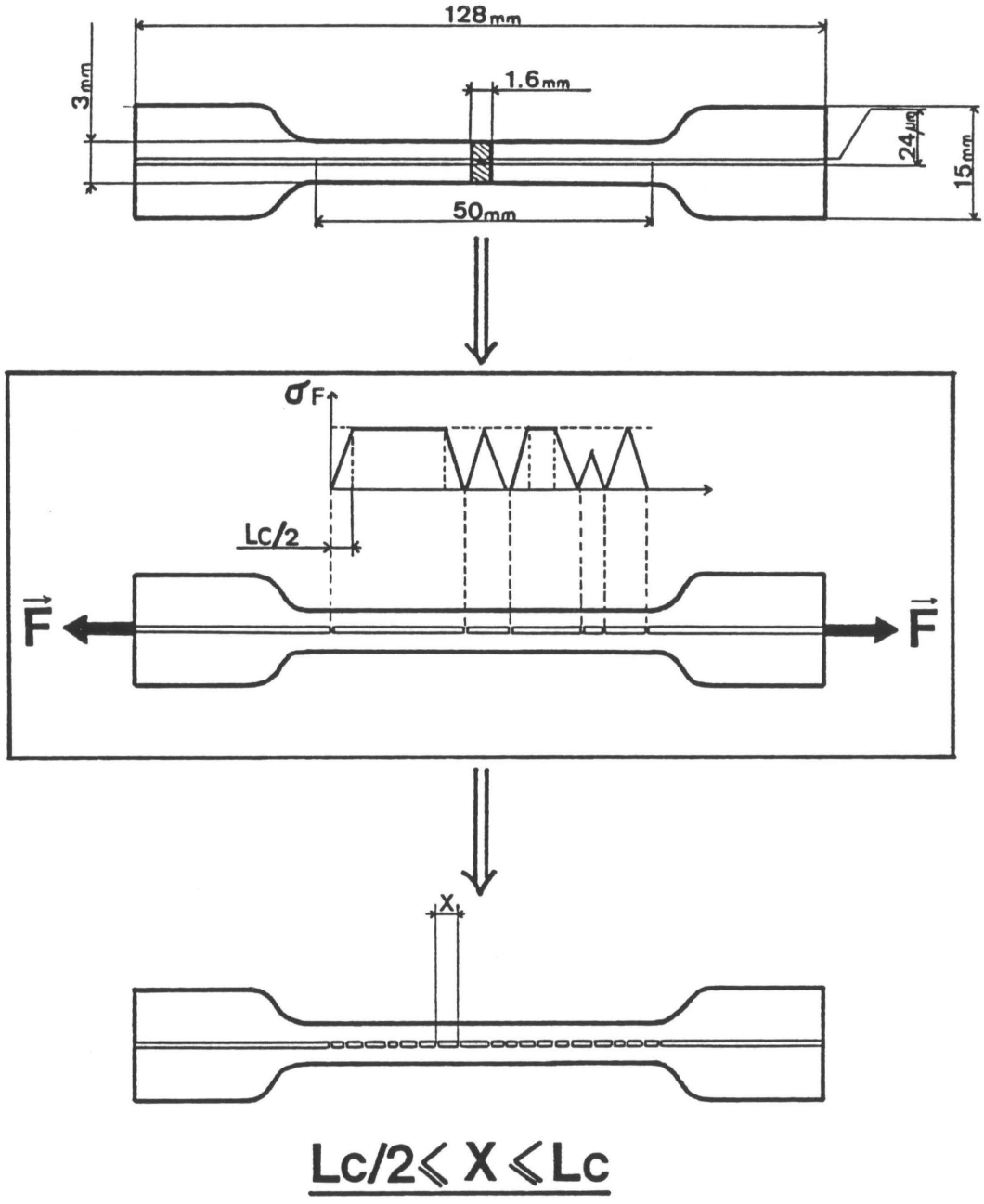

Figure 24. Critical fiber length test: Schematic diagram.

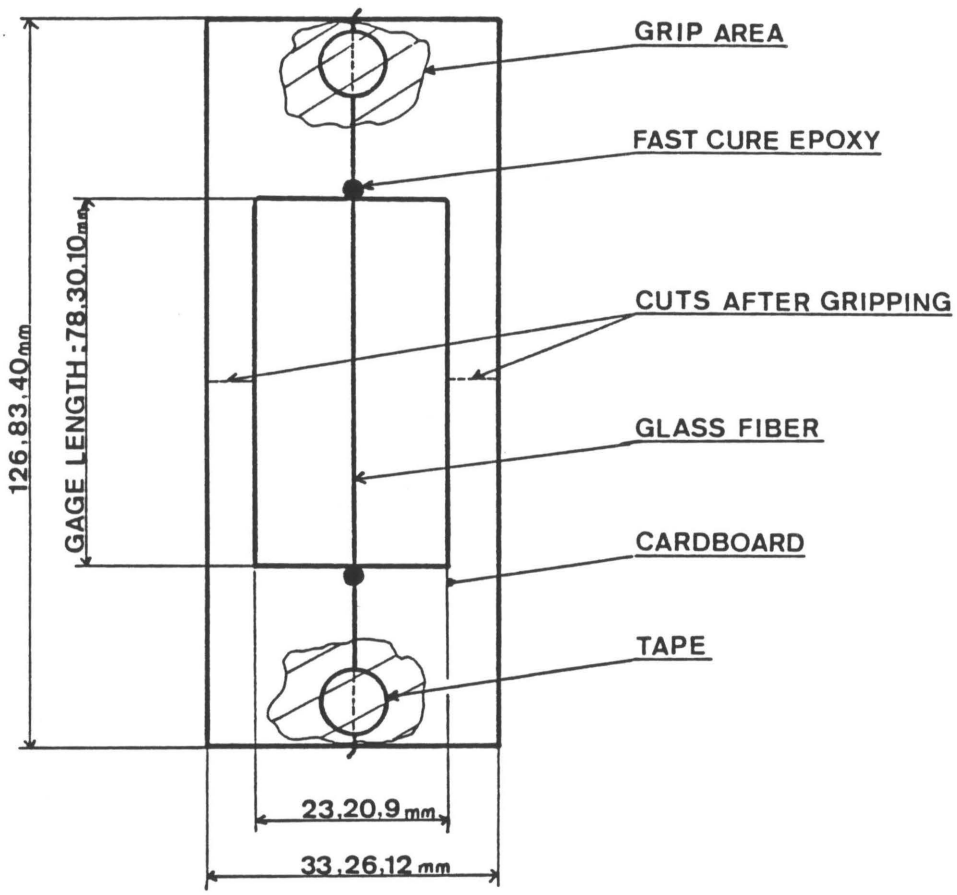

Figure 25. Tensile strength of the fiber: Sample description.

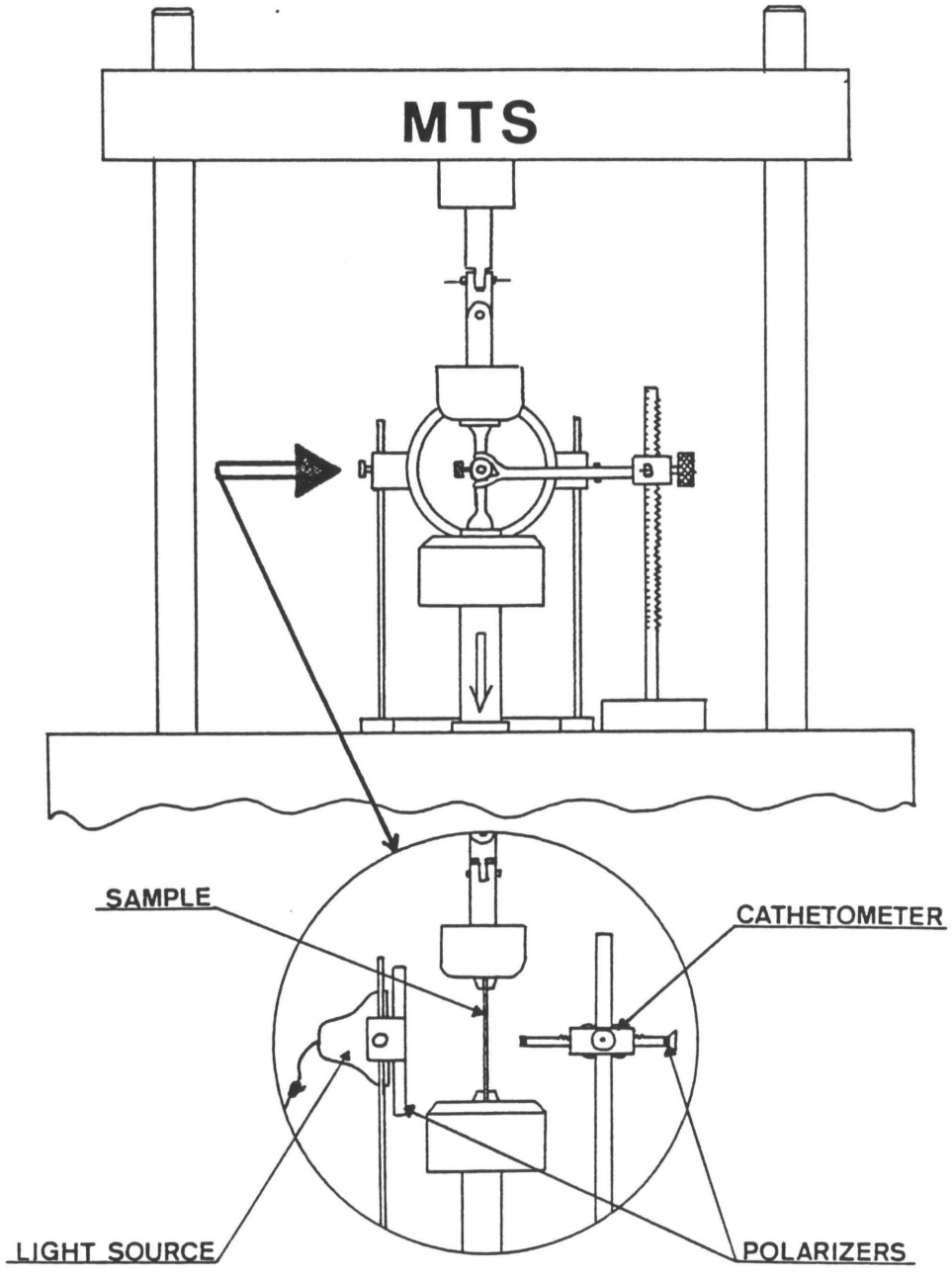

Figure 26. Critical fiber length test: Apparatus for loading with observation by polarized light.

Observations with polarized light.

Recalling Figure 3 and the section 'Model with an interphase', at fiber end stress transfer occurs between the matrix and the fiber through an interfacial shear stress. In that section the matrix was assumed to have elastic behavior. However the shear stress at the end of the fiber will probably exceed the yield point of the matrix. Therefore the matrix will deform plastically and one can approximate the shear state at the interface as in Figure 27.

One should notice that plastic deformation cannot occur without slippage of the fiber's end because the shear stress has to be zero at that point and thus cannot induce the matrix to yield. Moreover at fiber breakage, a very high strain energy has to be absorbed in the fiber break region. That may cause a combination of crack openings in the matrix, plastic deformation of the matrix along the fiber, and failure of the interphase. The predominance of one phenomenon over the others depends mainly of the quality of the fiber-matrix adhesion versus the matrix and fiber properties. If the adhesion is very good the matrix will deform plastically and/or cracks will occur in the matrix.

Any plastic zone is surrounded by an elastic one, therefore with polarized light one will observe an illuminated region

along the interface longer than the real plastic zone. This zone length should be characteristic of the quality of the fiber-matrix adhesion.

Using a Zeiss polar microscope at 160X and 320X magnification with measurement capability, measures and observations have been performed on one filament embedded samples. This experiment consists in recording the shape and length of the light zone at fiber breaks when:

1. The sample is stressed by a hand strain stage described in Figure 28.

2. The sample has been unloaded.

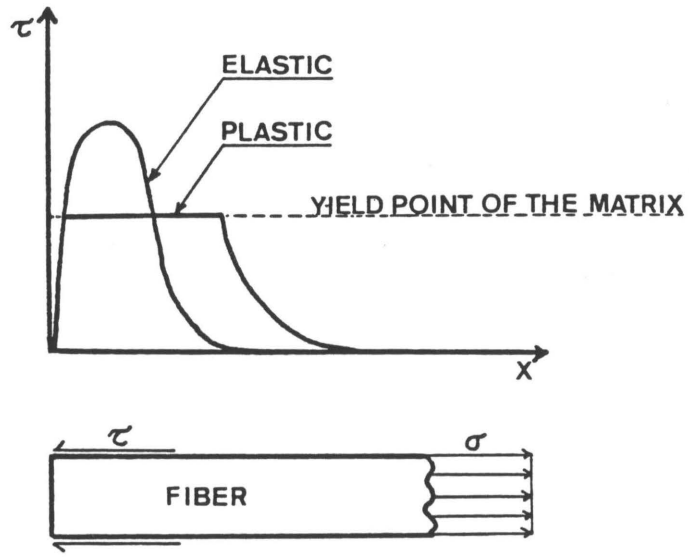

Figure 27. Elastic and plastic interfacial shear stress.

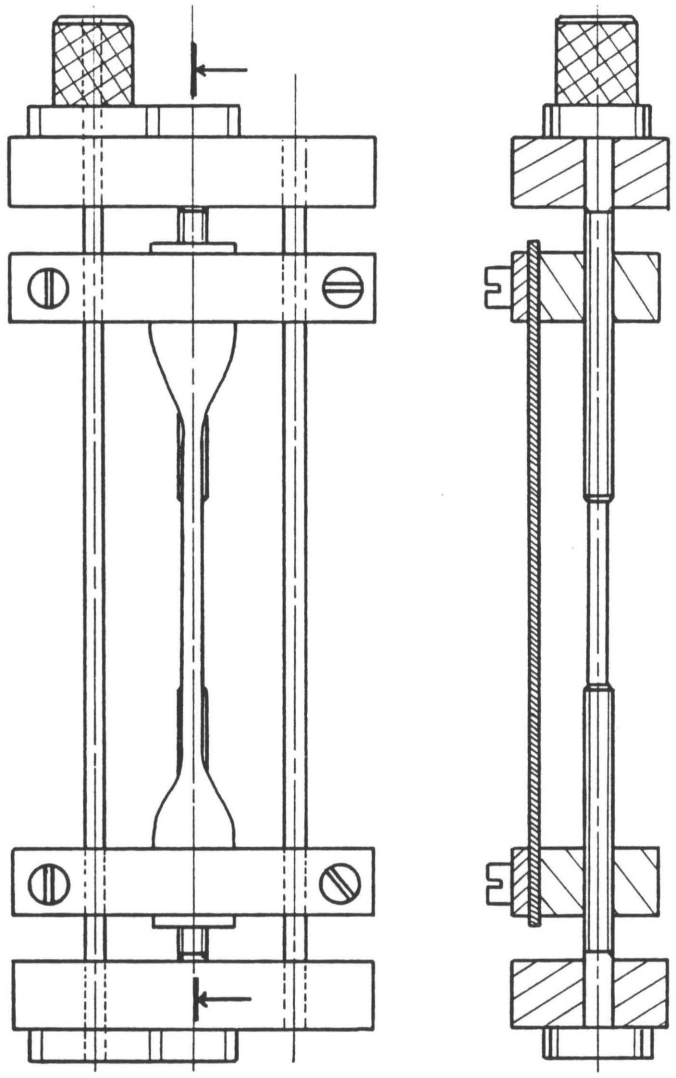

Figure 28. Observations with polarized light: Hand strain stage schematic diagram.

Short beam shear test (three point bending test).

The experiment has been done according to the ASTM 2344-76 (NF T 57 104) on ten beams for each kind of samples. The equipment used was an Instron (model 1125) , the cross head speed was 0.05 in/min. The schematic diagram of this test is given in Figure 29.

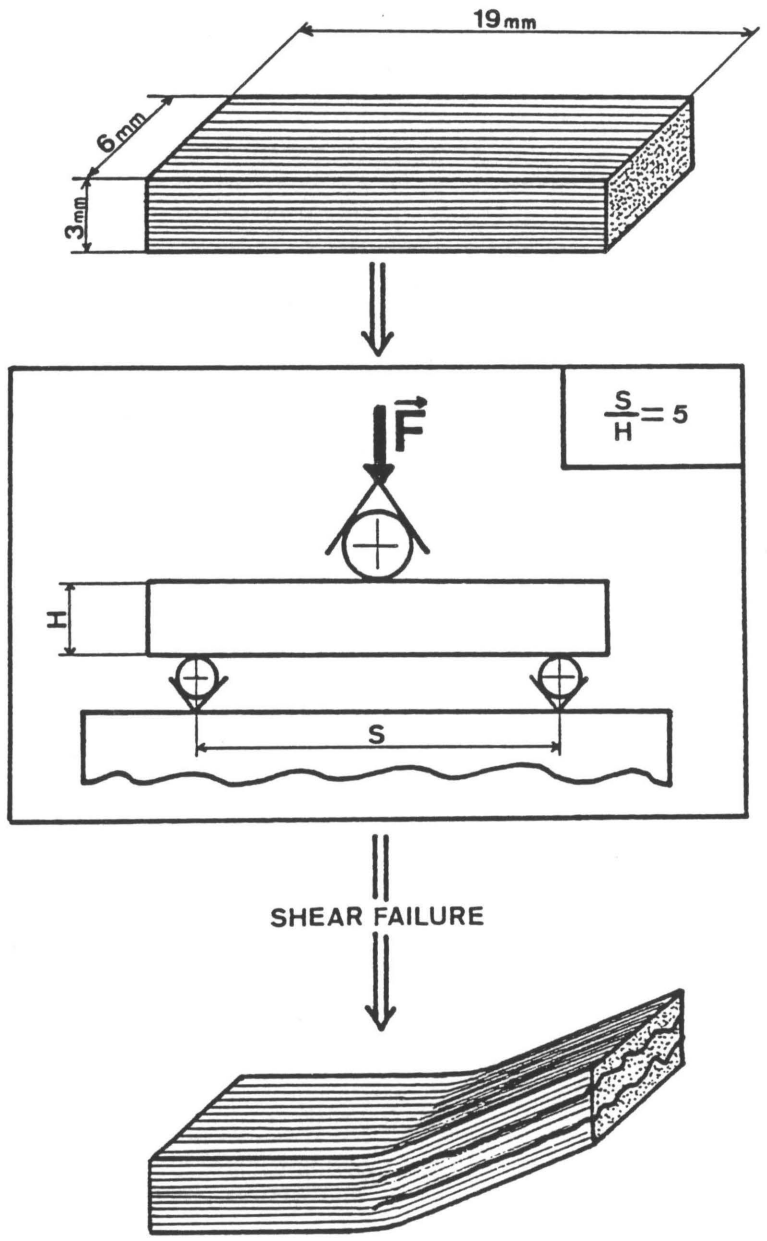

Figure 29. Short beam shear test: Schematic diagram.

ESCA analysis.

X-ray Photoelectron Spectroscopy (XPS or ESCA) is an analytical technique used to determine chemical composition and bonding in the top surface layers of materials (within 10 nm). The sample is illuminated with X-rays which excite photoelectrons from the surface. These photoelectrons are analysed for kinetic energy. Characteristic orbital binding energies (B.E.) can be calculated from measured photoelectron kinetic energies. These energies are dependant on the precise chemical configuration of the surface atoms. In an XPS spectrum one plots the number of electrons detected against their binding energy. The spectrum obtained with this technique is compared to reference spectra in order to determine the chemical composition of the surface. Then each peak is analysed considering its position on the spectrum, its intensity and width. That gives both chemical composition and bonding information.

A Kratos XSAM-800 Surface Analysis System, equiped with a dual (Mg/Ti) X-ray anode and ion gun, has been used to analyse the chemical composition of fiber coated with each surface treatment and of each kind of matrix (Table 5).

SIMS analysis.

Secondary Ion Mass Spectrometry, (SIMS), is a powerful technique for surface and materials analysis. It detects all the elements and their isotopes with an unequalled sensitivity. Additional chemical information can be obtained from examining characteristic fragmentation patterns. In SIMS, the surface to be analyzed is bombarded with a primary ion or neutral beam. Sufficient energy is transferred to the surface for molecular fragments and ions to be sputtered into the vacuum where the ionized material is analyzed using a quadrupole mass spectrometer. Static SIMS uses low energy, low dose argon ions or Fast Atom Bombardment (FAB) as the primary beam to obtain sensitive chemical analysis of the outermost atomic layer. This data is displayed as a mass spectrum.

A VG Scientific SIMSLAB with a FAB Ar° source at 5kev (6nA equivalent current) has been used to analyse the fracture surface of polyester samples tested with the short beam shear test. Mass spectra between 0 and 100 a.m.u. were recorded. Each spectra took 200 sec. It can be estimated that not more than 1-2 molecular layers were removed during the analyses.

SEM analysis.

Fracture surfaces of short beam composites and of one,three and seven filaments embedded samples were observed using a JEOL 35C SEM.

RESULTS AND DISCUSSION

ESCA analysis

The ESCA results give the chemistry one would expect on the fiber's surface and of the matrix from the kinds of treatment coated on the fiber and from the formulation of the matrices (Figures 30,31 and Table 6).

From Table 6 one can see that the two coupling agents (A1100 = γAPS and A174 = γMPS) do not cover the fibers uniformly or form on the fiber a very thin layer (< 10 nm). If the layer were thick the ESCA results should not show the Al2p and Ca2p peaks for the fiber coated with coupling agents because those two peaks are characteristic of the bare glass fiber as one can see in Table 6. SEM photomicrographs (a) of Plate 1 show that for the case of the fiber coated with A174, part of the coupling agent does not wet the fiber surface very well and that portions of coating layer have been peeled. That was not been noted for the case of the fiber coated with A1100 and

may explain why in Table 2 (Tensile strength of the fiber), A174 seems to offer less protection against flaw formation due to handling than did A1100.

On the other hand the fact that Al2p and Ca2p are absent in the chemistry of the fiber with the silicone treatment suggests a very thick layer of silicone around the fiber. That is also shown by the SEM photomicrographs (b) of Plate 1. The narrow Si2p peak for the fiber with silicone agent (2.1 eV at half-height) compared to the Si2p peak for the fiber without treatment (2.8 eV at half-height) indicates that the silicone on the surface of the fiber detected by ESCA comes from the silicone agent and not from the silicone contained in the glass.

The carbon 1s spectra in Figure 31 reveal no difference in chemistry between the pure epoxy and the epoxy containing one part of A1100 and a very small difference in the ester peak between pure polyester and polyester with one part of A174. Those differences are revealed more clearly by the percentage of Si2p on the surface in Table 6.

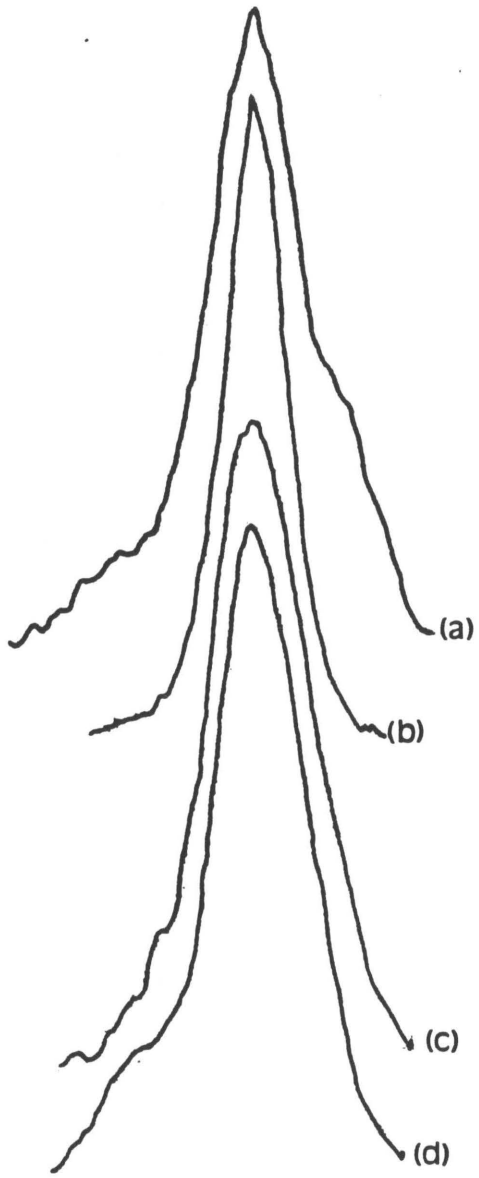

Figure 30. C 1s peaks of treated fibers: (a): bare fiber; (b): fiber with Si treatment; (c): fiber with A1100; (d): fiber with A174.

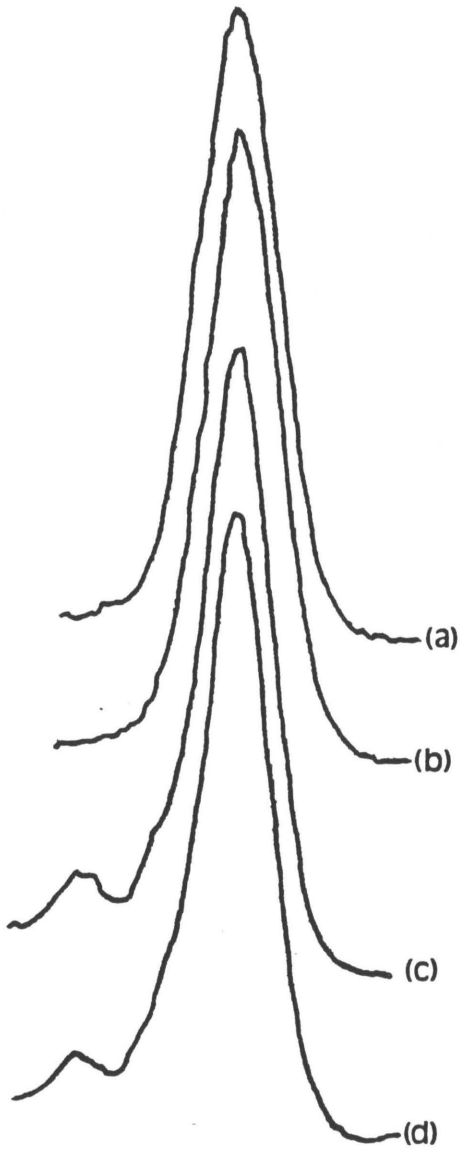

Figure 31. C 1s peaks of matrices: (a): pure epoxy; (b): epoxy with A1100 (1 part); (c): pure polyester; (d): polyester with A174 (1 part).

Table 6. ESCA results : chemical composition.

	C1S	O1S	SI2P	N1S	AL2P	CA2P	NA2S
FIBER + SURFACE TREATMENT							
FIBER	20.0% 285.0 3.1	41.8% 531.8 3.2	15.3% 102.2 2.8	0.0%	18.1% 76.0 .7	4.7% 347.9 3.0	0.0%
FIBER + SI	77.2% 285.0 2.0	12.1% 532.3 1.9	10.7% 102.0 2.1	0.0%	0.0%	0.0%	0.0%
FIBER + A1100	39.7% 285.0 3.1	35.3% 532.1 2.9	15.7% 102.6 2.8	4.1% 400.2 4.0	3.9% 73.8 2.5	1.3% 347.9 3.2	0.0%
FIBER + A174	42.5% 285.0 2.9	38.0% 532.5 2.7	14.2% 102.6 2.6	0.0%	2.7% 74.2 2.5	2.6% 348.4 2.8	0.0%
MATRICES							
EPOXY	75.1% 285.0 2.6	19.3% 532.9 2.5	1.6% 102.0 2.1	1.8% 399.8 1.7	1.4% 74.4 2.3	0.0%	0.9% 64.0 2.0
EPOXY + A1100	76.2 % 285.0 2.4	16.8% 532.7 2.4	3.8% 101.9 2.3	1.3% 399.7 1.7	1.2% 74.4 2.3	0.0%	0.5% 63.3 1.6
POLY	79.5% 285.0 2.1	19.8% 532.7 3.0	0.7% 102.1 2.3	0.0%	0.0%	0.0%	0.0%
POLY + A174	79.3% 285.0 2.0	18.8% 532.8 2.8	1.9% 102.1 2.9	0.0%	0.0%	0.0%	0.0%

	X	
I	*.*% ***.* *.*	PERCENTAGE OF X ON THE SURFACE OF I POSITION OF THE PEAK (BINDING ENERGY) WIDTH OF THE PEAK AT HALF-HIGHT

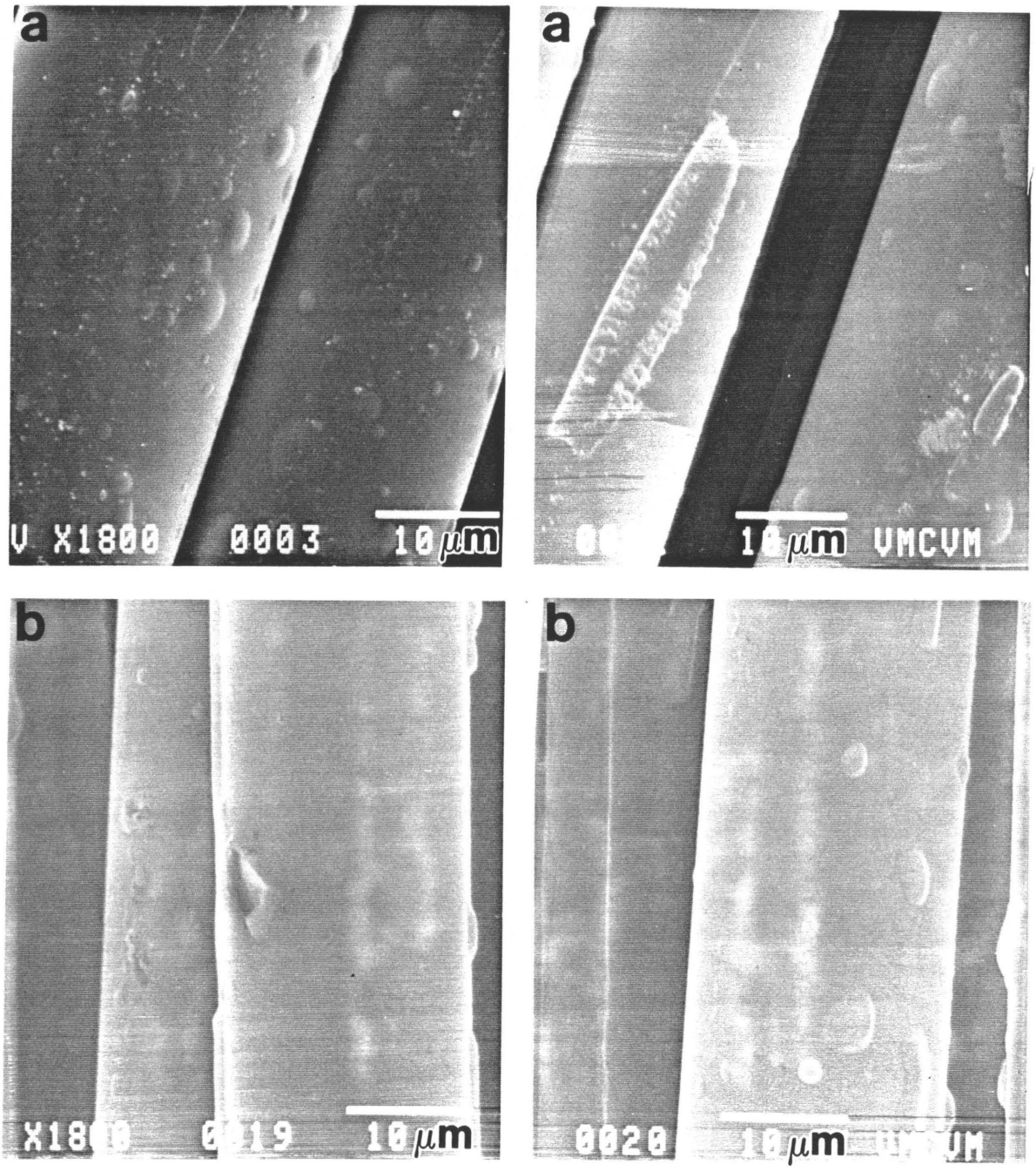

Plate 1. SEM photomicrographs of coated fibers: (a) fiber coated with A174 (γMPS); (b) fiber coated with Si agent.

Short beam shear test

Tables 7 and 8 give a schematic representation of the results of the three point bending tests. As one can see in those tables and as it has been said in the literature [64], that test induces very different failure mechanisms in the composite beams. Therefore one has to be careful in the analysis of the results. In tables 7 and 8, the load at failure has been indicated for each kind of composite beams in order to make the results complete and not in an attempt to perform comparisons between beams or to propose those values for design purposes. Four modes of failure have been observed in this research (1) shear failure (2) fracture of the beam perpendicular to the fiber direction called bending failure (3) microbuckling failure under the point where the load is applied (4) internal slipping failure due to the very bad fiber-matrix adhesion. Failure of the short beam can occur by one or a combination of those four mechanisms. The failure mechanism really depends on the matrix and fiber properties and on the quality of the fiber-matrix adhesion. If the matrix is brittle then the sample is more subject to shear failure because it will not deform plastically under the applied load and therefore will not fail by microbuckling. If the fiber has a low tensile strength, the fibers will break due to bending and the sample will fracture perpendicular to the fiber direction. Finally if the fiber-matrix adhesion is

poor the fibers will slip on the matrix as soon as the applied load overcomes the friction force. In that case no crack will be observed but a gradual deformation of the sample.

For the samples made of polyester resin, Table 7 indicates that only the beams with the fiber coated with A174 fail in pure shear. The samples made of polyester containing A174 fail mainly in shear but also in bending. This is due to the fact that the fiber are bare in that case and has been damaged during handling. That phenomena has already been reported in Table 2 where one can notice the large difference in strength between fiber coated with A1100, with A174 and bare fiber. It seems that the coupling agent formulation plays an important role in the protection of the fiber against flaw formation. However in the case of polyester plus bare fiber the samples do not fail in bending because the internal slipping becomes the predominent failure mechanism. One can notice the tremendous effect of the coupling agent in the matrix. This will be reinforced in the SIMS analysis. Without the A174 on the fiber or in the matrix the fiber-polyester matrix adhesion seems to be very poor but still greater than for the fiber coated with the silicone agent. Plates 2 and 3 show the SEM photomicrographs of the fracture surface for each kind of polyester sample. One can observe the fracture surfaces of (c) and (d) without matrix debris due to brittle failure compared to (a) and (b) in Plate 2. That confirms

completely the difference in failure mode. It may appear from the photomicrographs of Plate 3 that there is separation at the fiber-matrix interface in the two cases where A174 has been used. No matrix bonded to the fiber can be observed by using SEM after fracture. The next section about SIMS analysis will demonstrate that in fact there is a matrix layer around the fiber for those two cases.

Table 8 gives the results for the sample made of epoxy resin. Since the matrix is ductile it was impossible to obtain a pure shear failure in the case of the samples made of fiber coated with A1100. No difference can be noticed between the failure of the beam made of pure epoxy and bare fiber and those made of epoxy containing A1100. Both fail in bending. However it can be stated that the fiber-matrix adhesion is better for bare glass-epoxy than bare glass-polyester as no internal slipping has occured with the epoxy-bare fiber sample. Plate 4 shows the two kind of fracture obtained with the epoxy samples. Photomicrograph (b) reveals some matrix still bonded to the fiber after fracture. Therefore the coupling agent A1100 seems to promote a good fiber-matrix adhesion.

Table 7. Short beam shear test results: Polyester samples.

INTERPHASES	POLYESTER	
	BEAM FAILURE	STRAIN - STRESS CURVE
FIBER + A174	PURE SHEAR 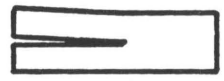	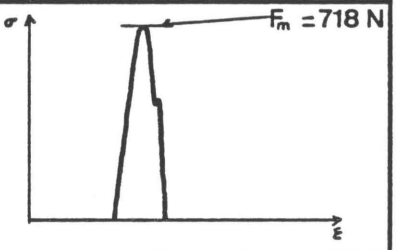
RESIN + A174	MAINLY SHEAR 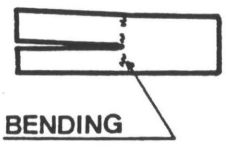 ALSO BENDING	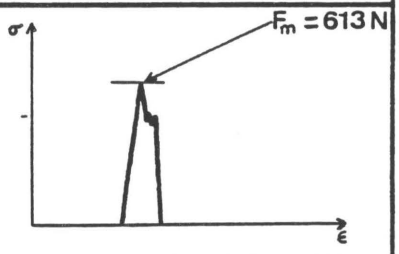
BARE FIBER	MAINLY INTERNAL SLIPPING  ALSO SHEAR	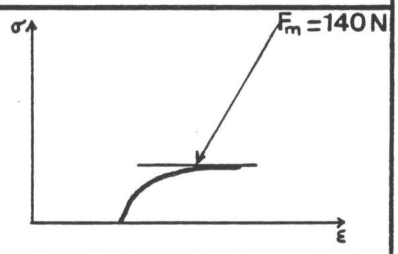
FIBER + SILICONE	PURE INTERNAL SLIPPING 	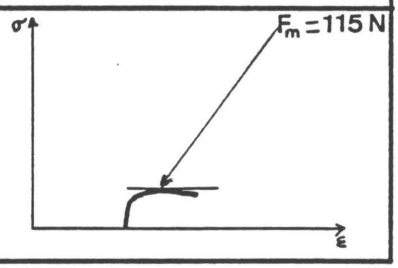

Table 8. Short beam shear test results: Epoxy samples.

INTERPHASES	EPOXY	
	BEAM FAILURE	STRAIN-STRESS CURVE
FIBER + A1100	SHEAR AND MICROBUCKLING 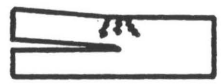	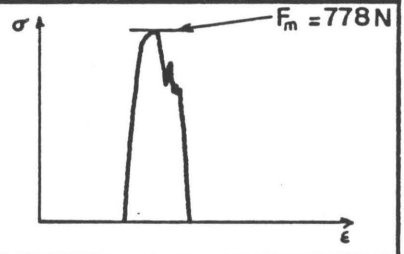
RESIN + A1100	PURE BENDING 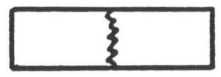	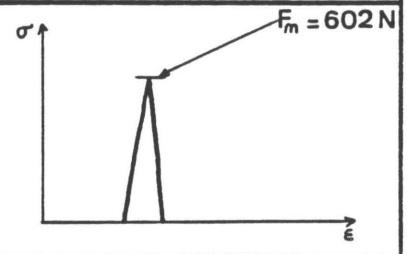
BARE FIBER	PURE BENDING 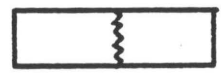	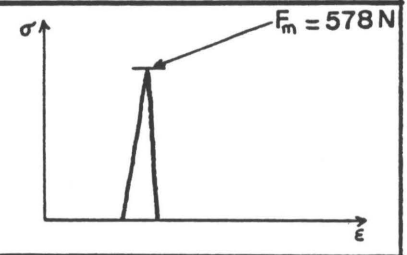
FIBER + SILICONE	PURE INTERNAL SLIPPING 	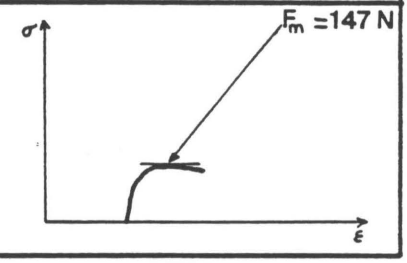

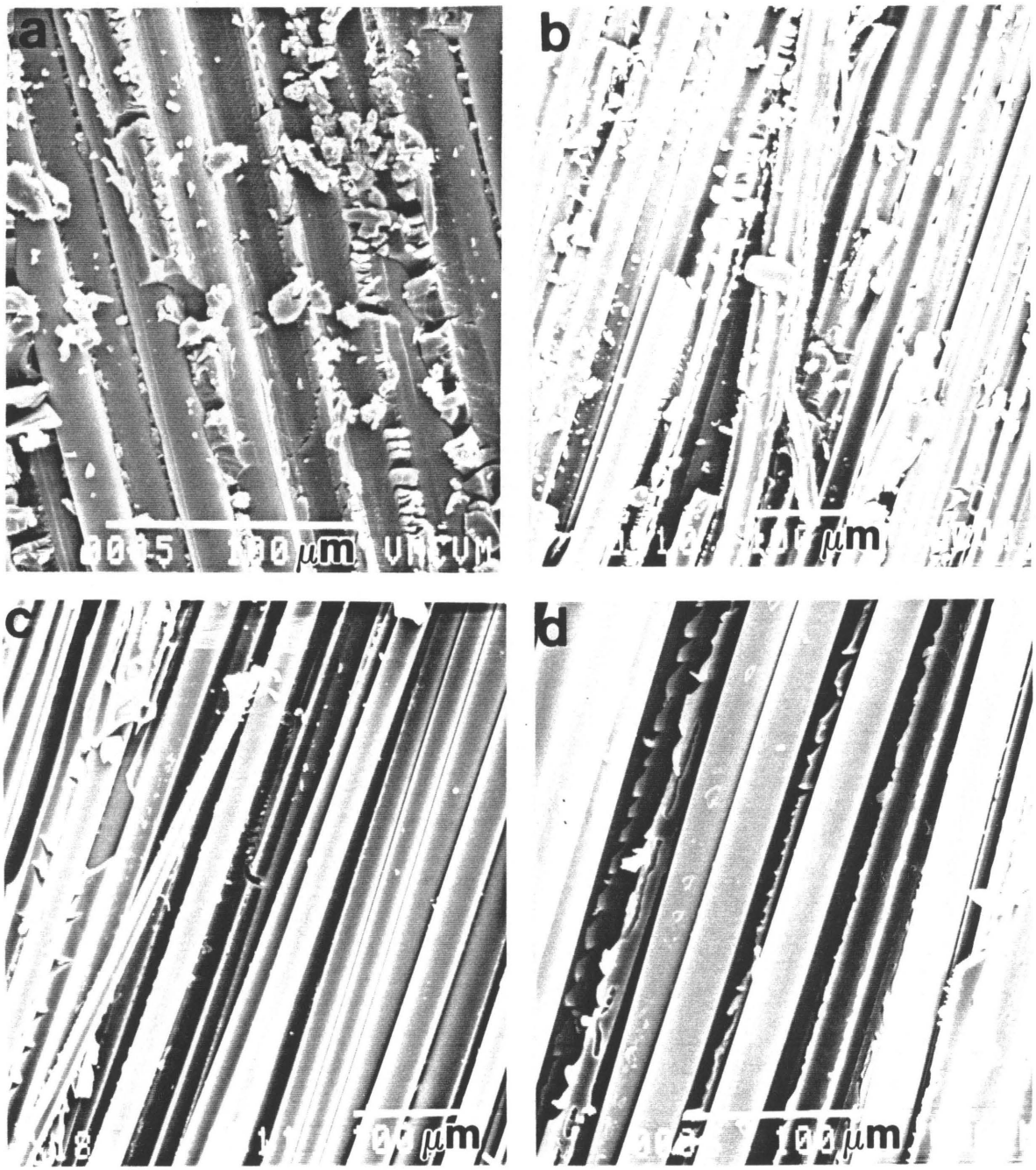

Plate 2. SEM photomicrographs of the fracture surface of short beams: Polyester samples. (a) fiber + A174, (b) polyester + A174, (c) bare fiber, (d) fiber silicone.

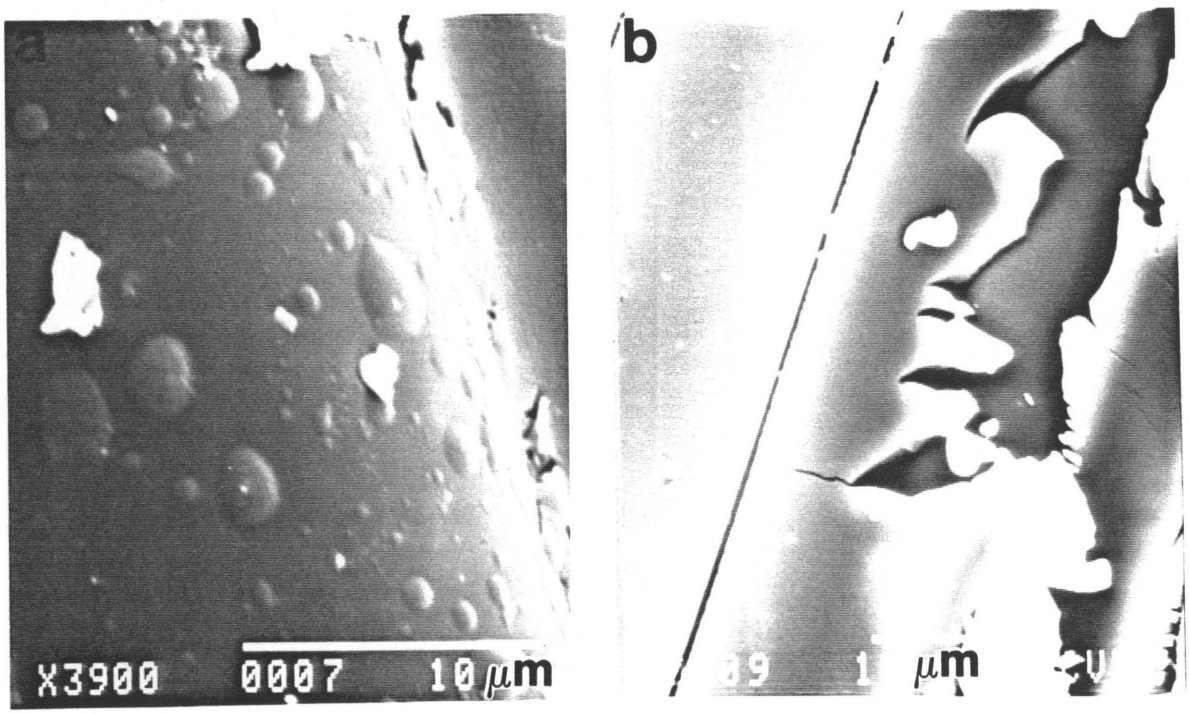

Plate 3. SEM photomicrographs of the fracture surface of short beams: Polyester samples. (a) fiber + A174, (b) polyester + A174.

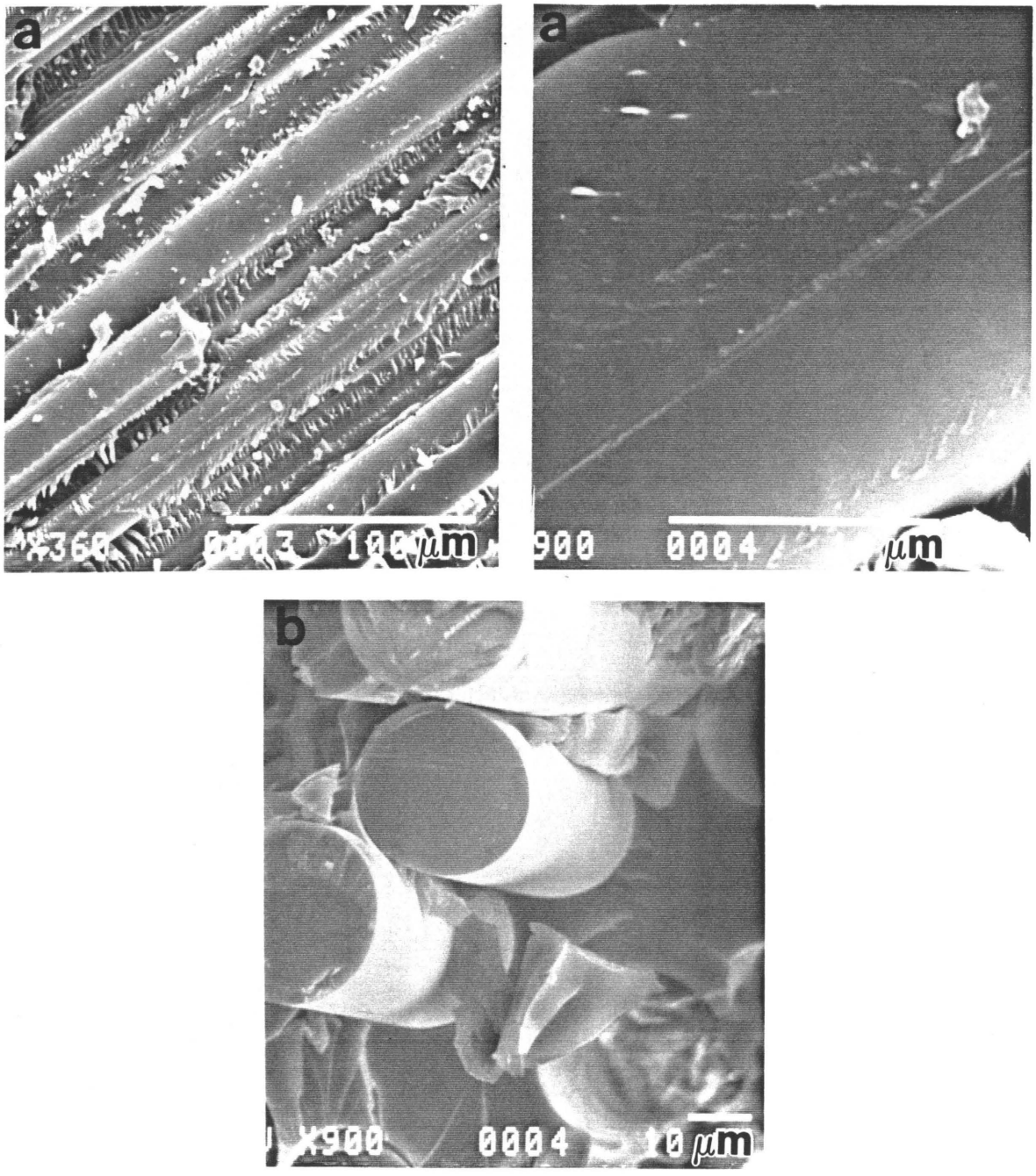

Plate 4. SEM photomicrographs of the fracture surface of short beams: Epoxy samples. (a) and (b) Fiber A1100, (c) bare fiber.

SIMS analysis

SIMS results from the fracture surfaces of short beams made of polyester give very interesting detail on the locus of failure in those samples. Shear failure occurred at the interface in the sample with no treatmemt on the fiber. Figure 34 shows that the mass spectrum is characteristic of a very clean glass surface (the reader has to be aware of the difference in count rate between the spectra presented in Figures 32-35. Those differences are indicated on the Y-axis. Therefore this indicates no bonding between bare fiber and polyester resin as has already been inferred from the SEM picture of the fracture surface in the previous section. For the beam made of pure polyester and fiber treated with γMPS, Figure 33 shows a mass spectrum characteristic of a polymer material with the clear sequence of C1 to C7 cluster peaks. Therefore shear failure has occurred in the matrix. The polyester layer is thick enough to hide the coupling agent coated on the fiber. Failure must be located relatively far from the interface. From the SEM picture of the fracture it was not possible to resolve that kind of failure. That demonstrates the value of the high resolution information provided by SIMS. For the case of the beam made of polyester containing one part of γMPS and bare fiber, the SIMS spectrum (Figure 34) demonstrates that failure has taken place in the matrix as one can note the presence of the C1 to C7 peaks,

as in the previous case. This was not obvious in the SEM picture in the previous section. The polymer spectrum, however, is quite different from the one in the pure polyester case with treatment on the fiber. This difference in chemistry of the two matrices (pure polyester and polyester + γMPS) was not as well defined by the ESCA analysis. Moreover, the peak at 73 mass units in Figure 34 verifies the presence of coupling agent in the matrix and demonstrates an enrichment of γMPS close to the interface because of the intensity of the peak. That the γMPS did not polymerize is indicated by the absence of peaks over 100 mass units. The spectrum of a siloxane-sulfone copolymer where the siloxane is of molecular weight over 5000 mass units, is shown in Figure 35 for comparison. The polysiloxane molecules produce high-molecular weight cluster fragments with regular spacing of one CH unit, well above 100 AMU.

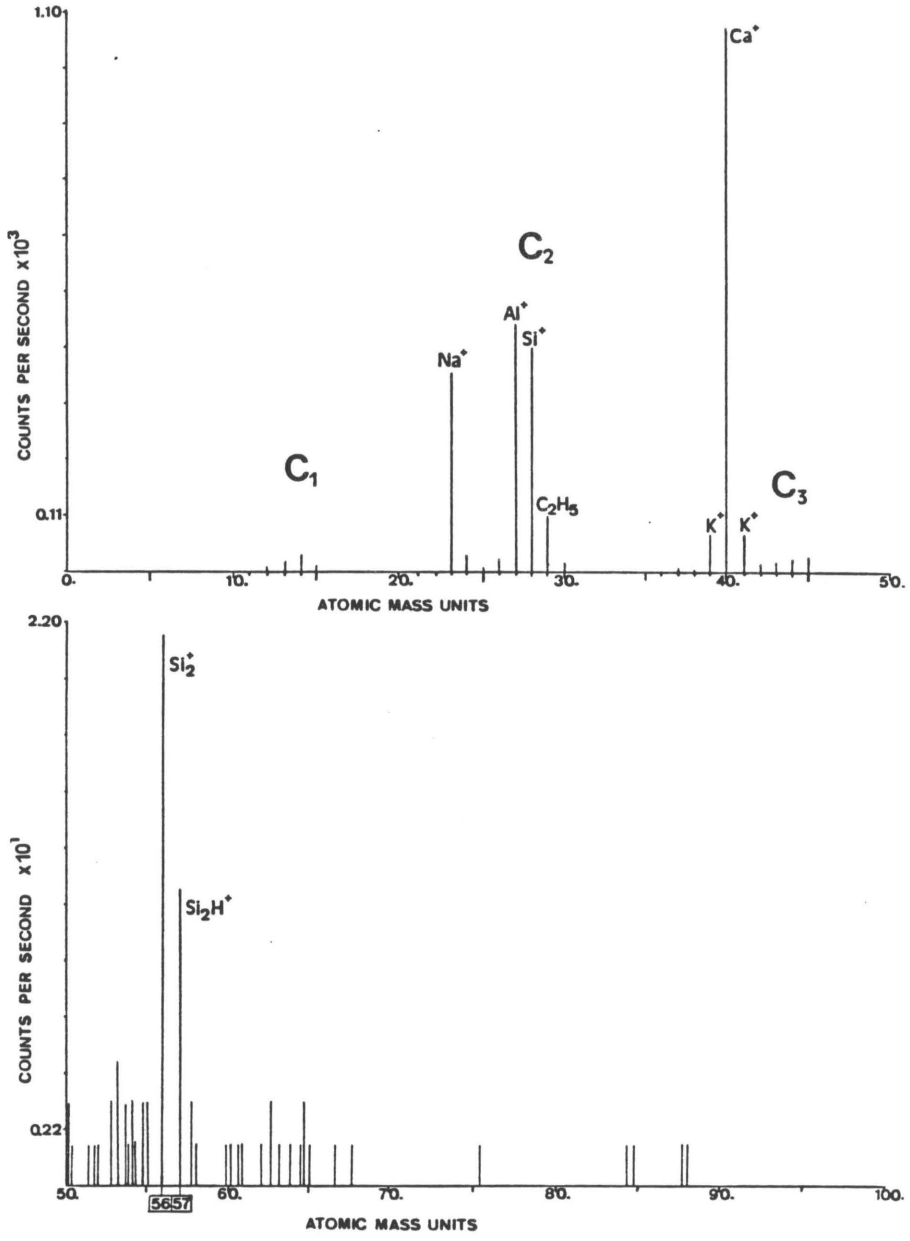

Figure 32. SIMS spectrum. Pure polyester + bare fiber

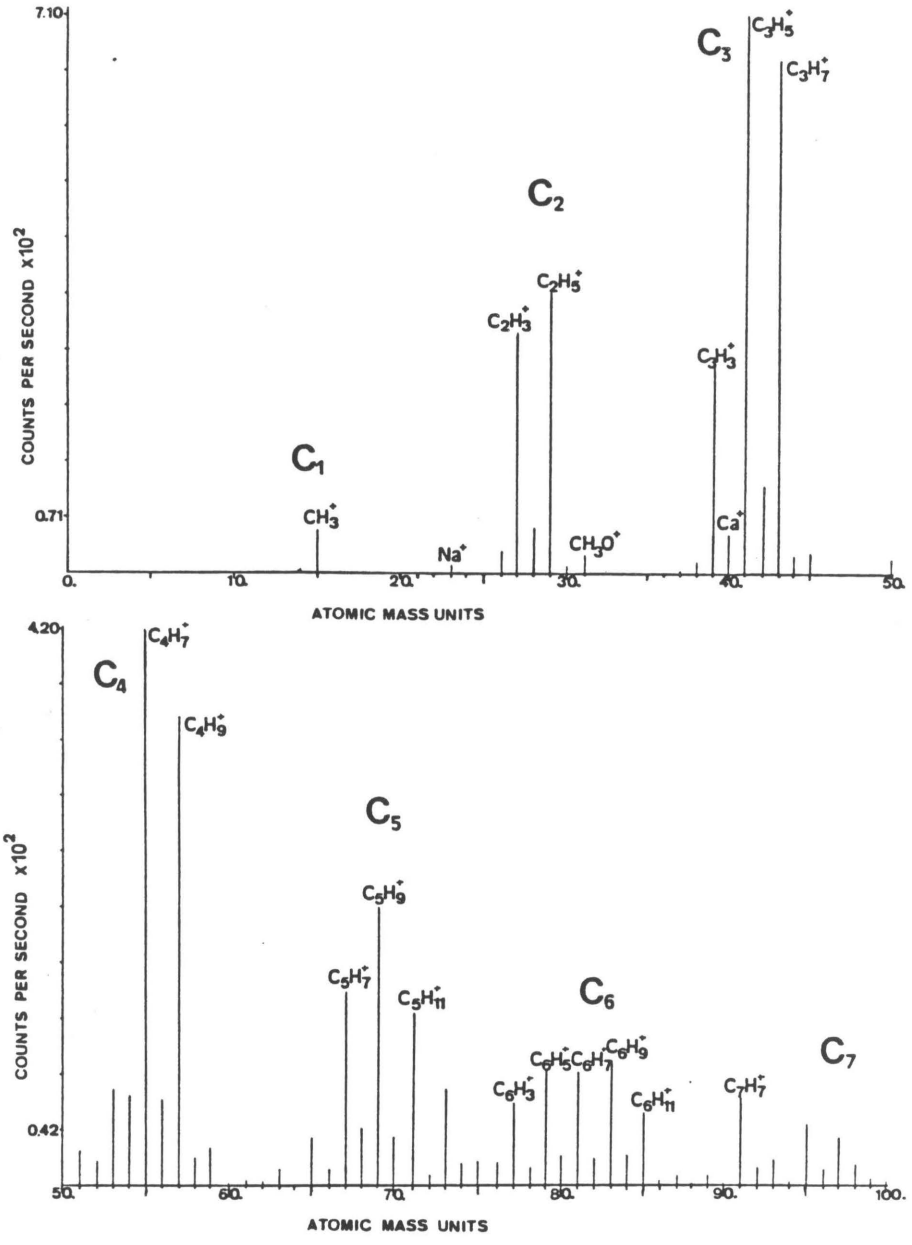

Figure 33. SIMS spectrum. Pure polyester + (fiber + γMPS)

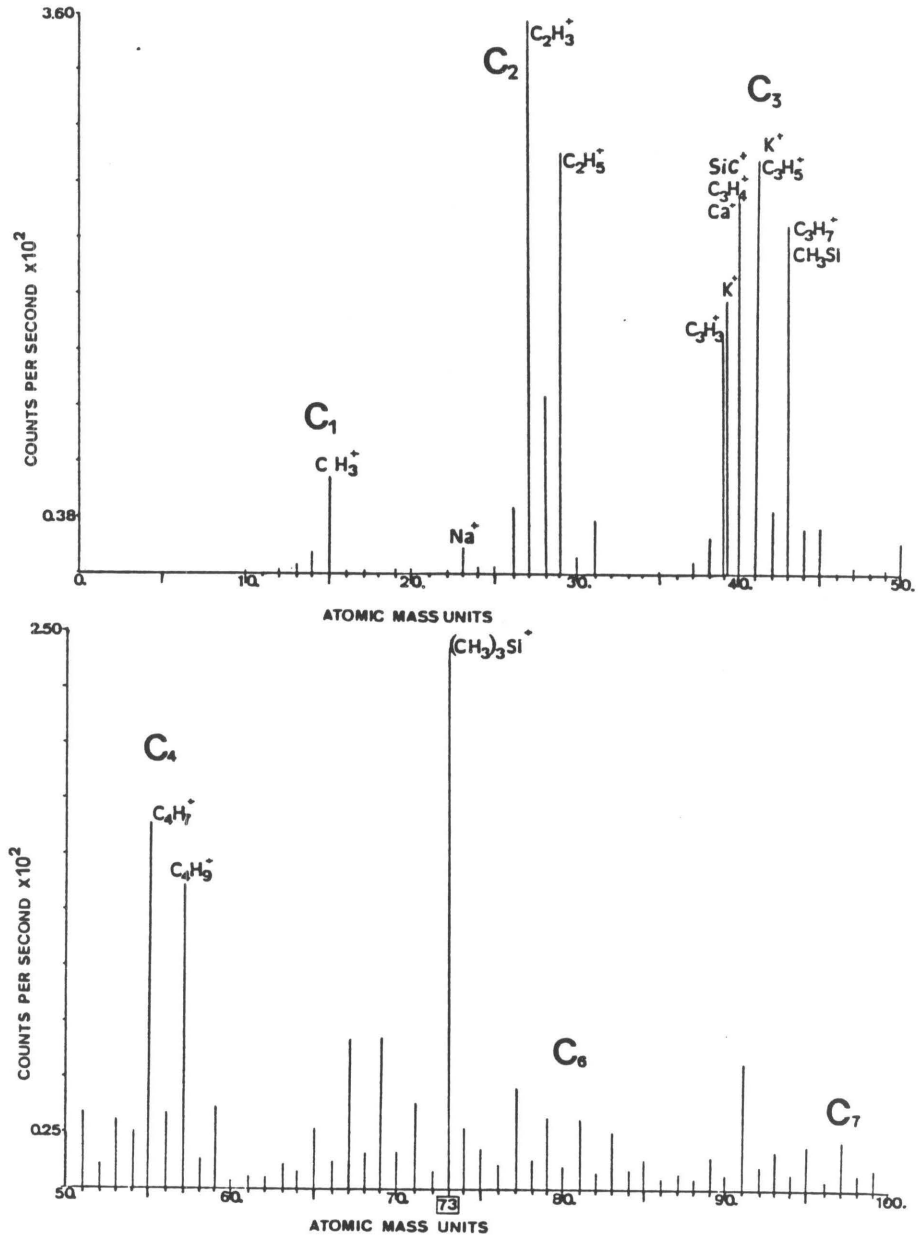

Figure 34. SIMS spectrum. (polyester + γMPS) + bare fiber

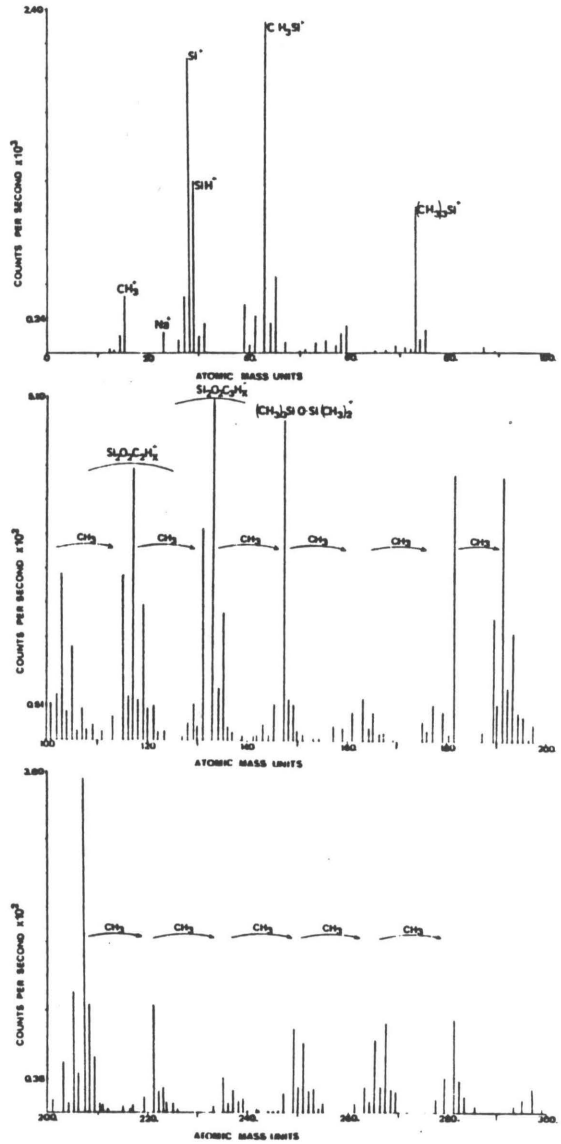

Figure 35. SIMS spectrum. Siloxane-sulfone copolymer: Positive SIMS, target bias 25 v, step size 0.1 AMU, 3 scans of 1001 channels at 100 ms per channel.

Critical fiber length test

The results for the samples made of epoxy resin are given in Table 9. According to that test the best fiber-matrix adhesion is for the case (fiber + A1100) then comes the case (bare fiber) and finally (epoxy + A1100). Very few breaks (3 to 5) were observed in the sample containing the fiber coated with silicone, demonstrating a complete lack of bonds between the fiber and the matrix. The few breaks probably occurred because of friction and due to the presence of some severe flaws on the fiber. In all the single fiber samples tested in this research one can observe three to seven early breaks due to severe flaws up to 1.5 mm elongation and then considerable strain must be applied to about 2 mm elongation before further breaks occur. The results of Table 9 tend to demonstrate that the coupling agent in the matrix induces a negative effect on the interfacial shear strength. That may be a premature conclusion because this statement supposes that the critical fiber length test evaluates only the fiber-matrix adhesion and nothing else.

As it has already been explained in the section on experimental procedures that a fiber break induces the release of a very high strain energy that may cause a combination of crack opening in the matrix, plastic deformation along the interface, or failure of the interphase. The perfect illus-

tration of that is the experiment performed on the single fiber samples made of polyester resin. In fact it was impossible to run the critical fiber length test at room temperature on those samples. The reason is shown in Plate 5: crack formation at fiber break (The dark particles on the photographs of polyester samples are due to the dust stuck on the samples because the polyester was still sticky after cure). On account of the brittleness of the polyester resin the first three to seven breaks always leads to fracture the specimen by propagation of those cracks. Plates 6 and 7 compare the fracture surfaces of polyester specimens with coupling agent on the fiber and in the resin, respectively. The large difference between those two Plates reinforces what has been said about the phenomena induced by the release of the strain energy upon fiber breaks. On account of the good fiber-matrix adhesion in the case of the fiber coated with A174 the strain energy released was not absorbed by complete fracture of the interphase. Therefore the fiber breakage will tend preferably to progate a matrix crack and to cause plastic deformation along the interface. Plate 6 shows that only small regions of the interphase have fractured. The strain energy released has induced the fiber crack to propagate so rapidly through the resin that no plastic deformation of the matrix has occurred. On the contrary, Plate 7 demonstrates that in the case of the coupling agent in the matrix, the strain energy released fractured the interphase all around

the fiber, despite the fact that the A174 in the resin makes the polyester more brittle, as will be shown later. In Plate 7 one can clearly see the mirror zone surrounded by the plastic zone and in Plate 6 only the mirror zone is present. An other cause of the difference between the two fractures is indicated in Table 2. The fact that the fiber coated with A174 has a tensile strength greater than for the bare fiber will cause the latter to break at a lower strain and thus release less energy.

In order to overcome the impossibility to perform the test on polyester samples at room temperature no matter how low was the strain rate, it was decided to increase the temperature to 60°C. The matrix becomes more ductile and crack propagation is reduced. Results are given in Table 10 and suggests the same interfacial shear strength for the cases (fiber A174) and (bare fiber) and a lower value for (polyester + A174). The reason for those very surprising results is shown in Plate 8. Good fiber-matrix adhesion induces crack formation at fiber breaks and the cracks open upon further increasing strain. Therefore the opening cracks tend to unload the fiber, reducing the probability of other fiber breaks. In fact one should only compare the results for (fiber + A174) and (polyester + A174) as it seems that fiber break induces the same kinds of failure phenomena (photographs (b) and (c)). Photograph (a) shows a poor

interfacial shear strength as fiber break leads to a fiber-matrix debonding. The role of A174 in the matrix is very important as can be noticed in Plate 8, and already indicated in the SIMS analysis and short beam shear test. A174 seems to elaborate the polyester more brittle and so more subject to crack propagation.

It stands to reason that the critical fiber length test does not evaluate only the interfacial shear strength but also the properties of the matrix in term of cracking and deforming plastically. Therefore, that test can be used only when all the parameters except the nature of the interphase are held constant and when the phenomena induced at fiber breaks are identical for each kind of sample. The question is: How can one be sure from a visual observation that there is no difference in failure mechanisms at fiber breakage? To answer that question one must make use of the high-resolution analytical techniques employed here in.

Table 9. Critical fiber length test: Epoxy samples.

EPOXY
Fiber + A1100 Lm = 369 μm Standard deviation = 133 μm δ = 264 μm τ = 215 MPa
Epoxy + A1100 Lm = 457 μm Standard deviation = 129 μm δ = 305 μm τ = 85 MPa
Bare fiber Lm = 367 μm Standard deviation = 109 μm δ = 245 μm τ = 130 MPa
Fiber + Si Very few fiber breaks

Table 10. Critical fiber length test: Polyester samples.

POLYESTER
Fiber + A174 Lm = 1412 μm Standard deviation = 465 μm δ = 941 μm τ = 31 MPa
Polyester + A174 Lm = 1143 μm Standard deviation = 289 μm δ = 762 μm τ = 27 MPa
Bare fiber Lm = 1126 μm Standard deviation = 258 μm δ = 751 μm τ = 30 MPa
Fiber + Si Very few fiber breaks

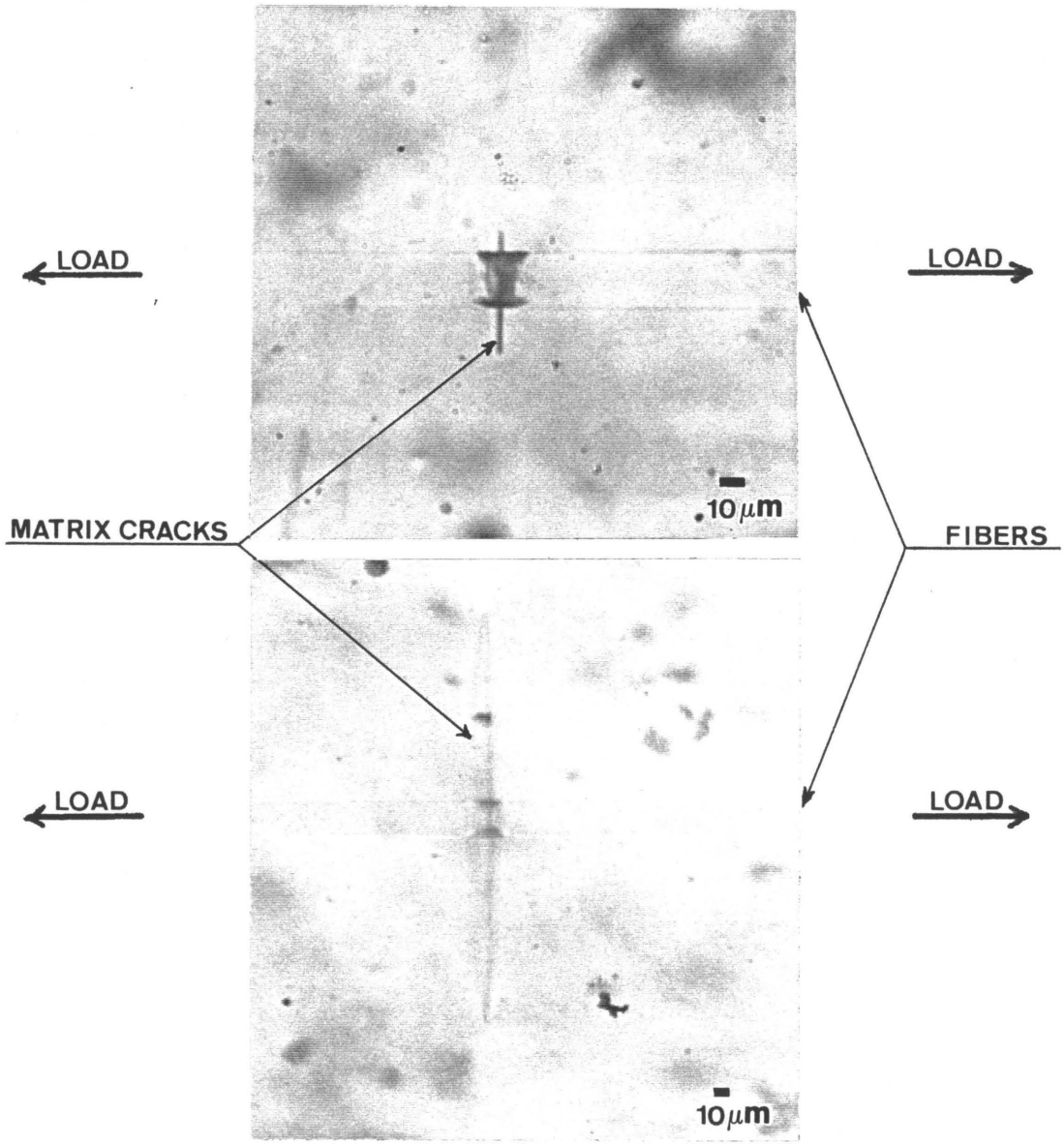

Plate 5. Two kinds of cracks at fiber break in single fiber samples made of polyester resin.

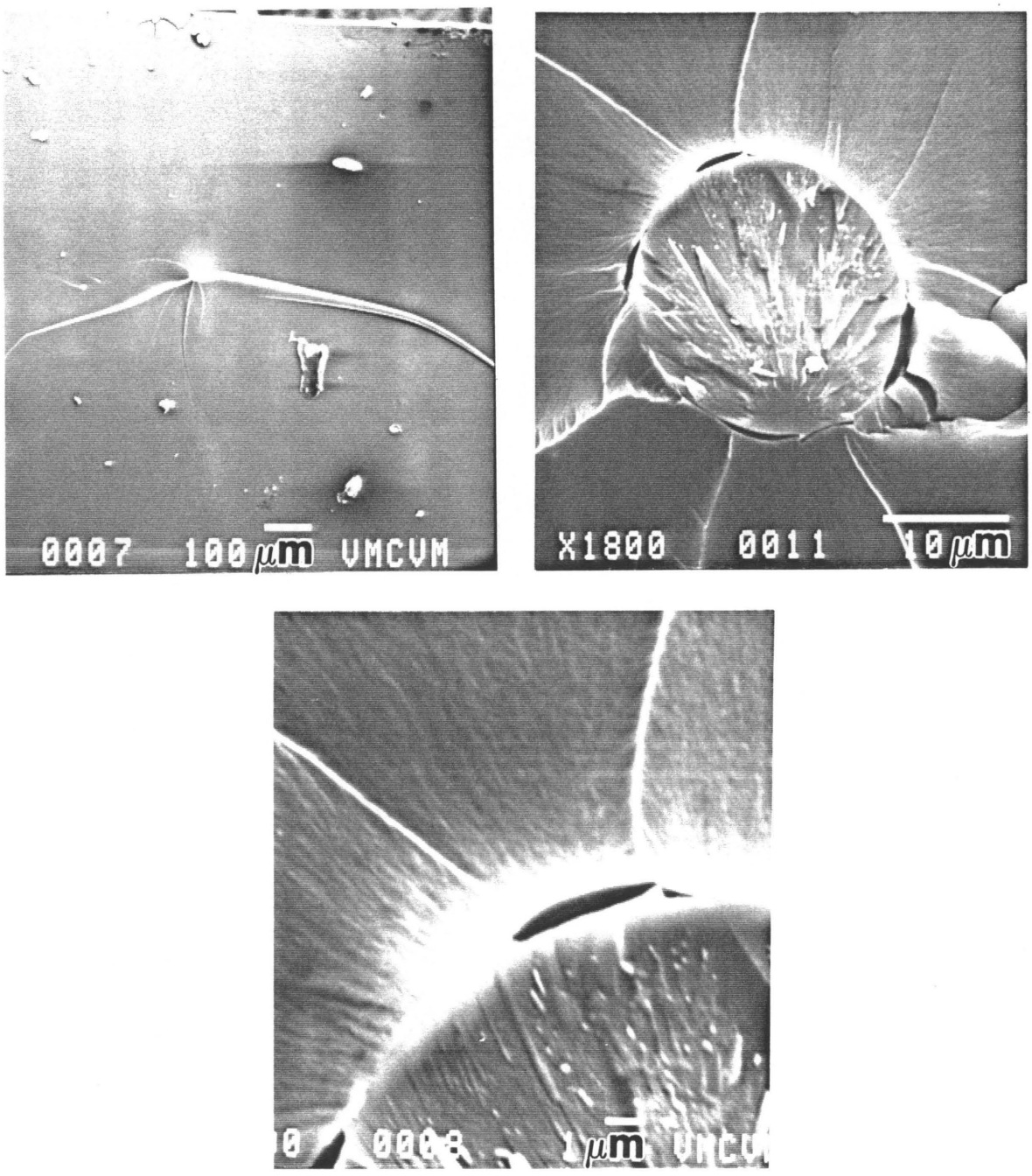

Plate 6. SEM photomicrographs of the fracture surface of a polyester sample containing one fiber coated with A174.

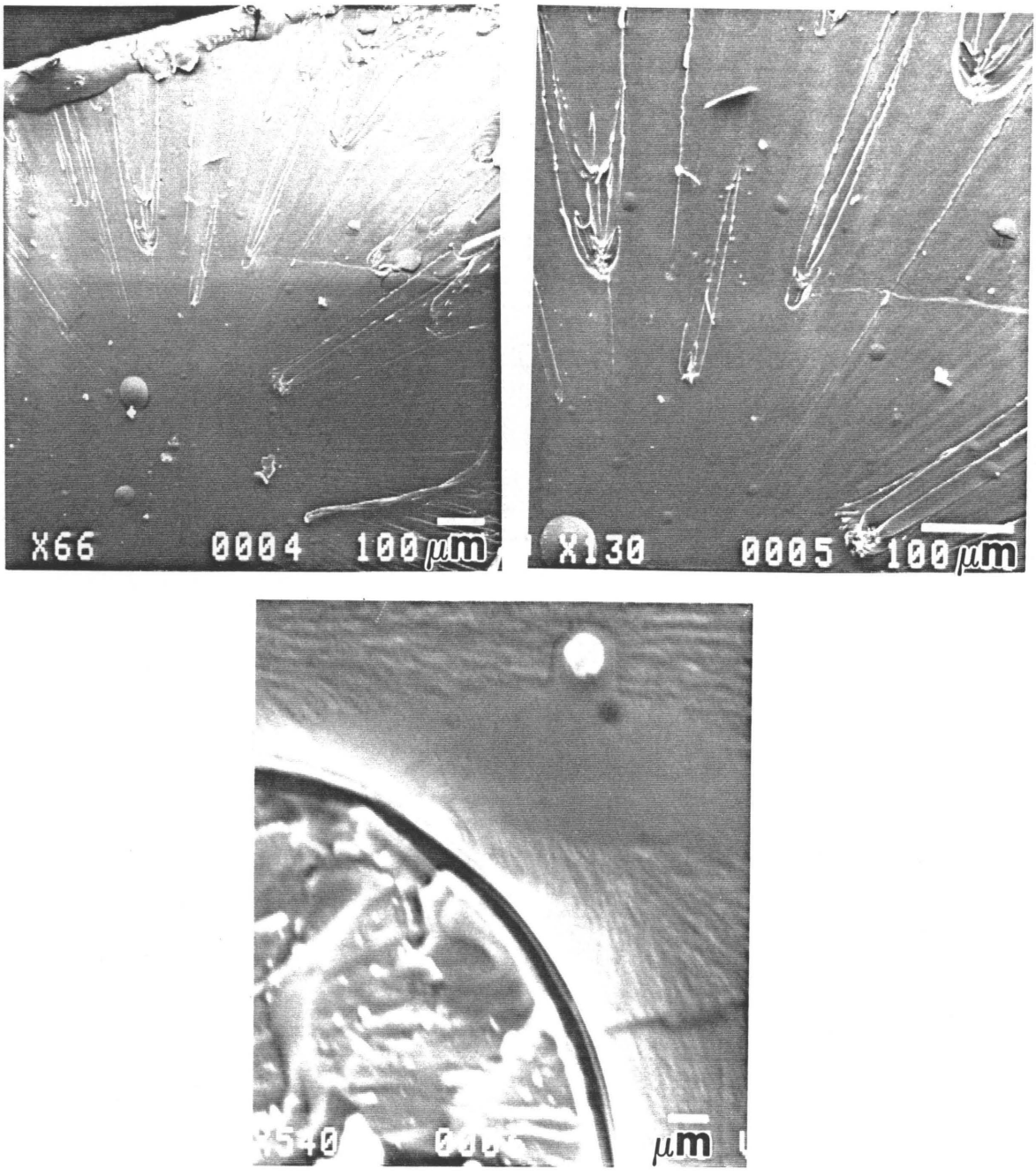

Plate 7. SEM photomicrographs of the fracture surface of a sample made of polyester containing A174 and bare fiber.

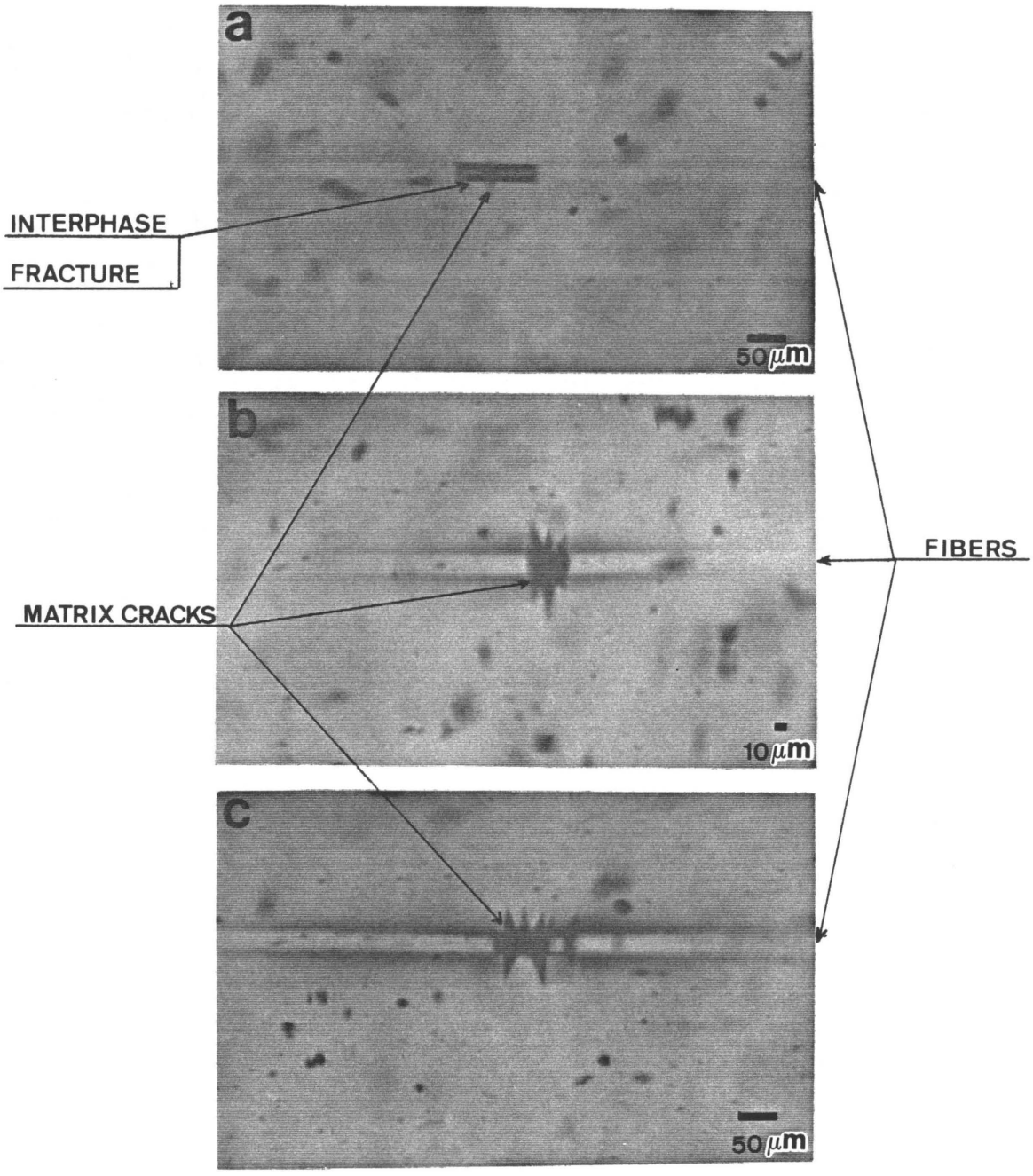

Plate 8. Three kinds of fiber breaks at 60°C in the single fiber sample made of polyester. (a) bare fiber, (b) polyester + A174, (c) fiber + A174.

Measurements and observations with polarized light

Contrary to what has been found [56] about carbon fibers in epoxy, no significant change was observed in the shape of the light zone around a fiber break when the specimen is loaded. Plate 9 shows an increasing degree of strain (therefore decreasing fragment lengths) for the case of a single fiber sample made of epoxy resin. It seems that the dimension and the shape of the illuminated zone are fixed definitively during the fiber breakage and probably depend on the properties of the interphase. However, it stands to reason from the diffused light zones shown in Plate 9 that it is impossible to perform any measures to study their variation from one kind of interphase to another.

If plastic deformation occurs along the interface upon fiber breaks one should see a residual light zone after the sample has been unloaded. It is shown in Plate 10 for the epoxy samples and in Plate 11 for the polyester samples (Photomicrographs of Plate 11 represent only half the light zone around the break) As it has been explained in the experimental procedures the better the fiber-matrix adhesion the more strain energy can be absorbed through plastic deformation at fiber break therefore the longer is the plastic zone. Table 11 gives the results of those measurements for both polyester and epoxy samples. For each matrix a better

adhesion is found for the fiber coated with a coupling agent, no difference is noted for the epoxy samples between the (epoxy + A1100) and (bare fiber) cases as their light zone's length are too close to one another to demonstrate a difference in adhesion. That may be related to the short beam test where the same mode of failure has been observed for those two cases (bending failure). On the other hand Table 11 indicates a difference in adhesion between the (polyester + A174) and (bare fiber) cases for the samples made of polyester resin. Here again, one can relate those results to what was found for the short beam shear test. Better fiber-matrix adhesion had been implied for the beam made of polyester containing A174 because that beam fails in shear and not by internal slipping which is the failure mode of the bare fiber sample.

Even if the results obtained by analysis of the residual plastic zone size seems to correlate with the observations made by SIMS analysis and the short beam shear tests one has to be aware of the difficulty in performing quantitative measurements. The way they have been done (polarizing microscope with 160X or 320X magnification) makes them subject to too large an imprecision (± 10 μm at 320X and ± 20 μm at 160X) to consider this technique able to distinguish a small difference in adhesion. This technique can be improved by using a higher magnification microscope in order to evaluate

precisely the influence of fiber end slipping and crack opening on the length measured, and by using photographic techniques to define more clearly the light zone. That experiment gives more reliable results than the critical fiber length test and refer more to the notion of ineffective length than of critical fiber length. Recalling the model with an interphase it has been found the lack of simple relation between the two notions exists. That test tends to reinforced that conclusion and shows that the ineffective length is more characteristic of the fiber-matrix adhesion than the critical fiber length as defined in the literature.

Table 11. Measurements with polarized light: Results.

	POLYESTER
Fiber + A174	zone length = 1121 µm
Polyester + A174	zone length = 841 µm
Bare fiber	zone length = 772 µm
	EPOXY
Fiber + A1100	zone length = 176 µm
Epoxy + A1100	zone length = 127 µm
Bare fiber	zone length = 135 µm

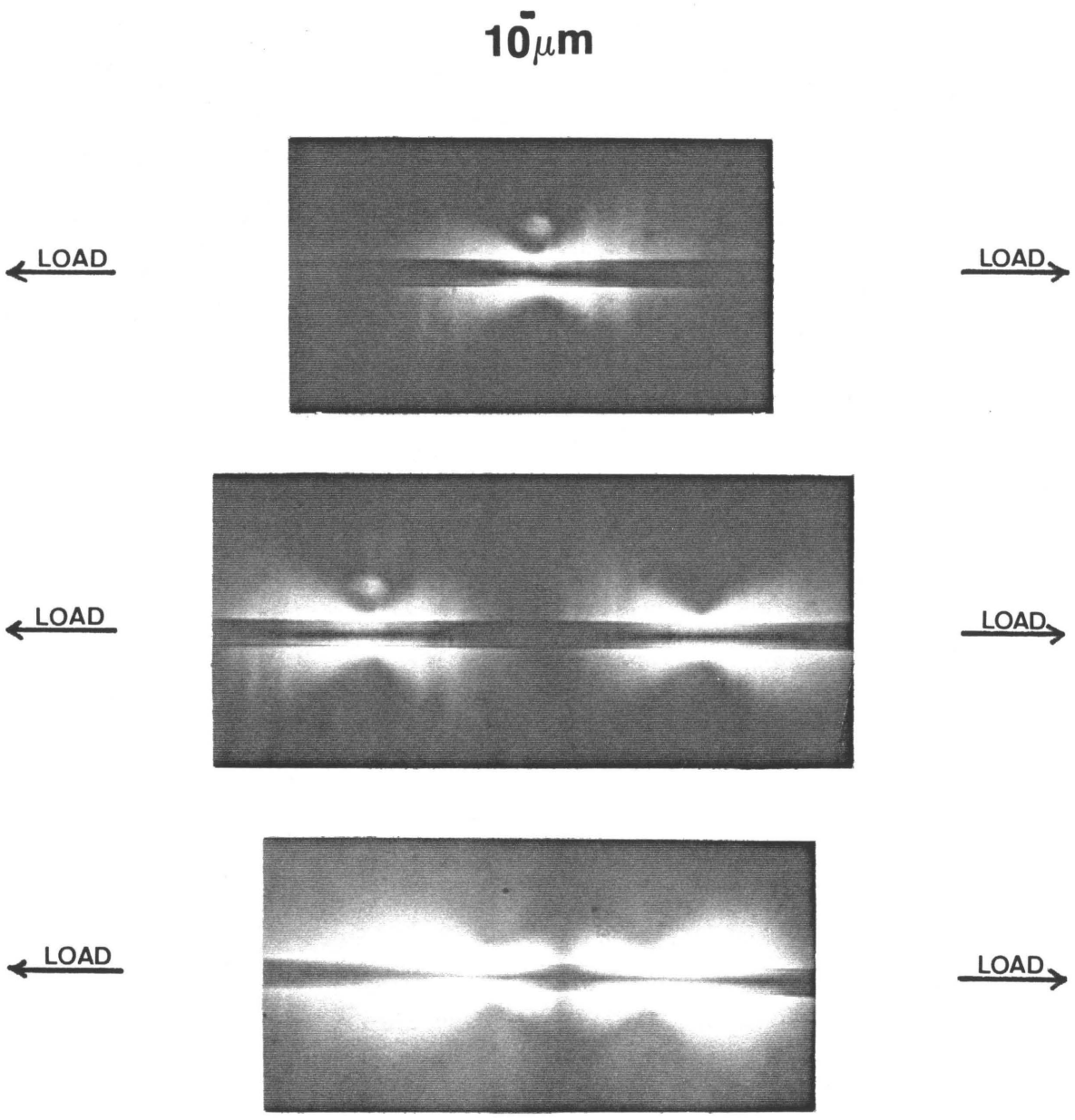

Plate 9. Polarized light photomicrographs of fiber breaks in epoxy resin when the sample is stressed.

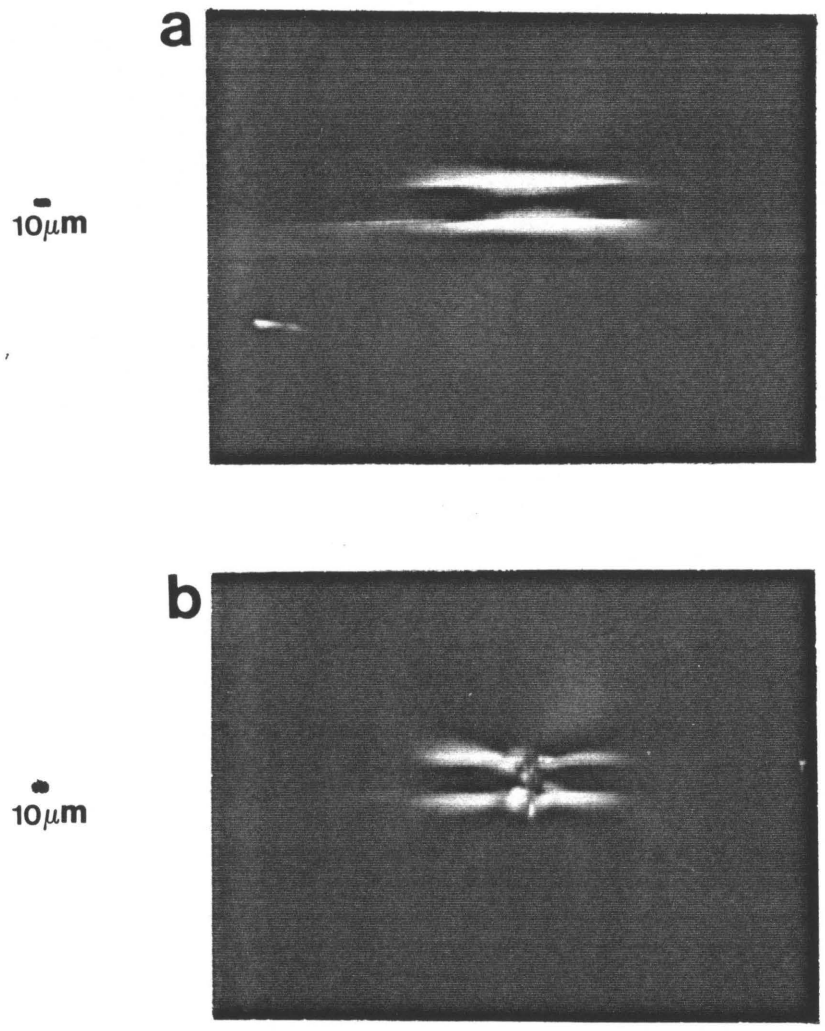

Plate 10. Polarized light photomicrographs of light zones for the epoxy samples after unloaded: (a) fiber + A1100, (b) epoxy + A1100.

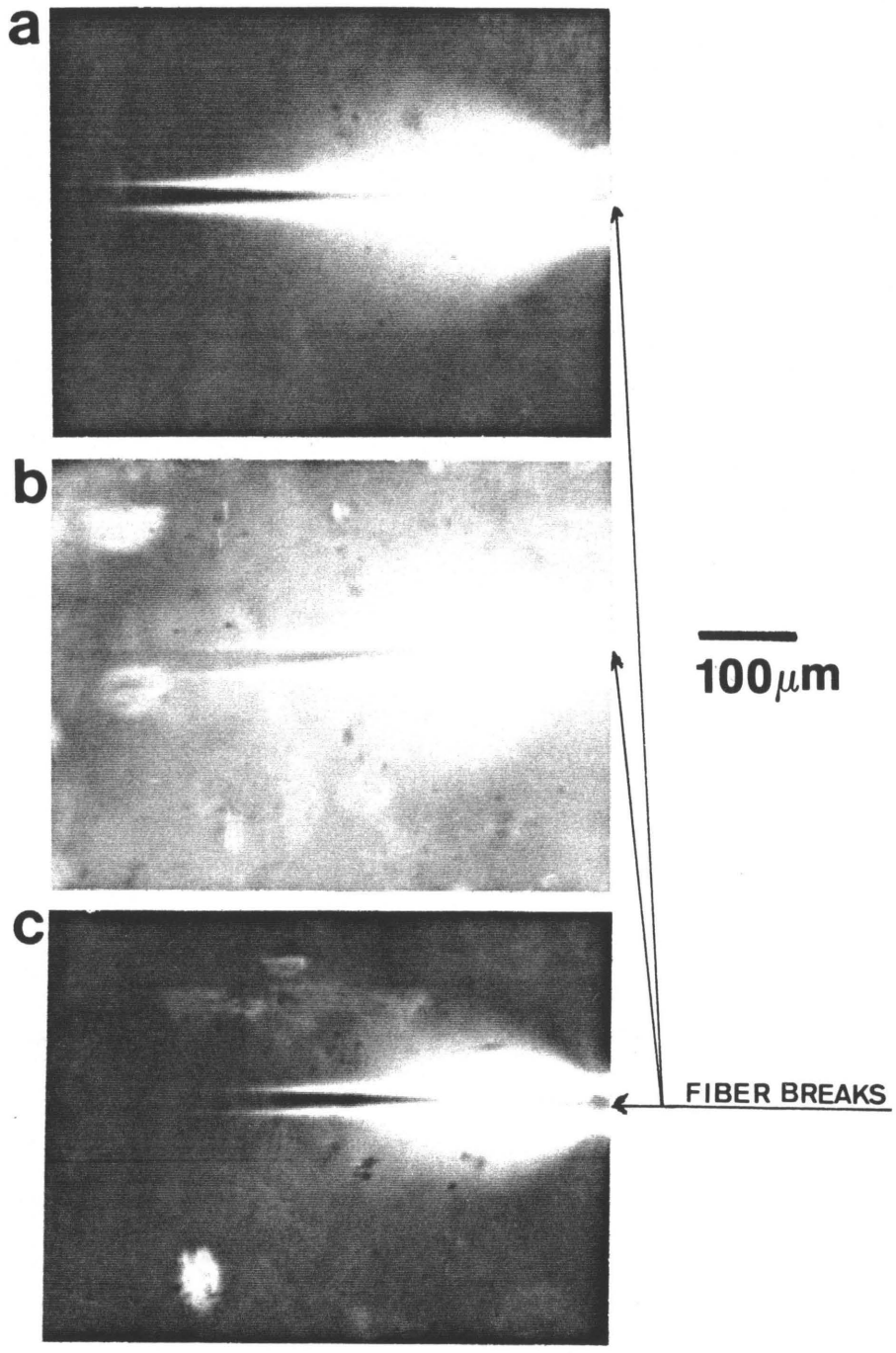

Plate 11. Polarized light photomicrographs of light zones for the polyester samples after unloaded: (a) fiber + A174, (b) polyester + A174, (c) bare fiber.

Comparison: Critical fiber length test / Short beam shear test

It is very difficult to relate the results of the two tests. In both cases the fiber-matrix adhesion, the strength of the fiber and the properties of the matrix play very important roles. However for the same matrix, fiber and interphase, the properties of those three constituents will not participate in the same way in the failure of the single fiber sample and of the composite beam. It has already been noticed that those two tests may give opposite results about the fiber-matrix adhesion (polyester case).

Besides the reasons given in the previous sections the two tests differ because of several other points:

- Stress concentration and constraints due to other fibers. Plate 12 shows the difference of stress concentration between one and three breaks in an epoxy sample containing three fibers. One has also to note on that photograph the crack induced by the two other fiber breaks in the neighborhood of the first break shown on the top picture. A more catastrophic influence of other fiber is presented by Plate 13 and 14. One has to remember from the critical fiber length test that no matrix crack occurs at the fiber break in the single fiber samples made of epoxy. However, if a tensile test if per-

formed on a sample containing more than one fiber the specimen will fracture similarly to what has been observed for the single fiber polyester test at room temperature. The contraint induced by adjacent fiber makes the matrix to behave in a more brittle manner. One can easily notice on Plate 13 and 14 the disk shape cracks around the fibers. Besides that, if the number of fibers increase the energy to be released does the same because several fibers may break at the same time. The mirror zone is bigger for the epoxy sample containing seven fibers than the one containing only three.

- Difference in the stress-strain curves. If one takes the simple case of a tensile load applied on both single fiber sample and composite, Figure 38 demonstrates that what is measured in the critical fiber length test is far from what one is interested to know about the composite. One wants to characterize the interface for a strain between 0 and ε_{cmax} and not at ε_s or ε_{smax}. The reasons inducing a certain value of the critical fiber length depend on the interphase and matrix properties at ε_s. Those properties may be quite different at ε_{cmax}. Even a comparison between surface treatments may be wrong because the reasons of the difference in fiber fragment length at the end of the test may have no relation with the difference in adhesion at ε_{cmax}.

- Fiber breaks. One of the main difference between the short beam test and the critical fiber length test is that no fiber break occurs in the shear failure of the beam. Therefore the influence of strain energy released is non existent in the short beam test. As it has been shown that energy has an important effect in the other test.

- Poisson effect and differential thermal expansion. On account that there is more glass than matrix in glass fiber reinforced composite the shrinkage of the matrix due thermal effects and loading may tend to debond the fibers from the matrix as shown in Figure 2.

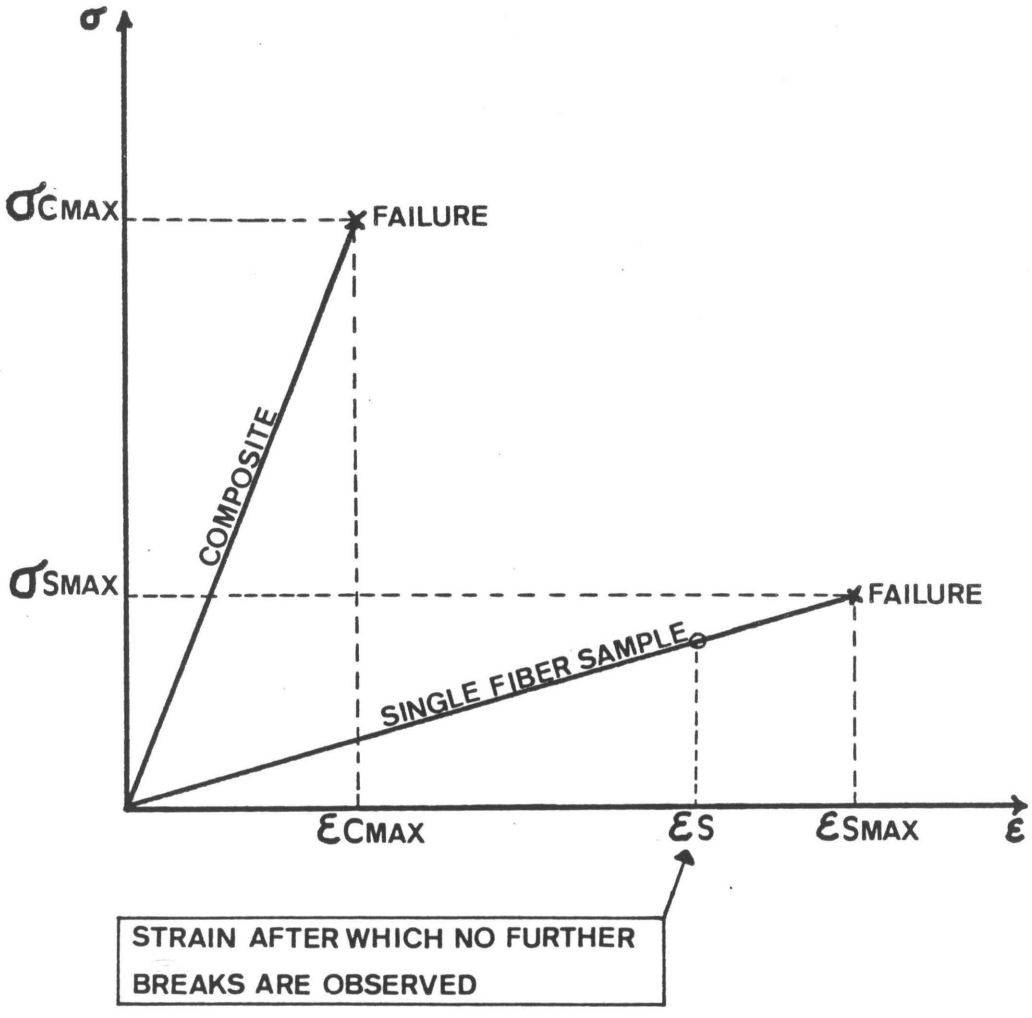

Figure 36. Stress-strain curves: for a composite and a single fiber sample.

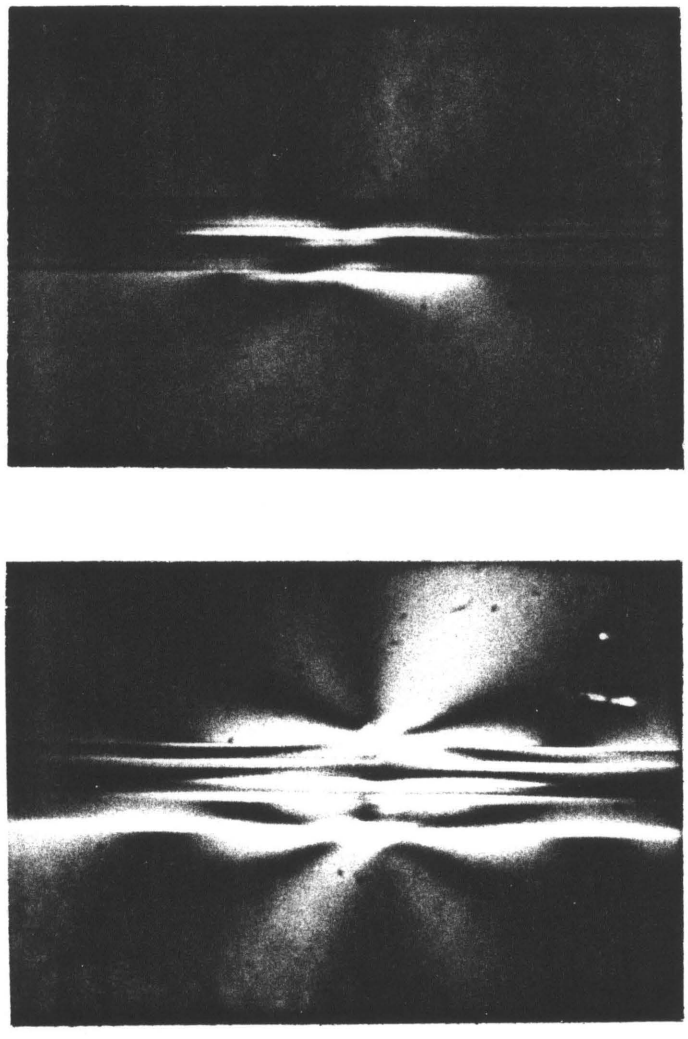

Plate 12. Polarized light photomicrographs of the breaks in a three fibers epoxy sample. (a) one break, (b) three adjacent breaks.

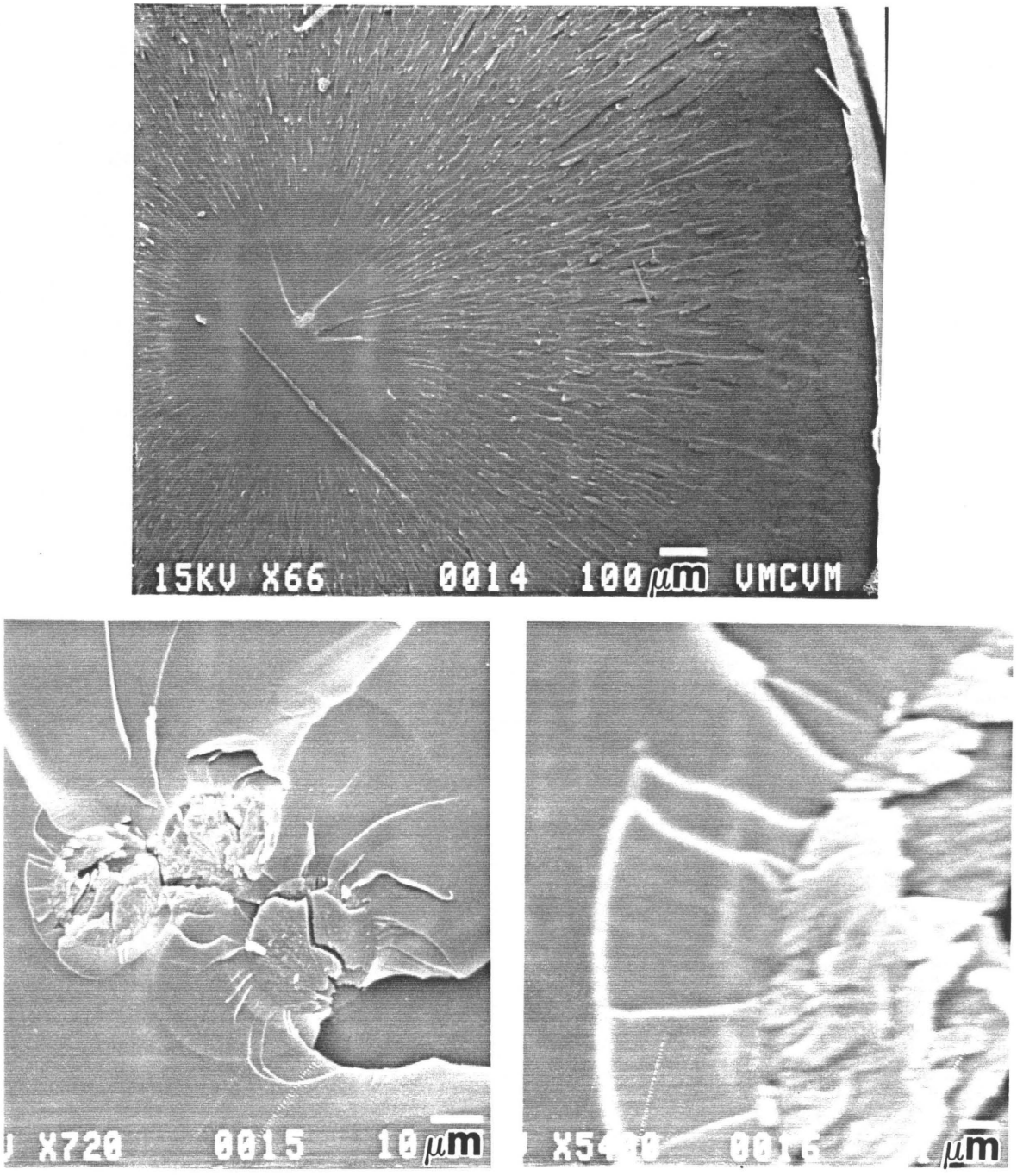

Plate 13. SEM photomicrographs of the fracture surface of an epoxy sanple containing three fibers coated with A1100.

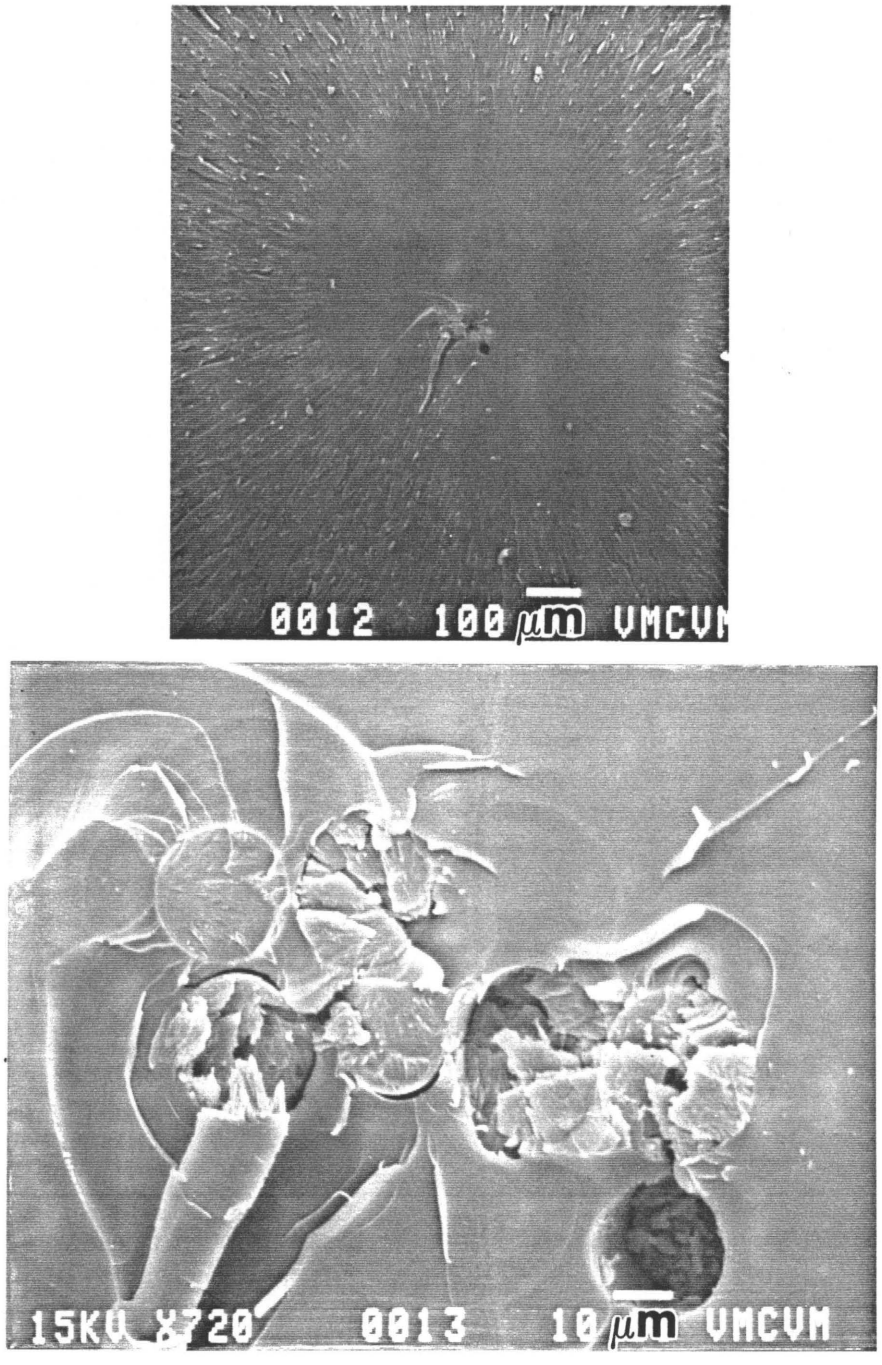

Plate 14. SEM photomicrographs of the fracture surface of an epoxy sample containing seven fibers coated with A1100.

SUMMARY AND CONCLUSIONS

The purpose of this research was to study the influence of the interphase on the properties of composite materials. Attention was focussed upon whether the evaluation of fiber-matrix adhesion with a single fiber specimen is suitable for the prediction of the interfacial shear strength in real composites. In order to achieve those goals the research program was designed by combining: (1) The analysis given by a new theoretical approachs, (2) mechanical tests on composite short beams and single fiber dogbones, (3) *in situ* optical microscopy with polarized light, (4) high resolution surface analysis with electron microscopy (SEM) and spectroscopy (XPS or ESCA) and mass spectroscopy (SIMS). Eight interphases were prepared by varying the matrix (epoxy or polyester, with and without silane) and fiberglass surface treatment (none, γAPS, γMPS, or silicone).

In the theoretical part, a shear lag model integrating the new characteristics of the interphase has been developed. It shows the difference between the concepts of the ineffective length and the critical fiber length, and that led to the new measurements performed in this research using polarized light microscopy. Also with the new model, it was possible to investigate the influence of the mechanical properties of each

consituent in a composite on the ineffective length. The statistics of fiber breakage was modelled with the assumption that the strength of a fiber as a function of its length can be approximated by a Weibull distribution. Combined with the shear lag model an accurate calculation of the interfacial shear strength was possible from the fiber fragment lengths measured in the critical fiber length test. The combined model takes into account the gradient of tensile stress near the fiber end, which is generally neglected in the literature, creating a significant difference in the results. Using more elaborate and realistic assumptions that model can be the basis of future work in order to improve the prediction of the stress transfer at the fiber-matrix interface.

The tensile tests performed on fibers alone in order to determine the Weibull parameters pointed out the great influence of the coupling agent formulation on the fiber strength (γAPS : γMPS : none ≈ 3.1 : 1.7 : 1.3). This important function of a "coupling" agent has not been highlighted before, perhaps because is related to protection and not to "coupling". ESCA and SEM analysis showed correlations in that each glass surface coating had specific composition and morphology.

The results of both short beam shear and critical fiber length tests demonstrate that neither is a good mechanical

technique to evaluate fiber-matrix adhesion. Both tests produced results that were impossible to interpret without the combined information from the polarizing microscope, ESCA, SIMS and SEM.

In both mechanical tests, the results depended not only on the fiber-matrix adhesion but also on the fiber and matrix properties. Therefore one cannot, in general, use either test to evaluate the interfacial shear strength simply. In fact, the results of the two test did not correlate with eachother.

An alternative method to evaluate the fiber-matrix adhesion is proposed: Measurement of the length of the residual birefringent zone adjacent to a fiber break on unloaded single fiber spacemens. That quantity is similar to the ineffective length and the results did show good correlation with the short beam data and the SIMS fractography in the cases studied in this research. Future work should refine the experimental procedure to obtain more precise values for the residual zone, and extend the data base to other combinations of fiber, surface treatment and matrix.

The short beam shear tests did provide fractured samples that could be analysed by SIMS. It was possible to determine the locus of failure in the polyester beam for each kind of

interphase, that γMPS on the fiber or in the resin did eliminate failure at the glass surface. Combining those results with the polarizing microscope observations on single fiber samples under stress, and on their fracture surfaces with SEM, the influence of fiber-matrix adhesion was investigated. Good adhesion gave rise to catastrophic brittle matrix crack propagation in the polyester case, but not in the epoxy. On the other hand, no adhesion led to no load transfer and simple slipping at the the interface. Those results illustrate the need to "custom design" the interphase with respect to the fiber and matrix properties, and the subsequent load distributions as well.

The in situ polarizing microscopy and SEM fractography was repeated using multiple filament samples, the mutual influence of adjacent fibers on the behavior of composite material was illustrated. The combined results were used to define in detail the differences in response between single fiber and composite specimens. This research exemplifies the multidisciplinary approach necessary to make progress in the future attempts to optimize composite properties through prediction and control of the fiber-matrix interphase.

REFERENCES

1. Theocaris, P. S., and Papanicolaou, G. C., "The effect of the boundary interphase on the thermomecanical behaviour of composites reinforced with short fibres," Fib. Sci. Tech., 1979.

2. Broutman, L. J., and Agarwal, B. D., "A theoritical study of the effect of an interfacial layer on the properties of composites," Poly. Eng. and Science, August 1974, No. 8.

3. Berger, E. J., and Eckstein, Y., "Epoxy resin wetting of E glass single filaments as it relates to shear strength," Adhesive Joints, 1984, edited by K.L. Mittal.

4. Wesson, S. P., and Jen, J. S., "Surface energetics and surface composition of fiberglass reinforcements," 16th National SAMPE Technical Conference, 9 , 11, 1984.

5. Wu, S., "Polymer interface and adhesion," E.I. Dupont de Neumours & Company, Marcel Dekker Inc.

6. Mc Mahon, P. E., and Ying, L., "Effects of fiber/matrix interactions on the properties of graphite/epoxy composites," NASA Contractor Report 3607, 1982.

7. Schultz, J., Caseneuve, C., Shanahan, M. E. R., and Bonnet, J. B., "Fibre surface energy characterisation," Journal of Adhesion, 1981, Vol. 12, pp 221-231.

8. Simon, H., "Proprietes interfaciales dans les composites: energie de surface et adhesion fibre de verre/matrice macromoleculaire," Doctorate thesis at the University of Haute Alsace, 1984.

9. Hammer, G. E., and Drzal, L. T., "Graphite fiber surface analysis by X-ray photoelectron spectroscopy and polar/dispersive free energy analysis," Applications of surface science, 4, 1980, pp 340-355.

10. "Surface characteritics of fibers and textiles". Part II edited by M.J. Schick, Marcel Dekker Inc New York and Basel, 1982.

11. Chauchard, J., Chabert, B., and Edel, G., Teintex, 6, 299, 1976.

12. Fowkes, F. M., Dwight, D. W., Lloyd, T. B., and Otischler, D., "Modification of surface acidity and

basicity of glass fillers," Proc. of the 40th Annual S.P.I. Conference, Section 17-E, Atlanta 1985.

13. Rynd, J. P., and Rastogi, A. K., Surface Science, 48, 1975, 22.

14. Rynd, J. P., and Rastogi, A. K.,American Ceramic Society Bulletin American Chemical Society Symposium, Surface chemistry of composite materials, Boston, 1972, 53, 1974, p 631.

15. Culler, S. R., Ishida, H., and Koening, J. L., "Non destructive FT-IR sampling techniques to study glass fiber composite interfaces," Applied Spectroscopy, Vol. 38, No. 1, 1984.

16. Miller, J. D., Hoh, Ka-Pi, and Ishida, H., "Studies of the stimulation of silane coupling agent structures on particulate filler: pH effect," Polym. Comp., January 1984, Vol. 5, No. 1.

17. Ishida, H., Polym. Comp., April 1984, Vol. 5, No. 2.

18. Dibenedetto, A. T., and Scola, A, D., "Chacterisation of S-glass/polymer interfaces using Ion Scattering Spectroscopy and Ion Mass Spectroscopy," J. of Colloid and Interface Science, Vol. 64, No. 3, May 1978.

19. Cupic, A., Berthelot, J. M., and Maufrat, J. M., "Resolution du probleme: milieu infini contenant une seule fibre cylindrique et soumis a des contraintes uniformes," Fib. Sci. Tech., 11, 1978.

20. Christensen, R. M., "Mechanics of composite materials," Willey-Interscience publiation, Chap III, p 84.

21. Arnoud, J. F., "Etude de l'endomagement des materiaux composites par decohesion fibre-matrice," Proc. of the J.N.C. 3, Paris, September 21-23 1982, p 159.

22. Carrara, A. S., and Mc Garry, F. J., "Matrix and interface stresses in a discontinuous fiber composite model," Journal of Composite Materials, 2, 222, 1968.

23. Agarwal, B. D., and Bansal, R. K., "Plastic analysis of fibre interactions in discontinuous fibre composites," Fib. Sci. Tech., 10, 1977.

24. Mac Laughlin, T. F., "A photo elastic analysis of fiber discontinuities in composite materials," Presented at the

Monsanto /Washington University association Annual symposium High performance.

25. Greszczuk, L. B., "Interfiber stresses in filamentary composites," AIAA journal, Vol. 9, No. 7, July 1971.

26. Tyson, W. R., and Davies, G., Brit. J. App. Phys., 1963, 10, 199.

27. Schuster, D. M., Scala, D., Trans. Met. Soc., 1965, AIME, 230, 1941.

28. Voloshin, A., "Stress field evaluation in photo elastic anisotropic materials: experimental numerical technique," Journal of Composite Materials, Vol. 14, 1980, p 342.

29. Chabert, B., Mermoz, G., and Vincent, L., "Role physicochimique de la fibre de renfort dans la mise en oeuvre et les proprietes d'un materiau composite," Composite, No. 2, March-April 1984.

30. Theocaris, P. S., and Milios, J., "The disruption of a longitudinal interface by a moving transverse crack," J. of Reinforced Plastics and Composites, January 1983.

31. Kaeble, D. H., "Theory and analysis of fracture energy in fiber reinforced composites," Journal of Adhesion, Vol 5, 1974.

32. Gaggar, S. K., and Broutman, L. J., "The influence of fiber and interface strength on toughness of glass reinforced plastics," Proceedings of the 31st Annual Technical Conference S.P.I., 1976, Section 6-F.

33. Atkinson, C., and Avila, J., "A comparaison of exact and model solutions for the initiation of debond fracture," Int. J. Eng. Sci., Vol. 21, No. 9, 1983.

34. Atkinson, C., Avila, J., Betz, E., and Smelser, R. E., "The rod pull out problem, theory and experiment," J. Mech. Phys. Solids, Vol. 30, No. 3, 1982.

35. Mullin, J., Berry, J. M., and Gatti, A., "Some fundamental fracture mechanics applicable to advanced filament reinforced composites," Journal of Composite Materials, Vol. 2, No. 1, 1968.

36. Rosen, B. W., "Tensile failure of fibrous composites," AIAA journal, Vol. 2, No. 10, November 1964.

37. Rosen, B. W., "Mechanics of composite strengthening, fibre composite materials," American Society for Metals, Metal Park, Ohio 1965, pp 37-75.

38. Kelly, A., and Tyson, W. R., "Fiber-strengthened material," High Strength Materials, V.F. Zackay edit, J. Wiley and sons Inc, Chap. 13, p 578.

39. Fukuda, H., and Chou, T. W., "An adcanced shear lag model applicable to discontinuous fiber composites," Journal of Composite Materials, Vol. 15, January 1981, p 79.

40. Fukuda, H., and Chou, T. W., "Stiffness and strength of short fibre composites as affected by cracks and plasticity," Fib. Sci. Tech., p 243, 15, 1981.

41. Bartdorf, S. B., and Ko, R., "Use of shear lag for composite microstress analysis," Advances in Aerospace Structures, ASME, 1983.

42. Piggott, M. R., "Expressions governing stress-strain curves in short fibre reinforced polymers," J. Mat. Sci., 13, 1978, p 1709.

43. Ostrowski, J., Will, G. T., and Piggott, M. R., "Poisson's stress in fibre composites I: analysis," J. of Strain Analysis, Vol. 19, No. 1, 1984.

44. Chua, P. S., and Piggott, M. R., "The glass fibre-polymer interface II and III," Composite Sci. and Tech., 1, 1985.

45. Lauke, B., and Schultrich, B., "Deformation behaviour of short-fibre reinforced materials with debonding interfaces," Fib. Sci. Tech., 19, 1983, pp 111-126.

46. Riley, V. R., "Fibre/fibre interaction," Journal of Composite Materials, 1968.

47. Hedgepeth, J. M., and Van Dyke, P., "Local stress concentrations in imperfect filamentary composite materials," Journal of Composite Materials, Vol 1, 1967, p 294.

48. Batdorf, S. B., "Tensile strength of unidirectionally reinforced composites I and II," J. Reinforced Plast. and Comp., April 1982, p 153.

49. Bergman, B., "On the probability of failure in the chain-of-bundles model," Journal of Composite Materials, Vol. 15, January 1981, p 92.

50. Manders, P. W., Bader, M. G., and Chou, Tsu-Wei, "Monte carlo simulation of the strength of composite fibre bundles," Fib. Sci. Tech., 17, 1982, pp 183-204.

51. Broutman, L. J., "Measurement of the fiber-polymer matrix interfacial strength," Interfaces in composite, ASTM STP 452, 1969, 27.

52. Broutman, L. J., "Mechanical requirements of the fiber-matrix interface," Proc. of the 25th S.P.I. Conf., Section 16-D, 1, 1970.

53. Broutman, L. J., "Glass-resin joint strength and their effect on failure mechanisms in reinforced plastics," Poly. Eng. and Science., 6, July 1966.

54. Fraser, W. A., Ancker, F. H., and Dibenedetto, A. T., "Evaluation of surface treatments for fibers in composite materials," Polym. Comp., October 1983, Vol. 4, No. 4.

55. Miwa, M., Ohsawa, T., and Tahara, K., "Effects of fiber length on the tensile strength of epoxy/glass fiber and polyester/glass fiber composites," J. Appl. Polym. Sci., Vol. 25, 1980, p 798.

56. Drzal, L. T., Rich, M. J., and Llyod, P. F., "Adhesion of graphite fibers to epoxy matrices: I the role of fiber surface treatment," Journal of Adhesion, 1982, Vol. 16, pp 1-30.

57. Jarvela, P., Laitinen, K. W., Purola, J., and Tormola, P., "The three-fibre method for measuring glass fibre to resin bond strength," Int. J. Adhesion and Adhesives, Vol. 3, No. 2, July 1983.

58. Miller, B., "Fiber/resin microbond shear strength measurements," Proc. of the 8th Annual Meeting of The Adhesion Society, February 24-27 1985, Savannah Georgia.

59. Sun, L. T., Lin, Y. T., and Wu, J. K., "The effects of fiber end geometry on the stress distribution of short fiber composites," Advances in Aerospace Structures, ASME, 1983.

60. Chua, P. S., Piggott, M. R., "The glass fibre-polymer interface: I-Theoritical consideration for single fibre pull-out tests," Comp. Sci. Tech., 22, 1985, pp 33-42.

61. Wells, J. K., and Beaumont, P. W. R., "Debonding and pull-out processes in fibrous composites," J. Mate. Sci., 20, 1985, pp 1275-1284.

62. Sarma, A. V. S. R. J., Murthy, P. N., and Kushwaha, P. S., "Stress diffusion in pull out model," Fib. Sci. Tech., 12, 1979.

63. Phan-Thien, N., "A contribution to the rigid fibre pull-out problem," Fib. Sci. Tech., 13, 1980, pp 179-186.

64. Stinchcomb, W. W., Henneke, E. G., and Price, H. L., "Use of short-beam test for quality control of graphite polyimide laminates," ASTM STP 626, 1977, pp 96-109.

65. de Charentenay, F. X., and Kamimura, K., Ann. Composites, Vol. 2, p 3, 1982.

66. Bayou, J. P., "Influence de l'interface charge/polymere sur les proprietes viscoelastiques des materiaux composites," Thesis at the university Lyon I France, 1980.

67. Gupta, A. K., Kar, B., and Mani, P., "Effect of binder content and coupling agents on mechanical properties of epoxy-aggregate composites," J. Reinforced Plast. and Comp., Vol. 1, October 1982, p 370.

68. Duttq, A., and Ryan, E., "Effect of fillers on kinetics of epoxy cure," J. App. Poly. Sci., Vol. 24, 1979, pp 635-649.

69. Ohsawa, T., Nakayama, A., Miwa, M., and Hasegawa, A., "Temperature dependance of critical fiber length for glass fiber-reinforced thermosetting resins," J. App. Poly. Sci., Vol. 22, 1978, p 3203.

70. Riefsnider, K. L., Course E.S.M. 6100 "Failure analysis in composite materials" at Virginia Polytechnic Institute and State university, Spring 1985.

71. Metcalf, A. G., and Schmitz, G. K., "Effect of length on the strength of glass fibers," ASTM Preprint, No. 87, June 1964.

72. Phoenix, S. L., "Clamp effect in fiber testing," Journal of Composite Materials, Vol. 6, July 1972.

The vita has been removed from the scanned document